Astro-oligodendrocytic gap junctional coupling and possible roles for Connexin 29 and Connexin 47.

By

Vlad-Andrei Ionescu

A Thesis

Submitted to the Faculty of Graduate Studies

in Partial Fulfillment of the Requirements for the Degree of

MASTER OF SCIENCE

Department of Physiology

University of Manitoba

Winnipeg, Manitoba

THE UNIVERSITY OF MANITOBA

FACULTY OF GRADUATE STUDIES

*****

COPYRIGHT PERMISSION PAGE

Astro-Oligodendrocytic Gap Junctional Coupling and Possible Roles for Connexin 29 and Connexin 47

BY

Vlad-Andrei Ionescu

A Thesis/Practicum submitted to the Faculty of Graduate Studies of The University of Manitoba in partial fulfillment of the requirements of the degree

of

MASTER OF SCIENCE

TABLE OF CONTENTS

I. ACKNOWLEDGEMENTS

Some of the most poignant experiences in our life are usually intensely defined by feelings of elation, awe, amazement, hardship, and at times frustration, but never boredom. Such moments stay with us for the rest of our life and have as common denominator the fact that they represent the foundation on which our personal identity becomes crystallized. However, during such times we would feel undoubtedly lost if not for the guidance and reassurance of the ones that have walked the path ahead of us. As I navigated my own journey as a graduate student I had the support and mentorship of Dr Nagy, my advisor, who has so unselfishly shared his knowledge and experience and taught me the fine art of scientific thought. There is an old proverb that says "teachers open the door, however you enter by yourself" Thank you Jim, you have done so much more! The lessons learned far exceed the bounds of this book!

The lessons learned would have not been completed without the help of my committee members, Dr. Elissavet Kardami, Dr. Brent Fedirchuk and Dr. Peter Cattini. Thank your for your helpful comments and for the intellectually stimulating conversations during oral evaluation.

My appreciation also goes to present and past member of our lab; Brett McLean for excellent technical assistance and Bruce Lynn who taught me "the tricks of the trade". My fellow graduate students Carl Olson, Myriam Lafreniere, Katinka Stecina and Arzu Ozturk for being there during difficult times.

I would like to especially thank my parents, Dan and Cristina, for unwavering love and support. Leading by your own example, you gave me the strength and passion to pursue my dreams and not to deviate from my goals, regardless of how unachievable they may have seemed at times.

Finally, my love goes to Maria-Josée whose support and patience has helped me navigate these difficult and unpredictable times. Thank you! You are my rock!

II. LIST OF ABBREVIATIONS

a.a.	amino acid
A/A	astrocyte/astrocyte GJIC
A/O	astrocyte/oligodendrocyte GJIC
AT	amino terminus of a protein
Ca^{2+}	calcium
CD	cytoplasmic domain of a transmembrane protein
CL	cytoplasmic loop of a multi-pass transmembrane protein
CT	carboxyl terminus of a protein
cDNA	complementary DNA
CMT	Charcot-Marie-Tooth peripheral neuropathy
CMTX	CMT X-linked peripheral neuropathy
CMT1A	CMT type I, associated with mutations or duplications in the gene encoding PMP22
CMT1B	CMT type I, caused by mutations in the gene encoding P0
CNS	central nervous system
Cx	connexin
DNA	deoxyribonucleic acid
E	extracellular loop of a multi-pass transmembrane protein
ED	extracellular domain of a transmembrane protein
EM	electron microscopy
FITC	fluorescein-5-isothiocyanate
FRIL	freeze-fracture replica immunogold labeling
GFAP	glial fibrillary acidic protein
GJIC	gap junctional intercellular communication
IP_3	inositol 1,4,5-triphosphate
IR	immunoreactivity
K^+	potassium
KO	knockout
kDa	kilodalton
LM	light microscopy
M	molar
MBP	myelin basic protein
ml	milliliter
mM	millimolar
MOBP	myelin-oligodendrocyte basic protein
MOG	myelin-oligodendrocyte glycoprotein
MW	molecular weight
N/N	neuronal/neuronal GJIC
NGS	normal goat serum
nm	nanometer
NMDA	N-methyl-D-aspartate
O/A/O	oligodendrocyte/astrocyte/oligodendrocyte GJIC
O/N	oligodendrocyte/neuronal GJIC
P0	myelin protein zero
PB	phosphate buffer

PBS	phosphate-buffered saline
PBST	PBS containing 3% Triton X-100
PDZ	PSD, Disc-large protein, ZO-1
PKA	protein kinase A
PKC	protein kinase C
PKG	protein kinase G
PLP	proteolipid protein
PMP22	peripheral myelin protein 22
PNS	peripheral nervous system
PSD	postsynaptic density
pS	picosiemens
RNA	ribonucleic acid
pH	potential of hydrogen
Ser	serine
TBS	20mM Tris-HCl buffered saline
TBS-T	TBS containing 0.2% Tween-20
μm	micron
Tyr	tyrosine
ZO-1	zonula occludens-1
WT	wild-type

III. ABSTRACT

It has been previously shown that oligodendrocytes in *vivo* are limited almost exclusively to heterologous gap junction formation with astrocytes (A/O), with little or no evidence of oligodendrocyte/neuronal (O/N) or homologous oligodendrocyte/ oligodendrocyte (O/O) gap junction formation. In this study we investigated the cellular localization, anatomical relationship to other glial connexins (Cx26, Cx30, Cx32, Cx43, Cx47) and developmental expression of Cx29 a newly discovered members of the gap junctions protein family.

Immunocytochemically, Cx29 was localized to oligodendrocytes and myelinated fibers throughout brain and spinal cord, with a developmental pattern that showed an onset of expression in a caudo-rostral progression, with a detection in hindbrain during the second postnatal week. Subcellular fractions of myelin were enriched for Cx29, with dense immunoractive bands migrating at 31-33 kDa and 51 kDa corresponding to Cx29 monomer and dimer forms. Immunoblotting indicated moderate levels in forebrain and highest levels in subcortical areas and hindbrain that increased during the postnatal week to stable levels expressed in adults. Following double labeling studies it was revealed that Cx29 partially co-associates with oligodendrocytic Cx32 and astrocytic Cx43 on the oligodendrocyte somata .This was in contrast to the almost total co-localization of Cx32 with Cx26, Cx30 and Cx43 along the same structures. Myelinated fibers, however, seemed to have very limited co-association of Cx29 and Cx32 with either Cx30 or Cx43. In the absence of Cx32 in Cx32 knockout (KO) mice, Cx30 immunolabeling on oligodendrocytic somata appeared to be virtually absent, while Cx26 was partially reduced and Cx43 remained unaffected. There were no differences in expression pattern in Cx32 KO or wild type (WT) brains for either of the remaining oligodendrocytic Cx29 and Cx47. These results suggest that Cx26 and Cx30 are abundantly present at A/O gap junctions and are implicated in heterotypic gap junction formation with Cx32. The persistence of Cx43 and Cx47 after Cx32 deletion suggests Cx43/Cx47 coupling at A/O junctions, while the sparse association of Cx29 with either Cx26 or Cx43, together with the apparent preferential transport of Cx29 to myelinated fibers suggests that Cx29 along with Cx32 may contribute to connexin-mediated autologous communications between adjacent layers of un-compacted myelin.

IV. INTRODUCTION

"In Act II, Scene V of Anthony and Cleopatra, the Queen of Egypt berates and finally beats the unfortunate messenger who tells her of Anthony's marriage to Octavia. Perhaps Shakespeare was anticipating the discovery of gap junctional communications when he penned this scene: Cleopatra clearly understands that, at least in some instances, the messenger is indeed responsible for the nature of the message."

Thomas H. Steinberg "Gap Junction Function"

IV.1. Gap junctions

In multicellular systems intercellular communication represents an important evolutionary adaptation that confers on cells involved the ability to organize in higher structures and coordinate specific functions. One form of intercellular communications is cell-to-cell coupling mediated by gap junctions (reviewed by Goodenough et al., 1996). Gap junctions are specialized cell-to-cell contact domains of plasma membrane regions enriched in intercellular channels that are composed of two oligomers with each cell contributing one oligomer. The channels are formed by the extracellular interaction of two opposing hemichannels or connexons, resulting in low resistance pathways that span the plasma membrane of the opposing cells and bypasses the narrow extracellular space (gap). Each connexon consists of a hexameric structure composed of six integral membrane-spanning subunits called connexins arranged to create a central pore (Bruzzone et al., 1996). Earlier observations of electron micrographs of adjacent cells in tissue revealed regions where the plasma membranes of the two adjoining cells came in close proximity, separated by regions of constant width (Robertson, 1963). Further studies with extracellular heavy metals tracers such as lanthanum and ruthenium revealed a heptalaminar structure composed of the trilaminar plasma membranes of the adjoining cells and a heavily stained gap region of approximately 2-3 nm (Revel and Karnovsky, 1967). In contrast, the electron opaque element lanthanum did not permeate tight junctions, suggesting that intercellular gap junctions are distinct from tight junctions (Goodenough and Revel, 1970). Further studies involving freeze-fracture and thin sections electron micrographs showed gap junction regions as dense arrays of homogenous intercellular channels forming intramembrane particles on the

protoplasmic fracture face (P-fracture face) and a complementary arrays of depressions on the ectoplasmic fracture face (E-fracture face) (Goodenough and Revel, 1970; Peracchia, 1980). Within these cell-to-cell contact regions the number of transmembrane channels and implicitly the size of the gap junctions region vary considerably according to the tissue examined. Bennett and Goodenough (1978) reported that gap junction formation between the rod and cone cells of the retina may contain no more than 30-50 connexons. At the other extreme, granulosa cells were shown to form aggregation of plaques in excess of 2000 connexons with gap junctions of approximately 35-40 μm^2 (Larsen et al., 1981).

Gap junctions are ubiquitously present in vertebrate and invertebrate tissues being expressed by virtually every cell type except mature skeletal muscle cells, erythrocytes and spermatozoa (Dermietzel and Spray, 1993). Intracellular injection of peptides of known molecular size conjugated to fluorescence dyes revealed that the intercellular channels have a pore diameter of approximately 1.5 nm and a molecular exclusion size of up to 1 kDa. (Simpson et al., 1977; Flagg-Newton and Loewenstein, 1979; Brink and Dewey, 1980; Imanaga et al., 1987).

A commonly used descriptive fingerprint for gap junctions is the unitary channel conductance with reported values varying from 15pS for chicken Cx36 to 300 pS for human Cx37 (Veenestra et al., 1994a; Spray et al., 1999). Gap junction mediated intercellular communication (GJIC) involves the exchange between the participating cells of ions, small metabolites such as amino acids and vitamins, messengers molecules, low molecular weight trophic factors and high energy compounds, while excluding macromolecules such as proteins an polysaccharides (for review see Paul, 1995; Kumar and Gilula, 1996). The relative large pore size of the channel allows a bidirectional exchange of molecules that is gate-regulated by intracellular or extracellular physiological factors such as pH, Ca^{2+}, voltage, connexin phosphorylation, neurotransmitters, growth factors and tumor promoters (Spray et al., 1982; Saez et al., 1986; Beyer and Veenstra, 1994; Veenstra, 2000). Moreover, the degree of coupling between participating cells can be also regulated at the level of connexin expression, connexin recruitment and junction assembly. Lipophilic compounds such as octanol, heptanol, halothane an ethrane are known to intercalate into the lipid bilayer of the plasma membrane at gap junction regions and block junctional communication (White et al., 1985; Burt, 1989; Burt and Spray, 1989).

Gap junctions provide a form of intercellular communication between the coupled cells mediating many physiological functions in both excitable and non-excitable tissue cells. In

myocardium, gap junctions allow rapid current flow through excitatory tissue and action potential propagation that ultimately leads to synchronous contraction of the (Weidmann, 1952; Bar et al., 1965). The extracellular K^+ spatial buffering, an important homeostatic process required for unimpaired neuronal excitability, is also mediated by gap junction interconnected glial cells (Newman, 1985a,b). Another relevant physiological process that has allowed multicellular organisms to integrate and coordinate the activity of cells organized in tissues is the rapid propagation of Ca^{2+} waves between coupled cells. Such a mechanism appears to be involved in the coordination of ciliary beating in airway epithelium (Sanderson et al., 1994; Felix et al., 1998), coordination of secretion in pancreatic acinar and islet cells (Meda et al., 1991), modulation and maintenance of vascular tone (Christ et al., 1996) and trigger propagated contractions generated by focal stretch in cardiac tissue (ter Keurs and Zhang, 1997). In the nervous system of cold blooded animals, electrotonic synapses formed by gap junctions between neurons allow a much faster propagation of information than classical chemical synapses (Bennett, 1977). Gap junctions are also involved in tissue differentiation, (Bonner, 1989) embryonic development (Warner, 1985) and coordination of intercellular communication mediated by growth regulatory signals (Stagg et al., 1990). Following a series of studies where it was observed that compromising the integrity of gap junctions results in complete uncoupling of metabolic and electric intercellular communication, events that are present exclusively in cells that are known to express gap junctions, strongly suggests that gap junctions may be the only communication channels between cells (Barr et al., 1965; Gilula et al., 1972). Considering the critically important roles mediated by gap junctions, it is thus not hard to understand that events that would interfere with the functionality of gap junction communication can and do have deleterious effects on tissue or the whole organism. To the present day, a long list of diseases, ranging from deafness, cataracts, heart malformations or neuropathy have been linked with mutations that are either deleterious or perturb the normal channel physiology (Willecke et al., 2002)

IV.2 Connexins

In vertebrates, gap junctions are assembled from a multigene family of proteins named connexins (Beyer et al., 1987). Interestingly, it has been discovered that gap junctions in invertebrates are constructed of functionally homologous proteins (innexins) that belong to a

completely different gene family (Phelan et al., 1998). Originally, connexins were classified according to the molecular weight as determined by SDS-PAGE and the tissue of origin. However, with the increasing number of connexins discovered, soon it became apparent that some connexins are expressed in more that one tissue type (Paul, 1986) and connexin mobility on SDS-PAGE may be influenced by electrophoresis conditions or other intrinsic factors relate to the state of the protein, such as its phosphorylation state (Green et al., 1996). Today, connexin nomenclature appends the molecular weight, as predicted by its cloned DNA sequence, to the family named connexin (Cx) together with the species name (eg. mouse: mCx32, human: hCx31.2).

In 1986, Cx32 was the first connexin gene to be identified and isolated using a cDNA expression library for the 27 kDa rat liver protein (Paul, 1986). In the same year, Kumar and Gilula (1986) cloned its human cDNA counterpart using a hybridization screening protocol mediated by an oligonucleotide complementary to the carboxyl terminus (CT) of the mouse Cx32. The high sequence homology of the connexin genes (59% as reported by Willecke et al., 1991), enabled Beyer (1987) to screen a rat myocardial library with Cx32 cDNA at reduced stringency and identify a 43 kDa polypeptide, known to be mouse Cx43. Cx43 shares 43% overall homology with Cx32 and to the present day it is considered to have the highest tissue and cellular distribution out of all known connexins as it has been identified to be expressed in heart, testis, skin and brain (Bruzzone et al., 1996). Cx26 was cloned by Zhang and Nicholson (1989) from liver. The same technique was employed to identify other members of the connexins family, rCx31 found in rat placenta (Hoh et al., 1991b), mCx33 expressed by Sertoli cells (Chang et al., 1996), mCx37 and mCx40 found abundantly in lung tissue (Willecke et al., 1991; Hennemann et al., 1992). To date, with 95% of the human and mouse genomes sequenced, it is likely that all the connexin genes are presently identified.

According to the degree of homology and length of the cytoplasmic domain, the connexin family has been subdivided in 3 groups; α, β and γ. For example, γ connexins have a predictably larger cytoplasmic loop (CL) and carboxyl-terminus (CT) than α and β connexins. So far only three connexins have been classified in the γ subclass (Willecke et al., 2002). Traditionally connexins with a molecular weight of less then 32 kDa were identified as α connexins. Each connexin gene follows the same architecture as it contains one large 5' untranslated exon that is separated from the second exon responsible for the complete reading frame necessary for

connexin synthesis (de Maio et al., 2002; Willecke et al., 2002). However, a few notable variations have been identified: The Cx32 gene appears to have at least three alternative transcript isoforms, directed by alternatively splicing of the promoter region (Söhl et al., 2001). Cx36, a γ connexin, is the only currently identified member of the connexin family that has the reading frame interrupted by an exon (Condorelli et al., 1998). This raises the possibility that genetic diversity of connexins extends beyond the gene family, as it has been proposed that isoforms of Cx36 may be generated by alternative splicing. Finally γ Cx45 is the only connexin gene identified to date, that contains three exons (Jacob and Beyer, 2001). While exon 1 and 2 contain the 5' untranslated region, the entire coding region of γCx45 is located exclusively on exon 3. Based on the connexin genes high tissue specificity (Piechocki et al., 1999) and differential expression patterns during embryonic development and adult age (Bierhuizen et al., 2000), it has been speculated that the promoter region of the connexin gene family displays a complex genomic organization that includes additional yet to be identified elements (Piechocki et al., 2000; Fernandez-Cobo et al., 2001; Teunissen et al., 2002). Presently, about 19 different murine connexin genes have been identified with a molecular mass ranging from 26 kDa to 57 kDa. In humans, the family consists of 20 connexin genes with predicted molecular weights (MW) from 25 kDa to 62 kDa; the largest connexin gene known, coding for a 541 a.a. protein (Willecke et al., 2002). The orthologous connexin genes across species, as determined by comparison involving human and mouse connexin genes, do not necessarily encode for proteins with identical MW. For example the human counterpart of mCx26 has been identified as a 26 kDa protein (hCx26); the human ortholog of mCx29 is a slightly larger protein hCx30.9. Moreover, direct extrapolation to human subjects of physiological studies involving animal models is hampered by the observation that identical connexins form gap junctions associated with distinct functions in human and in mice. While Cx26 deficiency is incompatible with life in mice, mutations associated with hCx26 are responsible for sensorineural hearing loss in humans (Thonnissen et al., 2002).

Recently it was uncovered, that Cx43 is involved in PDZ domain interaction, domain known to mediate G-protein coupled receptor transduction (Giepman et al., 1998). Moreover, it appears that connexin expression can confer protection to cellular injury at a level comparable to the widely known proto-oncogene *bcl2,* independently of gap junction formation and cellular coupling (Lin et al., 2003). The use of animal models where one or more connexin genes were

TABLE 1. Mouse Connexin Multigene Family

Connexin	Predicted MW (kDa)	Sub group	Examples of tissue expression	Protein (aa)	Cyt. loop	C-term
Cx26	26.41	β	astrocytes, hepatocytes leptomeninges	226	35	18
Cx29	28.98	n.d.	oligodendrocytes, Schwann cells	258	30	50
Cx30	30.36	β	astrocytes, leptomeninges	261	35	55
Cx30.2	30.31	β	n.d.	278	n.d.	n.d.
Cx30.3	30.38	β	kidney, skin	266	30	65
Cx31	30.9	β	keratinocytes	270	30	65
Cx31.1	31.19	β	keratinocytes	271	30	70
C32	32	β	oligodendrocytes, Schwann cells	283	35	75
Cx33	32.86	α	Sertoli cells	286	55	60
Cx36	36.08	γ	neurons	321	100	50
Cx37	37.59	α	cortical neuroblasts, endothelium	333	55	105
Cx39	39.99	n.d.	n.d.	n.d.		
Cx40	40.41	α	endothelium, conductive myocardium	358	55	135
Cx43	43	α	astrocytes, heart, fibroblasts, vascular tissue	382	55	155
Cx45	45.66	γ	neurons, heart	396	80	150
Cx46	46.3	α	heart, lens fibers,	417	50	190
Cx47	47.6	γ	oligodendrocytes	437	105	155
Cx50	49.59	α	lens fibers, heart, kidney, testis	441	50	210
Cx57	57.14	α	ovaries	505	55	275

Table was compiled with data from (Söhl et al., 2001; Willecke et al., 2002 and Nagy et al., 2003b)

deleted or rendered nonfunctional, should allow a greater understanding of connexin biology as it is becoming evident that connexins are not only the functional unit of gap junctions, but are also involved in complex cellular events.

III.3. Three-dimensional structure of connexins and gap junctions

The molecular complexity of gap junctions has been slow and at times challenging to decipher, as early structural studies were hampered by technical limitations such as purification of gap junction proteins or successful protein crystallization protocols (Hand et al., 2002). Gap junction plaques are formed by connexons packed together into a quasi-hexagonal lattice that combine areas of short range packing disorder with long range hexagonal order (Hirokawa and Heuser, 1982). Successful crystallography investigation required that sufficient quantities of gap junction proteins be available, and the connexon hexamers are crystallized into high resolution three-dimensional crystals that consist of tightly packed hexagonal lattices (Hand et al., 2002). While the first problem was circumvented by the advent of tissue culture cell lines expressing sufficient quantities of the desired connexon isoforms (Elfgang et al., 1995), the development of a successful purification protocol remained the greatest challenge. Intensive efforts to purify gap junctions have allowed researchers to prepare useful crystals that were suitable for both structural and biochemical analysis. Therefore, as early as 1977 X-ray crystallography studies and EM analysis revealed the standard gap junction to have a torus-like structure that contained six cylindrical subunits oriented perpendicular to the cellular membrane (Caspar et al., 1977; Unwin and Ennis, 1984; Unwin and Zampighi, 1980).

An important advancement in understanding of gap junction secondary and tertiary structure was performed by Unger and colleagues (1999), using transfected baby hamster kidney cells expressing a truncated form of Cx43 (refer to Figure 1). The connexin protein, despite the absence of most of the carboxyl terminus (263 amino acid residues as opposed to the full length Cx43 that has 382 residues), was capable of assembling into functional junctions. Three dimensional reconstruction of the individual gap junction channel revealed that the connexon structure protrudes approximately 1.4 nm on the extracellular side and has an outer diameter of ~7.0 nm within the membrane region that narrows abruptly to an outer diameter of ~5.0 nm at the lipid membrane extracellular region, creating the impression of a "waist". Interestingly the

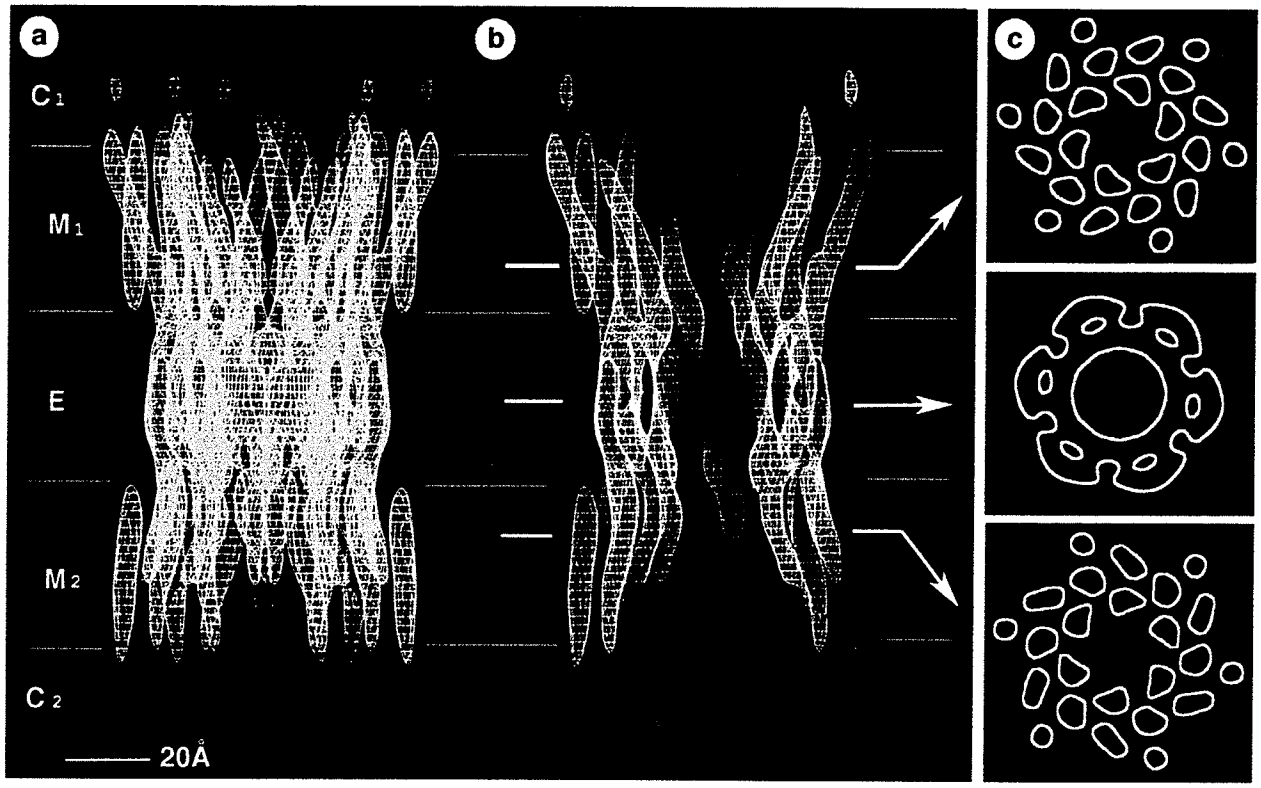

Figure 1. Projection density map of recombinant Cx43 gap junction, as derived by electron crystallography. (**a**) A full side 3D view of the intact channel and (**b**) a section through the channel interior. (**c**) Cross sections, parallel to the membrane bilayer, of the gap junction channel at level indicated by white arrows. The gap junction map is shown in reference to the boundaries of the membrane bilayer (M), extracellular space and the cytoplasmic space (C). The red asterisk marks the narrowest section of the channel interior (from Unger et al., 1999).

pore diameter follows a similar pattern of variability with respect to size. However, the pore itself does not contour to the outer size of the connexon. The internal diameter of the pore ranges from ~2.5 nm at the extracellular domain, thane narrows to ~1.5 nm diameter at the extracellular side of the lipid bilayer and then it opens to ~4.0 nm diameter at the cytoplasmic side (Hoh et al., 1991a, 1993; Lal et al., 1995; Unger at al., 1999). This study also confirmed the earlier hypothesis that docking of opposite hemichannels requires a mandatory 30° rotation between the partnering connexons (Unwin and Ennis, 1984; Perkins et al., 1988). The high degree of disorganization characteristic of the cytoplasmic domain of gap junctions has rendered this structure highly susceptible to beam damage and dehydration, conditions that are normally associated with X-ray crystallography (Baker et al., 1983; Sosinsky et al., 1998). To the present day, little is known about the ultrastructural organization of the cytoplasmic aspect of gap junctions.

IV.4. Connexins structure and topology

Hydropathy plots of the primary amino acid sequence of the connexin have predicted four hydrophobic amino acid domains separated by stretches of hydrophilic amino acids (Paul, 1986; Gilula, 1987; Goodenough et al., 1988). Further studies involving proteolytic enzymes and antibodies specific to small peptides in the primary sequence have shown that all connexin proteins traverse the cytoplasmic membrane four times and have such an orientation so that the carboxyl-terminus (CT) and amino-terminus (AT) are located within the cytoplasmic environment (Zimmer et al., 1987; Hertzberg et al., 1988; Bennett et al., 1991). By convention the connexins are devised in three structurally distinct domains (refer to Figure 2). The transmembrane domain, composed of four α-helical segments; M1, M2, M3 and M4, the cytoplasmic domain that contains the CT and AT, as well as a cytoplasmic loop (CL) that joins M2 and M3 transmembrane segments and the extracellular domain, defined by two loops E1 and E2 are comprised of two β-sheet 33-38 amino acid stretches that connect M1 to M2 and M3 to M4 (Unger et al., 1999). Typically the amino acid primary sequence of the CL and CT display the highest variation between different connexins, while E1 and E2 are very well conserved across the connexin protein family (Dahl et al., 1994).

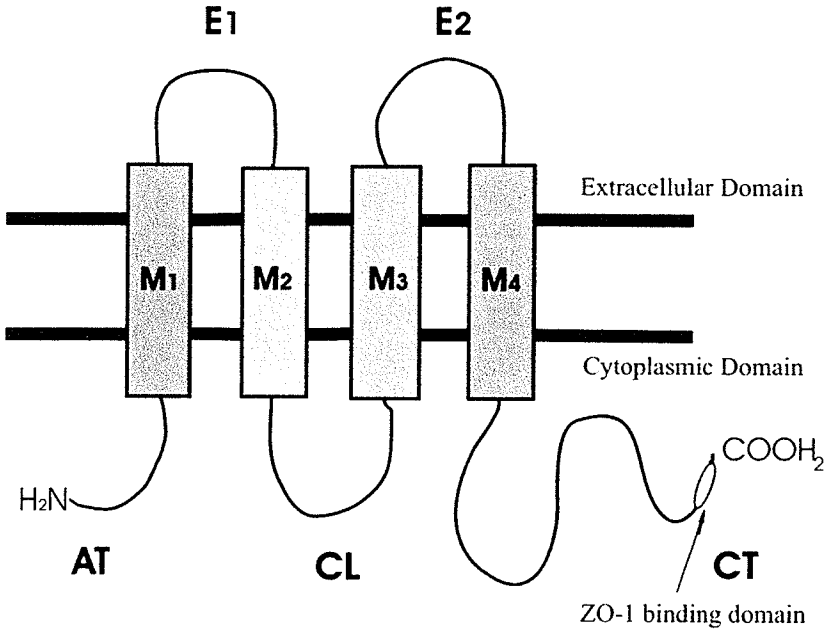

FIGURE 2. The topological arrangement of the transmembrane connexin protein at the plasma membrane. Extracellular loops 1 and 2 (E1 and E2), transmembrane domains 1-4 (M1-M4), amino terminus (AT), cytoplasmic loop (CL), and carboxyl terminus (CT). (Based on the review by Goodenough et al., 1996)

IV.5. Secondary structure of the extracellular domains

The extracellular domains are highly conserved regions that play a crucial role in docking (White et al., 1994a), heterotypic interactions (Goodenough et al., 1996) and voltage gating of gap junctions (White et al., 1994b;, White et al., 1995). The observation that both E1 and E2 extracellular loops are composed of significant continuous stretches of hydrophobic amino residues was unexpected, considering the extracellular exposure of this domain to an aqueous environment. Given the short length of the peptides, it was suggested that a β-sheet conformation for E1 and E2 is the only arrangement compatible with channel formation (Dhal et al., 1994).

Following the observation that the loss of any of the six highly conserved cysteine residues present in E1 and E2 results in loss of channel function, suggested that intramolecular disulfide bridge formation between E1 and E2 is "sine qua non" requirement for viable gap junction formation (Dhal et al., 1992, Foot et al., 1998). Support for this hypothesis came from the observation that gap junction formation can be rescued by insertion of two cysteine residues in a tandem fashion, one in each extracellular loop (Foote et al., 1998). Analysis of intact and

proteolysed connexin protein mobility in reducing and non-reducing SDS-PAGE have revealed that while there is supporting evidence for the existence of disulfide bonds between E1 and E2 of a single connexin, no such connections occurs between connexin subunits that form the channel (John and Revel, 1991; Rahman and Evans, 1991).

The requirement for precise alignment between the cysteine residues becomes evident with the observation that Cx31, characteristic for its unique spacing of the cysteine residues on the extracellular domains, is incapable of forming heterotypic functional channels (Hoh et al., 1991b). Recently, Unger et al. (1999) determined that the extracellular domain density map of Cx43 "was in distinct contrast to the characteristic signature for α-helices in cross section" and it was concluded that at least a portion of the polypeptide of E1 and E2 does not adopt a α-helical conformation, suggesting the presence of an anti-parallel β-sheet folding pattern for E1 and E2.

The presence of anti-sense β-sheet extracellular domains that are structurally reinforced by three disulfide bridges between the E1 and E2 loops of a single connexin would allow the extracellular domain to achieve the proper conformation and to interdigitate with its counterpart in the opposing connexons (Foote et al., 1998). This "lock and key" arrangement of the six protrusions that form each hemichannel would drastically increase the available surface area, and allow the formation of potentially large numbers of H-bonds, and other types of attractive interaction between the partnering connexons (Sosinsky, 2000). Such an arrangement would explain the relative harsh chaotropic conditions required to separate the gap junction structure to its individual hemichannels, as well as the observation that the docking domains of compatible connexons are able to form a uniformly impermeable seal that guards against the leakage of small ions between the gap junction lumen and the extracellular space (Stauffer et al., 1991).

Studies involving both mutational analysis and chimeric constructs have determined that E2 domain is responsible for heterotypic selectivity between connexins (White et al., 1995). The ability of Cx46 to form heterotypic channels with Cx43, was eliminated by the substitution of the E2 domain of Cx46 for its Cx50 counterpart (Cx46 is unable to form functional channels with Cx50). Reciprocally, the replacement of the E2 domain of Cx50 with the E2 domain of Cx46 enabled the chimeric $Cx50E_246$ to readily form functional channels with Cx43 (White et al., 1994a). Thus it has been suggested that the ability of chimeric connexin to form heterotypic gap junctions is dictated not by an incompatibility of the extracellular domains of the two connexons as by the inability of the two extracellular domains E1 and E2 to form functional disulfide bonds

(Foote et al., 1998). While the extracellular domains of gap junctions are primarily responsible for the docking interaction of partnering connexons, it appears that at least E1 domain is involved in the regulation of voltage gating of the channel (Suchyna et al., 1993).

IV.6. Secondary structure of the transmembrane domains

With respect to membrane topology, connexins are probably one of the best characterized channel forming proteins (Evans and Rahman, 1989). However, for a long time the information available with respect the 3D arrangement of the conserved trans-membrane domains remained speculative and at times contradictory (Sosinsky, 2002). It was speculated that, like many other integral membrane proteins, the four trans-membrane domains are constrained to adopt the thermodynamically favorable α-helical conformation, with one or more peptide segments lining the pore (Cascio et al., 1990). Recently, this was confirmed by Unger et al. (1999) following an electron crystallographic reconstruction of a truncated Cx43 gap junction channel (Figure 1). They were able to indisputably confirm the α-helical arrangement of all trans-membrane domains, and were also able to determine that the pore structure is lined along its entire length by one of the trans-membrane segments, while a second domain contributes at the cytoplasmic pore opening region. Unfortunately, the physical limitations associated with the technique used, precluded them to assign any of the four trans-membrane domains (M1-M4) to the specified position. Nevertheless, it was widely believed that the main pore lining domain is likely to be M3, since it is the only trans-membrane domain that has an amphipathic nature, and hence capable of forming aqueous channels (Milks et al., 1988).

In 1997 Zhou et al. attempted to identify the exact amino acids residues responsible for pore lining by using mutation analysis studies of a chimeric connexin constructs ($Cx32E_{1}43$ in which the sequence representing the extracellular loop E1 of Cx32 was replaced by the corresponding sequence of Cx43) capable of forming constitutively opened hemichannels with Cx46 in non paired Xenopus oocytes. The elegant premise of their investigation dictated that if the pore lining amino acids residues are one at a time mutated to cysteine residues, treatment with a membrane non-permeant thiolating agent such as maleimido-butyryl-biocytin (MBB), would disrupt the conductive properties of the wild type mutant hemichannel. It was thought that two possibilities for the thiol reagent block of gap junction conduction exist: steric block of the hemichannel, or by an induced conformational change resulting from the direct interaction between the connexins

and the thiol reagent (Zhou et al., 1997). The observation that the degree of inhibition is dependent on the size of the thiol reagent and that the mutated amino acids could be reached only by way of the pore seems to support the former hypothesis (Zhou et al., 1997). Much to the authors surprise it was revealed that the M1 segment (believed to be too short to encompass the complete channels lining) is the primary contributor to the channel region, while inconclusive results were obtained for M3, previously thought to be the main candidate for this function.

Recently, an interesting development has been achieved by Skerrett et al. (2002) who reproduced Zhou et al. experiment, however with a few important distinctions. First, their study used Cx32 expressing *Xenopus* paired oocytes, capable of forming functional gap junctions. Second, there was no bias in deciding what amino acids should be investigated as they probed a large number of amino acids on all four trans-membrane domains. Finally, in their assay system the introduction of the thiol reagent was achieved from the cytoplasmic opening of the pore, following a complete wash-out of the reducing environment characteristic of the cytosol. While the mutation of residues in all segments interfered with gap junction conductivity, it become evident that M3 is the primary pore lining segment, while M2 may contribute to the pore while in the open state. An important finding of the study revealed that all amino acids residues thought to belong to the M3 pore lining segment are hydrophobic, thus creating a precedent in the family of "aqueous channels" (Skerrett et al., 2002). The existence of a predominantly hydrophobic channel that allows the passage of hydrophilic small molecules and ions, departs gap junction channel physiology from the traditional ion channel, and implicates that a different set of mechanisms govern passage of ions and molecules through these channels (Skerrett et al., 2002).

It is now believed that the passage of ions and metabolites between coupled cells is not nonspecific and that connexins have high degree of selective permeability (Bevans et al., 1998). It has been reported that Cx32 and Cx43 have over 100-fold difference in their permeability to ATP and ADP, anionic molecule of similar size, despite almost identical permeability to anionic dyes (Goldberg et al., 1998). Such discrepancy in selectivity can not be explained in terms of size and charge alone. Thus the presence of a differential binding system between permeates and the pore structure that would involve weak intermolecular interactions was proposed (Skerrett et al., 2002).

IV.7. Secondary structure of the cytoplasmic domains

The cytoplasmic domain (CD) is the term used to refer to the cytoplasmic exposed regions of the individual connexin protein, such as the amino acid terminus (AT), cytoplasmic loop (CL) and the carboxyl terminus (CT). However, recently it has been also used to describe the cytoplasmic aspect of an entire connexon. Due to the flexibility and relative disorder of the CD, there is a paucity of information with respect to the 3D arrangement of this structure (Sosinsky et al., 2000). The CD represents the region of greatest amino variability within the connexin family, with CL and CT conferring most of the diversity among connexin subtypes (Duffy et al., 2002). According to recent connexin topography the CD can account for as little as ~33% in Cx26, to more than half the size of the connexin protein as it is the case with Cx43 (~61%) and other larger MW connexins. The exposure of this region to the cytoplasmic environment and hence to a whole plethora of cellular factors, makes the CD region a good candidate for involvement in tissue specific functions involving protein-protein interactions. In recent years a series of cytoplasmic binding partners, some of which contain known signaling domain motifs have been shown to interact with the CD region. Some of the first proteins identified to be localized at gap junctions plaques are the tight junction proteins zonula occludens (ZO-1) reported to interact with Cx43 (Toyofuku et al., 1998). Occludin and proteins belonging to the claudin family, both were reported in association with Cx32 (for review see Duffy et al., 2002).

The discovery that Cx43 associates with the non-receptor tyrosine kinase proto-oncogenic signal protein Src, suggests that connexins may play secondary roles that extend beyond just intercellular channel formation. Src is an effector molecule implicated in a large number of pathways involving mitogen-activated protein kinase (MAPK) and protein kinase C (PKC) (Loo et al., 1995; Batias et al., 1999). While the exact role of src at gap junction plaques is not well understood, reports suggest that src phosphorylation of tyrosine residues 247 and 265, located on CT region of Cx43 are required steps in order to inhibit intercellular communications in oocytes expressing Cx43 (Kanemitsu et al., 1997; Loo et al., 1995). However, it appears that src may be implicated in more than just gating regulation of gap junction channels as it was reported that binding of c-src to Cx43 interferes with the interaction between ZO-1 and Cx43 (Toyofuku et al., 2001).

IV.8. Gap junction gating

While gap junctions mediate the transfer of small molecules between coupled cells, by no means should they be perceived as passive conduits, but as dynamic filters that are constantly modulated by local environmental factors. Regulation occurs through modification of protein conformation by voltage and/or changes in the intracellular environment. Uncoupling is primarily a protective mechanism that enables healthy cells to isolate themselves from damaged neighbors in a fashion that would minimize injury. This phenomenon, where cells around an injured area are sealed over after the potential for injury is present is known as "healing over" and it was observed more than a hundred and twenty years ago by the German physiologist Engelmann who stated that "Die Zellen leben zusammen, aber sterben einzelen"; cells live together but die alone (Engelmann, 1875). Interestingly this chain of events is initiated by the "altruistic" behavior of the damaged cells, as gap junction closure is usually mediated by factors, such as pH and Ca^{2+}, at physiological levels that are incompatible with life and are synonymous with apoptosis (De Maio et al., 2002).

Lowering of the cytosolic pH (Liu et al., 1993; Morley et al., 1996), elevation of the cytoplasmic Ca^{2+} concentration (Baux et al., 1978), some types of phosphorylation (Ismailov and Benos, 1995) and trans-junctional voltage gradients are all parameters that affect the opening state of gap junctions. It has been proposed that at least three mechanisms are associated with the modulation of the opening state of gap junctions (Skerrett et al., 2002). A docking gate that would prevent the hemichannels to open unless their docking connexon partner is present, a chemical gate and a transjunctional voltage sensitive gate (V_J). It has also been postulated that gap junctions may be sensitive to a fourth factor, the transmembrane voltage potential (V_m), however this has not been conclusively demonstrated (Trexler et al., 1996; Bario et al., 1997). Channel gating sensitivity to the above mentioned factors has been demonstrated to also occur at nearly physiological calcium and hydrogen ion concentration. This suggests that modulation of the intercellular permeability by means of gap junction closure can also occur in healthy cells and it may play a significant role in normal cellular physiology (for review see Peracchia et al., 2000).

IV.9. Chemical gating

The CT domain has been associated with the chemical gating behavior of gap junctions induced by intracellular pH, insulin or v-src mediated phosphorylation (Swenson et al., 1990). It was observed that intracellular acidification following myocardial ischemia is associated with reversible closure of Cx43 and hence uncoupling of the myocytes (Muller-Borer et al., 1995). In a series of experiments involving mutational analysis it was determined that the truncation of the CT region of Cx43 impaired pH gating (Liu et al., 1993). Interestingly however, following the coexpression of the CT domain together with the truncated form of Cx43, pH sensitivity was partially restored (Morley et al., 1996; Ek-Vitorin et al., 1996). Therefore it was proposed that acidification-induced uncoupling mediated by Cx43 is governed by a "ball-and-chain" model, where a decrease in pH induces a conformational change in CT, which physically blocks the cytoplasmic opening of the connexon pore (Morley et al., 1996). This hypothesis was further supported by the observation that CT terminus contains a relatively conserved proline rich sequence commonly found in left-handed α helices, often involved in protein-protein interactions. (Adzhubei et al., 1994; Williamson et al., 1994; Cohen et al., 1995; Yu et al., 1994). It is important to mention that the exact requirements for the proposed mechanism appear to differ for different chemical stimuli. It was observed that deletion of Cx43 CT at an amino position that completely abolishes the effect of acidification does not interfere with v-src-mediated phosphorylation gap junction gating (Zhou et al., 1999). On the other hand it appears that the gating process involves additional factors that can not be explained by simple interaction between the CT domain and the cytosolic aspect of the pore opening. Calero et al. (1997) reported that by injection of excess exogenous Cx43 CT domain acidification-induced uncoupling of non-truncated Cx43gap junctions was disrupted. Such an event would not be consistent with a direct protein-protein interaction, where the CT domain would bind to a specific cytoplasmic region, as an excess of CT domain should enhance, not interfere with the closing of the wild-type channel. The apparent competitive inhibition exerted by the exogenous CT region suggests the possible participation of a cytosolic intermediary molecule in pH gating of Cx43 gap junctions (Calero et al., 1998).

IV.10. Voltage gating(V_J)

The removal of the carboxyl terminus of Cx43, while interfering with the pH induced gating of gap junctions, does not affect the voltage sensitivity of the channel (Liu et al. 1993). Further studies have revealed that pH induces uncoupling by activating a slow gating mechanism that functions independently of the V_J gating mechanism. However, an interesting question still remains whether the chemical and voltage induced gating mechanisms operate in an independent fashion from each other. While it is clear that the V_J gate operates independently of the presence of chemical factors, it was not clear whether the chemical gate is modulated independently of the state of the V_J gate (Bukauskas and Peracchia, 1997).

The evidence for the presence of distinct gating mechanisms induced by voltage or cellular acidification also comes from the observation that while the gap junction channel rapidly flickers between a main conductance state and a lower conductance state, in the presence of trans-junctional voltage, intracellular acidification completely induces junctional blockade (Weingard and Bukauskas, 1993; Bukauskas and Peracchia, 1997) Accumulated evidence suggests that the voltage sensor in gap junctions is not a localized structure but constitute the concerted interaction between molecular domains that line the pore structure and other domains that do not, that result in a global conformation change that constrict the pore (for review see Skeret et al., 2000). The exact mechanism responsible for voltage gating is yet to be fully elucidated, however it is evident that more than one region of the connexin molecule is involved in this process, as it has been observed that the voltage gating behavior can be affected by mutations of at least seven distinct regions (AT, M1, E1, M2, E2, CL and CT) (Rubin et al., 1992; Verselis et al., 1994; Oh et al., 1997; Skerrett et al., 1998; Haubrich et al., 1996; Ressot et al., 1998; White et al., 1994b; White and Bruzzone, 1996; Skerrett et al., 2002). Another possible mechanism proposed by Dahl (1996) would involve a pore-plugging molecule or a diffusible membrane-bound factor that would physically obstruct the pore opening. However, some characteristic of the voltage mechanism do not seem to be explained by this hypothesis. The mechanics involved in the diffusion of such factors does not reconcile with the fast kinetics (~2 ms) of gap junctions closure, and there is no supporting evident that voltage gating characteristics are drastically altered by different expression systems (Dahl, 1996).

Recently one form of Charcot-Marie-Tooth disease was associated with deficient gating properties of Cx32 gap junction in response to trans-junctional voltage (V_J). In this instance

disruption of the voltage gating properties of otherwise seemingly functional gap junctions capable of forming competent channels, appears to be of sufficient pathological significance (Oh et al., 1997; Ressot et al., 1998).

IV.11. Multimeric connexin interactions

With the constant addition of new connexins to the gap junction family, it soon became evident that some cells may and do express more than one connexin isotype, thus allowing for several possible ways in which a connexin can contribute to the formation of gap junction channels (for review see Goodenough et al., 1996)`. First, a connexon can be formed by six identical connexin proteins (homomeric channel) or by the interaction of at least two distinct connexins (heteromeric channel). This arrangement would therefore impact on the possible types of intercellular channels that could be generated from the interaction of heteromeric or homomeric connexons. Second, the association of two homomeric hemichannels composed of the same connexin subunits would yield a homotypic channel. However, if the two opposing connexons have a distinct makeup with respect to connexin composition two generic types of channels can exist. Gap junctions can be formed by two homomeric hemichannels that are composed of different connexins, resulting in a heterotypic/homomeric interactions, or the assembly of two heteromeric channels composed of distinct connexins species would generate a heterotypic/heteromeric channel (refer to Figure 3). The existence of multiple connexin proteins expressed within the same cell has been demonstrated in a large number of cells such as, hepatocytes, lens fibers, cardiac myocytes, keratinocytes, macroglial cells and possibly neurons (for review see Willecke et al., 2002). It appears that cellular expression of multiple connexins is the rule more than the exception, as only pinealocytes are the only cell type known to express Cx26 as the sole connexin species (Saez et al., 1991).

It was observed that gap junction plaques can either be homogenous with respect to the type of connexin present (i.e. only homomeric connexons are present at a specific gap junction plaque), or have a heterogeneous makeup where both homomeric and heteromeric connexons are present within the same plaque (Nicholson et al., 1987; Traub et al., 1989). The homomeric and heteromeric connexons at a heterogeneous plaque could be either randomly distributed within the gap junction plaque, or the two types of connexons can be segregated to distinct areas (Risek et al., 1994; Spary et al., 1991; Laird et al., 1992). The existence of heterotypic channels has been

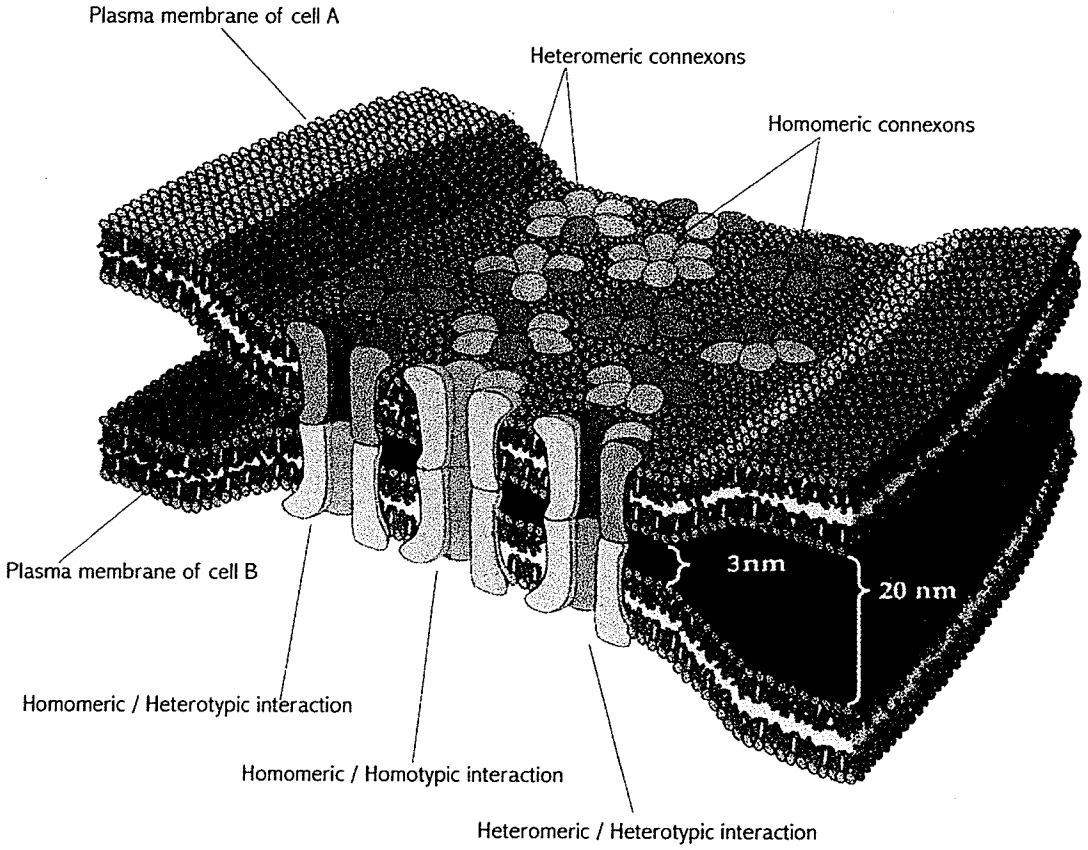

FIGURE 3. Schematic representation of the large number of possible interactions in gap junction channel formation between cell A and cell B. Each individual color represents a distinct connexin (modified from Neuroscience second edition, Dale Purves, Sinauer Associates Inc. pg.101)

successfully demonstrated in double whole cell patch clamp studies of paired *Xenopus* oocytes, where each oocyte expressed a different connexin, and it was observed that some but not all heterotypic combinations can form (Werner et al., 1989; White et al., 1994). On the other hand, the existence of heteromeric channels is inheritably more difficult to demonstrate, since there are no reliable methods to ascertain that single connexons are indeed comprised of two or more different proteins. To date, the most reliable evidence that favors the existence of mixed hexamers, comes indirectly from electrophysiological studies of cells expressing two different connexins. In these experiments single channel studies have revealed a large number of different conductance intercellular channels (Brink et al., 1997). Such an observation would be difficult to reconcile in the absence of heterogeneous population of heteromeric connexons (Steinberg, 1998).

As it can be envisioned the number of heterotypic/heteromeric channels types possible with only two connexins is huge. It has been predicted that if no six fold symmetry axis is assumed and the location of the two connexins within the hemichannel generates distinct channel characteristics, then in any individual cell there are 64 possible connexon types, and two cells would be able to form 4096 heterotypic/homomeric interactions (Beyer et al., 1997). Therefore, the chances of forming a homotypic gap junction channel are diminishingly small 1/4096 or (0.0002). As it is known today this estimate does not reconcile with the actual number of homotypic gap junction channels found in a cell (Beyer et al., 1997), suggesting that the assembly of connexin subunits into connexons is not a random process and cells have the ability to actively control this process. Cells regulate the assembly of multimeric connexins as a potential strategy of modulating the intercellular communication characteristics between coupled cells (Das Sarma et al., 2001). The physiological characteristics of hemichannels are dependent on connexin composition (Diez et al., 1999; Martinez et al., 2002). Therefore, the electrophysiology of heterotypic gap junctions is often asymmetric and results in rectifying gap junction channels (Suchyna et al., 1999). The conductance properties of such heterotypic gap junctions can not be predicted from the corresponding homotypic connexons electrophysiological profile (Bukauskas et al., 1995).

IV.12. Gap junction synthesis and assembly

It is known that most cells express more than one connexin type, with some connexins ubiquitously expressed in a variety of tissues, while others such as Cx33 present a highly restricted distribution (for review see Willecke et al., 2002). Moreover, the high turnover rate of gap junctions, some less than 2 hours (Laird et al., 1995), suggest a highly active protein synthesis, oligomerisation and transport mechanism in cells capable of GJIC (Beardslee et al., 1999). In addition, evidence is accumulating that the connexin expression levels can be drastically influenced by physiological states such as: injury, cellular proliferation or various signaling factors (Spray et al., 1987; Rosenberg et al., 1992; Bruzzone et al., 1996). It appears that the exquisite regulation of gap junction production is the result of both transcriptional and translational mechanisms. For example, just prior to parturition Cx43 gap junction are rapidly up regulated, an event mirrored by an increase in Cx43 mRNA (Lang et al., 1991; Winterhager et al., 1999). During hepatocarcinogenesis however, Cx26 and Cx32 protein levels are not paralleled by a similar change in mRNA levels (Neveu et al., 1995).

Expression of functional connexins capable of assembling into viable gap junctions has been achieved in cell free systems (Falk et al., 1997). Moreover the assembly of heteromeric connexons was not impaired in microsomal systems (Falk et al., 1997). It is believed that the specificity of connexins assembly rests with the connexin subunit as it was observed that out of a large number of heteromeric gap junctions possibilities, only the hemichannels composed of compatible subunits were present (Beyer et al., 1997). However, the exact location of connexin assembly into multimeric hemichannels remains controversial.

While it was proposed that connexins are atypical among other multimeric proteins, as evidence suggested *trans*-Golgi network as the potential assembly site (Musil and Goodeneough, 1993; Koval et al., 1997), it was revealed that connexins can also assemble in the endoplasmic reticulum (Kumar et al., 1995; George et al., 1999).

IV.13. Connexins in diseases

In most organisms formation of GJIC begins during early stages of embryonic life and it is believed that the establishing of GJIC represents a critical stage in the coordination of complex events such as tissue differentiation and pattern formation (Guthrie et al., 1984; Guthrie and Gilula, 1989, Valdimarsson and Kidder, 1995). Thus, it should come as little surprise that the

blockade of GJIC either chemically, or as result of connexin mutations, can have at times serious pathological consequences, as summarized in Table 2. In the mouse, Cx37 deficiency causes maternal infertility (Goodenough et al., 1999), Cx26 has been linked to decreased glucose transport in syncytiotrophoblasts in rat placenta (Gabriel et al., 1998). Cx26 was demonstrated to be highly expressed in human cohlear cells, and mutations in the Cx26 gene have been associated with autosomal recessive non-syndromic deafness in humans (Scott et al., 1998). It has been suggested that Cx26 mediated GJIC are involved in recycling of K^+ ions back to endolymph following stimulation of the sensory hair cells (Kelsell et al., 1997). The role of gap junctions as passageways for ions and metabolite transport is reflected in the morphology of the crystalline lens of the eye, a structure devoid of blood vessels due to its role and dependent on the diffusion of oxygen and nutrients from the surrounding vascularized epithelia. Deficiency of Cx46 and Cx50, the only known connexins expressed in the lens, leads to cataracts (Shiels et al., 1997; Pal et al., 2000). A peculiar aspect of gap junction associated diseases is the apparent expression of a pathological phenotype only in selected tissues or cell types, regardless of the fact that some connexins are widely expressed by more than one cell type. Probably the most notable example is human Cx32, expressed by Schwann cells and oligodendrocytes, that when mutated it adversely impacts only on the peripheral nerves and not the liver where it is also highly expressed (Ressot and Bruzzone, 2000).

Charcot-Marie-Tooth (CMT) disease is the most common inherited peripheral neuropathy, with an estimated frequency of about 1 in 2500 births (Harding, 1995). Clinically, the disease is characterized by progressive weakness of the distal leg, absent or diminished deep tendon reflexes and variable degrees of sensory loss (Skre, 1974). The onsets of symptoms appear to vary greatly, ranging between the first year and the sixth decade of life. The symptoms associated with CMT arise in a size dependant fashion, meaning that the largest nerves which have thicker myelin sheets are affected first (Abrams et al., 2000). The clinical features can differ in severity among affected patients of the same family and, in some forms of CMT, 10–20% of individuals identified with a mutated gene present no symptoms, but only abnormalities at neurological and electromyographic examinations.

TABLE 2. Phenotypes of Cx-deficient mice or human mutations

Connexin	Knock-out and mouse mutations	Human mutations
Cx26	Death at the embryonic day 11 due to decreased trasplacental transport of glucose analogous	Hearing loss
Cx30		Disorders of epidermal keratinization. Dominant hearing loss, Clouston's hydroticectodermal dysplasia, skin disease, hair loss, hail defects, and often mental retardation.
Cx30.3		Dominant: skin diseases
Cx31	Transient placental dysmorphogenesis	Recessive: nonsyndromic moderate-profound sensorineural hearing loss, skin disease and neuropathies.
Cx32	Normal appearance and behavior. Peripheral premature neuropathy. Lower hepatic glucose mobilization in response to electrical stimulation. High incidence of spontaneous or chemically-induced liver tumors.	Type X of Charcot-Marie-Toot characterized by myelin disruption and axonal degeneration of peripheral nerves.
Cx36	Weaker and greatly restricted spatially synchronous activity of inhibitory networks in neurocortex. Deficient in early visual transmission.	Linked to a juvenile form of myoclonic epilepsy and an inherited abnormality in sensory responses associated with predisposition to schizophrenia.
Cx37	Infertility in females	
Cx40	Major alterations of heart function. Development of arrhythmias dependent on the genetic background	
Cx43	Death at perinatal period. Malformation of the conus region overlying the pulmonary outflow tract. Failure at the pulmonary gas exchange. Heart embryonic alteration. Delayed ossification and osteoblast dysfunction.	Visceroatrial heterotaxia.
Cx45	Death around embryonic day 10 due to heart failure. Impairment of epithelial-mesenchymal transformation of the cardiac endothelium. Failure to develop a smooth muscle layer surrounding the major arteries of the embryo proper.	
Cx46	Development of senile cataract after 3 weeks of age due to aberrant proteolysis of crystalline proteins. Microphtalmia.	Autosomal dominant congenital zonular pulverulent cataracts.
Cx47*	Sporadic vacuolation of nerve fibers.	
Cx50	Development of cataracts during the first week after birth.	Congenital autosomal dominant zonular pulverulent cataracts.

Table is from De Maio et al., 2002, except (*) from Odermatt et al., 2003.

In general, the disease progresses slowly over the years, but can lead to severe functional impairment. Current treatment is only symptomatic and is based on physical therapy and/or corrective orthopedic surgery. Based on electrophysiological findings two major forms of CMT have been classically distinguished: Type I (CMT1), a demyelinating neuropathy associated with decreased nerve conduction velocity, and Type II (CMT2), a non-demyelinating neuronal disorder with normal or near normal nerve conduction velocity. The most common form of Charcot-Marie-Tooth, CMT1A, is an autosomal dominant neuropathy, associated, with duplication or mutations in the gene encoding myelin protein 22 (Nelis et al., 1999). Mutations in another major component myelin protein gene have been linked to CMT1B, a rare form of the disease (Suter et al., 1995).

Studies on families affected by a form of CMT, appeared to be inherited primarily by male family members via maternal, but not paternal transmission, revealed linkage to a region near the centromer of chromosome X (Fischbeck et al., 1986). Recent studies have revealed that in reality there are at least three forms of CMTX, characterized by either dominant or recessive inheritance pattern (Ionasescu et al., 1996). The dominant CMTX form is associated to Cx32 mutations and represents approximately 90% all X-linked cases, and is the second most common form of CMT (Hahn et al., 1990). Dominant CMTX is characterized by the early appearance of clinical symptoms and in males, by a more rapid progression to moderate disability. The dominant form accounts for 10–20% of all cases of CMT and is probably the second most frequent cause of hereditary motor and sensory neuropathies after CMT1A. To date, there is still debate whether the dominant form of CMTX and the recessive forms (CMTX2 and CMTX3) are demyelinating (type I) or axonal (type II) forms of CMT, as both demyelization and reduced nerve conduction velocities have been observed in CMTX patients (for review see Ressot and Bruzzone, 2000).

IV.14. Gap junctions in central nervous system

The brain! Out of all other organs no other has been so authoritatively deterministic of whom we are as human beings. It is hard to believe, as it was for Aristotle, more than 2000 years ago who considered that intelligence lay in a person's heart, that 1.5 kilograms of flaccid matter and convoluted folds is indeed responsible for *La Boheme, Divina Commedia* or our desire and capacity for scientific research. Hence, it should come at no surprise that to the present day the quest to determine the special and functional relationship of gap junctions in the brain has been

an arduous and at times a slow process that had to be precluded by advances in understanding the morphological complexity and neural architectonics of the brain.

Out of all 19 mouse connexins known today, at least ten (Cx26, Cx29, Cx30 Cx31, Cx32, Cx36, Cx37, Cx43, Cx45, Cx47) have been either identified at ultrastructurally defined neuronal and glial gap junctions, or were reported to be expressed within the central nervous system (CNS) (Willecke et al., 2002). Early observations that connexins in the brain are expressed in a heterogeneous spatial and temporal fashion, combined with functional studies in diverse neural cell type have revealed that intercellular coupling involving macroglia or neurons are specific events mediated by distinct connexins subtype. In an attempt to reconcile the proposed theory of physiological and metabolic compartmentalization of various neural components as dictated by local homeostatic factors, with the apparent expression of different connexins by various cell types, Mugnaini (1986) first proposed that cells in CNS form a panglial syncytium. It was suggested that astrocytes would form both homologous junctions with other astrocytes (A/A coupling) as well as heterologous junctions with neurons (A/N coupling). It was also proposed that neurons are restricted only to interneuronal junction formation (N/N coupling), while oligodendrocytes would be involved in little if any homologous inter-oligodendrocytic gap junction formation (O/O coupling). At the time it was believed that astrocytes, oligodendrocytes and neurons express distinct subsets of connexins, however a great deal of controversy persisted due to conflicting reports regarding the identity of the connexins expressed by different neural cells, as well as the exact coupling partnership existent between cells involved (for review see Nagy and Rash, 2000; Rozental et al., 2000).

In an attempt to identify the exact subtype of connexins expressed by various cells in the CNS, extensive studies involving immunocytochemical as well as grid map freeze-fracture analysis, attempted to eliminate the vague criteria for cellular identification at ultrastructural level, one factor believed to have fueled the controversy behind this issue (Nagy et al., 1997; Nagy et al., 1999; Nagy et al., 2001; Rash et al., 1997; Rash et al., 1998). It was determined that there is strong support for the existence of a functional panglial syncytium and it was confirmed that astrocytes express Cx26, Cx30 and Cx43 as the main astrocytic connexin (Rash et al., 2000). Finally, compelling evidence emerged that oligodendrocytes express Cx32, while neurons express Cx36 (Rash et al., 2001). The evident segregation of connexin subtypes to different cell types raised new questions concerning the permissiveness of gap junction formation in the CNS

and its implication on intracellular communication (The available data concerning CNS gap junction compatibility is presented in Table 3).

	Cx26	Cx29	Cx30	Cx31	Cx32	Cx36	Cx37	Cx43	Cx45	Cx47
XeCx38	-		-		-		+	+	-	
Cx47										+
Cx45	-		+	-	-		+	+	+	
Cx43	-		+	-	-		+	+		
Cx37				-	-		+			
Cx36						+				
Cx32	+	-	+	-	+					
Cx31	-			+						
Cx30	+		+							
Cx29		-								
Cx26	+									

TABLE 3. The formation of functional heterotypic/homomeric gap junctions in CNS as dictated by connexins compatibility. XeCx38, it is the endogenous *Xenopus* oocytes connexin. (table compiled with data from Manthey et al., 2001; Nagy et al., 2003c; White et al., 1995; White and Bruzzone, 1996; Willecke et al., 2002)

IV.14.a. Neuronal gap junctions

The first evidence for intercellular electrical coupling in neural tissue came from the observation made by Furshpan and Potter (1959) that the synaptic transmission from the presynaptic lateral giant fiber to the postsynaptic giant motor fiber displayed a delay of about 0.1 ms, an interval much less than the 0.5 ms normally associated with traditional synaptic transmission mediated by chemical messengers in cold blooded animals. A few years later,

Robertson (1963) provided the first conclusive ultrastructural evidence for the existence of gap junctions with the observation that pre- and postsynaptic membranes of the synaptic disk between the neuronal cells of the gold fish are separated by specialized intercellular junctions that are different from chemical synapses. At the time electrical synapses were considered a primitive form of inter-neuronal communication, evolutionary replaced in higher animals by the more advanced chemical synapse (for review see Nagy and Rash, 2000; Rozental et al., 2000). Recently however, it was reported that mixed synapses (both chemical and electrical) are more abundant that previously thought and it was proposed that the bidirectional communication offered by gap junctions would somehow complement the fundamentally unidirectional chemical synapses (Rash et al., 1996; Bennett, 2000). To date, gap junctions have been positively identified in almost all neuronal structures including the cerebral cortex (Sloper, 1972), hypothalamus (Perez et al., 1990), inferior olivary nucleus (Rutherford and Gwyn, 1977), hippocampus (Yamamoto et al., 1989), olfactory bulb (Reyher et al., 1991), the striatum, substantia nigra, cerebellum, lateral vestibular nucleus, trigeminal mesencephalic nucleus, inferior olive, anterior cochlear nucleus, the spinal cord and the retina (Rash et al., 2000, 2001). Since the discovery of gap junction communication in neural cells, direct electrotonic coupling was considered to be the mechanism mediating the flow of information between neurons, hence the name electrical synapses. Recently however, Kandler and Katz (1998) have argued that electrical coupling between developing neurons is relatively weak and unable to account for the neuronal synchronization recorded. Thus it was proposed that "biochemical waves" generated by direct exchange of IP_3 may provide the main functional route between the coupled neurons in developing and adult brain, however the possible coexistence of the two pathway has not been excluded.

More than half of the connexins known to be expressed in CNS (Cx26, Cx32, Cx36, Cx43, Cx45, Cx47) have been reported in neurons in normal and pathological conditions, as well as during development (Nagy et al., 2003c). However, only Cx36 has been unequivocally determined to be expressed exclusively by neurons in CNS, hence gaining acceptance as the only unambiguously recognized neuronal connexin (Condorelli et al., 1998; Rash et al., 2000). Consistent and specific labeling for Cx36 has been found in the nuclear complex of the inferior olive, the inner plexiform layer of the retina, the olfactory bulb and the molecular layer of the cerebellum (Meier et al., 2002). Recently, Teubner et al. (2001) reported the cloning of a new

connexin (Cx47) and following mRNA *in situ* hybridization studies it was proposed to be a novel neuronal connexon. It was reported that Cx47 localizes in α-motoneurons of the spinal cord, pyramidal cells of the cortex and hippocampus, granular and molecular layers of the dentate gyrus and Purkinje cells of the cerebellum. Interestingly and to the author surprise, Cx47 gap junction channels have a unitary conductance of 55 pS, much higher than 15 pS as it was reported for neuronal Cx36 (Teubner et al., 2001). In a recent turn of events, suggestive of the controversial and at times contradictory evidence surrounding the cellular identity of neural connexins, evidence emerged from the same research group that Cx47 is expressed in oligodendrocytes and not in neurons as they first postulated (Odermatt et al., 2003).

The functional significance of gap junction mediated neuronal coupling is not well understood, however a few possible roles have been postulated. First, it is believed that gap junctions between neurons allows bidirectional signaling between the pre- and post-synaptic elements, thus facilitating the synchronous firing pattern of the involved neurons (Bennett, 1977; Bennett, 2000). It was hypothesized that such a mechanism is responsible for the firing burst of the oxytocin producing cells of the supraoptic nucleus during milk ejection (Hatton et al., 1987). Also in the retina, a preferred model for the study of gap junctions in neural cells, interneuronal coupling is responsible for the high sensitivity of receptor cells to minute quanta of light (Hecht et al., 1942; Condorelli et al., 2000). Second, it has been proposed that electrical and mixed synapses may play a role in neural pathway plasticity for such cognitive processes as perception and attention (for review see Nagy et al., 2003c). Finally, following a series of observations that neocortical cell coupling changes throughout development, and the inhibition of gap junction coupling during corticogenesis inhibits progenitors from reentering the cell cycle, it has been postulated that gap junctions may play an active role in normal neurogenesis (Fulton et al., 1995; Bittman et al., 1997).

IV.14.b. Astrocytic Gap Junctions

In contrast to its physical size, only 2% of human body mass, the brain is responsible for more than 20% of the total glucose consumption of the body, thus making it one of the most metabolically active organs. While the functional unit of the brain is the neuron, as irony has it, these cells are completely dependent on the supporting tissue for homeostatic balance and survival. Observing the close apposition existent between astrocytes and neurons, more than a

century ago, Golgi proposed that astrocytes exist solely to provide physical and metabolic support for neurons. To date we confirmed Golgi's intuition, however emerging evidence suggests that astrocytes are more than passive elements that allow the trafficking of metabolites to and from neurons (Hatton, 2002). Recently, it has been reported that astrocytes are involved in bidirectional communications with neural cells, receiving and modulating the release of neuronal neuroactive substances and implicitly affecting the synaptic transmission (Araque et al., 1999; Smit et al., 2001).

Astrocytes derive their name from the stellar morphology observed in early histological observation of brain tissue, however their architecture can differ widely and to date astrocytes are classified in to two major subgroups. Fibrous astrocytes found in the white matter, and protoplasmic astrocytes that comprise the majority of cells found in the gray matter. The latter class of astrocytes, has been subdivided in two morphologically distinct subgroups. Müller cells located in the retina and pituicytes in the neurohypophysis aspect of the pituitary gland (for review see Barr and Kiernan, 1993). It is known that all astrocytes express glial fibrilary acidic protein (GFAP) believed to confers additional rigidity to the intermediate filaments supporting the cytoplasm (Pekny et al., 2001). The exclusive expression of GFAP by astrocytes has made this protein a useful marker in the identification of astroglia in immunocytochemical studies (Pixley et al., 1984).

Astrocytes are physically interposed between neurons and cerebral capillaries, their long processes associated with synaptic junctions and nodes of Ranvier. It is believed that astrocytes compartmentalize neurons according to their metabolic and electrophysiological needs (Nagy et al., 2003c). The dependence of neurons on astrocytes became evident when it was discovered that astrocytes and not neurons express enzymes essential for neuronal metabolic processes, such as amino acid metabolism, carbohydrate metabolism or glutamate-glutamine cycle (Norenberg and Martinez-Hernandez, 1979; Hetz et al., 1999; Kirchhoff et al., 2001). In the glutamate to glutamine cycle, the neuroactive glutamate release by neurons is taken up by astrocytes and is amidated to glutamine, a substance that has no neurotransmitting properties and is readily taken up by neurons. Another important physiological function is the spatial buffering of the K^+ ions exuded by neurons following periods of intense activity. This homeostatic event is mandatory for the preservation of K^+ at physiological levels in the relatively small extracellular spaces surrounding neurons. An increase in the level of K^+ could have disastrous effects for the

neuronal cell membrane potential and implicitly for the neuron's conductive properties. Therefore, it was proposed that the astrocytic network acts as a "potassium sink" that involves the redistribution of K+ to the perivascular tissue ions via gap junction interconnected astrocytes. It is believed that this direct pathway for the redistribution of K^+ is highly controled by constant modulation of gap junction coupling states between astrocytes (for review see Nagy and Dermietzel, 1999; Nagy and Rash, 2000).

The expression of connexins by astrocytes commences in late embryonic stages and continues through adult life. To date Cx26, Cx30 and Cx43 have been identified by freeze-fracture replica immunogold labeling (FRIL) and EM at astrocytic gap junction plaques forming the principle coupling partner in A/A and A/O gap junctions (Nagy et al., 2001). It appears that Cx30 is expressed exclusively by gray matter astrocytes and is not found in white mater in CNS (Nagy et al., 2001). Cx31.1 has been reported in cultured astrocytes however it is still debatable if the published observation was the result of specific antibody recognition (Naus et al., 1997).

Cx43 is expressed by both fibrous and protoplasmic astrocytes and displays a heterogeneous immunolabeling distribution, suggesting a regional diversity in astrocytic gap junction concentration (Yamamoto et al., 1990a,b). Interestingly, it was observed that Cx43 mRNA distribution does not completely mirror the distribution of Cx43 puncta, suggesting that Cx43 is also regulated at the translational level. Ultrastructural studies concerning the regional distribution of Cx43 have revealed that highly dense Cx43 immunolabeling is concentrated on astrocytic processes surrounding synaptic glomeruli, neuronal somata and dendrites (Yamamoto et al., 1999a,b). In spinal cord white matter Cx43 was localized between cytoplasmic processes of fibrous astrocytes suggesting homologous coupling, however Cx43 was also present at asymmetric labeling between astrocytic processes and unstained oligodendrocytic elements (Ochalski et al., 1997).

The association of astrocytes and neurons is so intimate that these cells can be used as surrogate markers for the physiological state of the neurons. Within hours following neuronal insult, drastic morphological changes such as cellular swelling can be observed in astrocytes surrounding the site of injury (Chen et al., 1993; Garcia et al., 1993). The gap junction coupling state of these reactive astrocytes (term coined to distinguish them from astrocytes found in healthy tissue) is not well understood, however it is believe that an increase and decrease in gap junction coupling state between astrocytes can coexist. It has been demonstrated that following

ischemic injury, astrocytes can reorganize the distribution of Cx43 formed gap junction in such a fashion that while the connection with the damaged area decreases, there is a notable augmentation in coupling between the astrocytes surrounding the injury site (Hossain et al., 1994). While reduced coupling confines the reactive gliosis to the damage area and prevents the noxious "bystander effect" on the surrounding healthy cells, the increase in coupling is responsible for the "good Samaritan" effect that allows astrocytes to share the toxic load and thus reduce the risk of injury (Ripps, 2002; Asklund et al., 2003). The opening state of gap junctions in astrocytes is modulated by factors such as Ca^{2+} concentration, phosphorylation state of the connexin protein or cytosolic H^{+} concentration (Bennett and Verselis, 1992)

Until a few years ago it was believed that even a modest increase in intracellular Ca^{2+} would reduce GJIC by rapid closure of the gap junction channel. Therefore, it came as a surprise when it was observed that intracellular injection of Ca^{2+} in one cell led to a substantial increase of Ca^{2+} levels in gap junction interconnected adjacent cells (Saez et al., 1989). The intercellular coordinated calcium wave propagation is mediated by the direct passage of Ca^{2+} and/or inositol 1,4,5-triphosphate (IP_3) from the cytosolic space of one cell to the next via gap junction intercellular communications (Bruzzone and Resssot, 1997). Recently however, following the observation that Ca^{2+} wave propagation only slightly retarded in uncoupled astrocytes, it was proposed that an additional, dominating extracellular path complements the gap junction mediated Ca^{2+} wave transmission (Guan et al., 1997; Naus et al., 1997, 1999). It has been proposed that the paracrine release of active factors such as ATP, endothelin, glutamate, acethylcholine may activate receptor systems on adjacent astrocytes and thus the production and propagation of Ca^{2+} waves in the absence of gap junction intercellular communication (for review see Scemes, 2000).

According to recent gap junction literature, there is no clear pattern to the effect of connexin phosphorylation on gap junction gating. In mammals, with the exception of Cx26 all known connexins are phosphoproteins (Lampe and Lau, 2000). It has been determined that phosphorylation of connexins can either reduce or increase gap junctional coupling according to the type of phosphokinase involved (for review see Jongsma et al., 2001). For example, phosphorylation of Cx43 by v-sarc tyrosine kinase or phosphorylation of serine/threonine residues by protein kinase G (PKG) decreases gap junctional coupling (Kwak and Jongsma, 1996; Contrell et al., 2003). In contrast, it has been observed that activation of PKC increases

junctional conductance in Cx43 expressing cardiomyocytes (Kwak et al., 1995). A unique aspect of Cx43 physiology is that in the normal brain, Cx43 exists exclusively as a phosphorylated species that rapidly dephosphorylates posthumously, or under local focal ischemic conditions (Hossain et al., 1994; Li et al., 1998). Dephosphorylation of Cx43 does not necessarily reflect on the pathological state of astrocytes. It has been reported that acute activation of the proximal sciatic nerve reduces the phosphorylation level of Cx43 expressed by the astrocytes of the dorsal horn (Li and Nagy, 2000).

IV.14.c. Gap junction in oligodendrocytes and Schwann cells

The production and maintenance of myelin, the electrically insulating protein that surrounds the axons is the responsibility of oligodendrocytes in the CNS, and Schwann cells in the PNS. Oligodendrocytes are highly branched microglial cells that are found predominantly in white matter and can be morphologically sub-classified into interfascicular oligodendrocytes (along myelinated axons) and satellite oligodendrocytes (closely associated with the cell bodies of large neurons). Each oligodendrocyte can myelinate 20-60 internodal segments of about 40-50 different axons, and adjacent myelin segments on the same axon belong to different oligodendrocytes (for review see Baumann and Phanm-Dinh, 2001). Such a relative discontinuous arrangement of myelin nodes may account for the paucity of remyelination following loss of myelin in CNS (Carroll and Jennings, 1994). In contrast, along large diameter myelinated fibers (1-2 μm) in PNS, Schwann cell associates with only one axon. However, for small diameter fibers such as C-fibers a single Schwann cell may surround a group of axons in what is known as a Remark fiber bundle (Waxman, 1996).

Extensive morphological and electrophyiological studies have provided compelling evidence of the existence of gap junctions in oligodendrocytes and Schwann cells (Kettenmann et al., 1983; Massa and Mugnaini, 1985; Robinson et al., 1993; Li et al., 1997; Rash et al., 1997, 2000). While it is believed that *in vivo*, mature oligodendrocytes do not form homologous coupling (Rash et al., 1997), during development it was observed that contacting oligodendrocytic progenitor cells are electrically coupled, but not dye-coupled (Butt et al., 1993). However, recently it has been reported that dye coupling between mature oligodendrocytes may be somehow influenced by local environmental factors, as it was shown that oligodendrocytes in gray matter are dye-coupled, whereas their counterparts in white matter are not (Pastor et al.,

1998). Although the existence of gap junctions in plasma membrane of oligodendrocytes was readily accepted, as in other CNS cell types a recurring theme remains the establishing of the exact identity of connexins expressed by oligodendrocytes (Nagy et al., 2003). With a large number of connexins reported to be expressed by oligodendrocytes at different stages of development, the strongest candidates however, remain Cx29, Cx32 and Cx47. In a recent study involving Cx47-null mice, Odermatt et al. (2003) revealed that Cx47 is mainly expressed in oligodendrocytes in highly myelinated CNS structures.

A good example concerning the conflicting evidence surrounding the exact cellular identity of glial connexins is represented by the literature related to expression and anatomical localization of Cx45. Following detection of Cx45 mRNA in adult rodent brain (Kunzelmann et al., 1997), incongruous evidence started to accumulate regarding the type of cells expressing Cx45. *In vivo*, Cx45 was immunohistochemically associated exclusively with oligodendrocytes; whereas no evidence of Cx45 expression was found in cultured oligodendrocytes (Dermietzel et al., 1997). In contrast, a subsequent study reported that Cx45 is highly expressed during embryonic development in a large number of motorneurons of rat spinal cord, however Cx45 expression appears to decrease soon after birth to lower yet detectable levels (Chang et al., 1999). Neuronal expression of Cx45 was further supported by examination of heterozygous $Cx45^{-/+}$ mice expressing β-galactosidase (β-gal) under the control of Cx45 promoter (Kruger et al., 2000). Finally, a new study indicates that Cx45 is expressed exclusively by unidentified cells associated with brain capillaries (Li et al., 2001).

Cx32 is a myelin associated protein that is also responsible for gap junction formation in hepatocytes, where it is also highly expressed (Yamamoto et al., 1991; Li et al., 1997). In CNS, double immunolabeling of Cx32 with the oligodendrocytic marker 2', 3'-cyclic nucleotide 3'-phosphodiesterase (CNPase) revealed that Cx32 is consistently co-localized with the outer aspect of oligodendrocytic somata. However, it appears that Cx32 detection remains restricted to a subpopulation of myelinated fibers arising from the cerebellar Purkinje cells (Li et al., 1997). Similarly, in a recent investigation Altevogt et al. (2002) reported that Cx32 in spinal cord is associated only with large diameter myelinated fibers. Following extensive FRIL studies it is believed that oligodendrocytes are involved exclusively in A/O heterologous coupling with little evidence for O/O homologous coupling (Rash et al., 1997). Interestingly, the rare instance when O/O are observed has been attributed to anatomical organization of oligodendrocytic processes

and it was proposed that such coupling may in fact be evidence for sparse autologous gap junction formation between adjacent cellular processes pertaining to the same oligodendrocyte (Nagy et al., 2003c).

In peripheral nerves, Cx32 was localized at the outer aspects of Schwann cell paranodes and at Schmidt Lantermann incisures (Bergoffen et al., 1993; Scherer et al., 1995; Altevogt et al., 2002). Whereas gap junction-like particles were identified more than 20 years ago by EM at the periaxonal regions in Schwann cells (Sandri et al., 1977), conclusive ultrastructural evidence for the existence of gap junctions at Schmidt Lantermann incisures still remains elusive. This contrasts with the reported rarity of Cx32 localization at paranodal regions in CNS (Spray and Dermietzel, 1995; Li et al., 1997). While the exact roles of autologous gap junctional communications between successive layers of myelin at paranodal regions and Schmidt Lantermann incisures is not clear, possible roles include dissipation of K^+ gradient following neuronal excitation, and/or creation of a radial diffusion route, estimated to be approximately a 1000 times shorter than the circumferential pathway (Scherer et al., 1995; Balice-Gordon et al., 1998).

IV.14.d. Myelin structure and Schmidt-Lanterman incisures in CNS

Myelin is a multilaminar specialized membrane that completely encircles the myelinated axons, except at nodes of Ranvier, and represents an important evolutionary adaptation that facilitates faster impulse conduction in myelinated nerves (for review see Garbay et al., 2000). Due to its multilaminar aspect, mature myelin displays a periodic arrangement of the intraperiod line (thin extracellular space that separates the opposing membranes) and the major dense line that is contiguous with the cytoplasm (refer to Figure 4). Traditionally, the myelin sheet has been divided into two distinct domains that contain a non overlapping set of proteins. Compact myelin, the predominant portion of the myelin sheet, and non-compact myelin found in paranodes (the myelin aspect that borders the nodes of Ranvier) and in Schmidt-Lanterman incisures (for review see Arroyo and Scherer, 2000). In PNS, myelin is formed by the wrapping of Schwann cells around axons and is largely composed of lipids (mainly cholesterol and sphingolipids) and myelin proteins: protein zero (P_0), peripheral myelin protein (PMP22) and myelin basic protein (MBP).

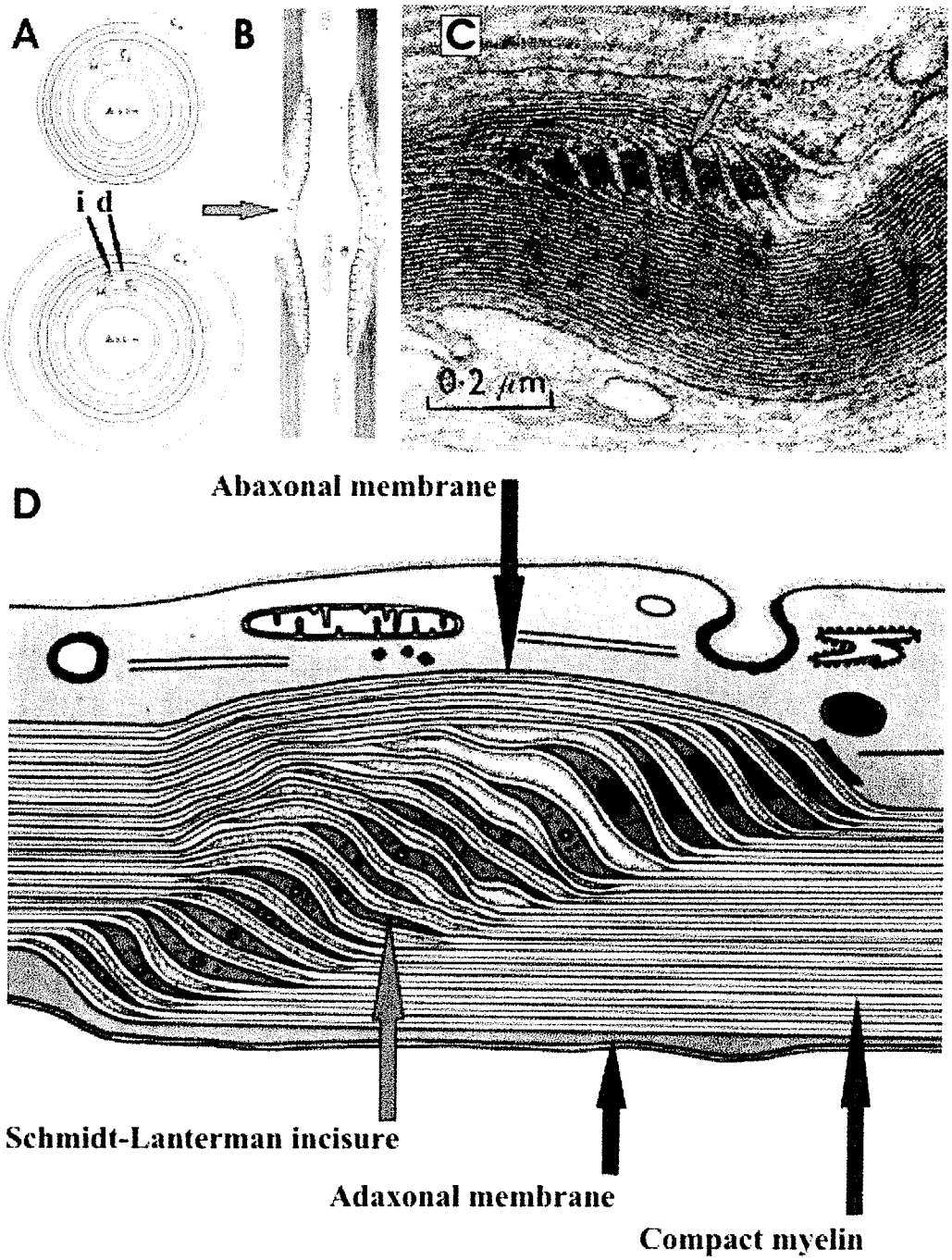

Figure 4. Schematic representation of a myelinated peripheral nerve axon in cross section (**A**) and longitudinal section (**B**). EM detail of a incisural cytoplasmic spiral from a mouse sciatic nerve. (**C**). Diagrammatic representation of a Schmidt-Lanterman incisures in a Schwann cell (**D**). Schmidt-Lanterman incisures are marked by blue arrows. (**i**) intraperiod and (**d**) major dens line of compact myelin. (Figures were taken from Hall and William, 1970).

The compact portion of CNS myelin is biochemically distinct from its CNS counterpart, with proteolipid protein (PLP) as the main protein. Oligodendrocytes, the myelinating cells of the CNS, express two proteins that are absent in Schwann cells, myelin-oligodendrocyte glycoprotein (MOG) and myelin-oligodendrocyte basic protein (MOBP).

Schmidt-Lanterman incisures were observed more than a century ago, as conical discontinuities located in compacted myelin between the internodal region of the peripheral myelinated nerve fibers (for review see Ghabriel and Allt, 1981). Initially, the existence of Schmidt-Lanterman incisures was much debated, believed to be nothing more than a postmortem artifact generated by fixation and tissue extraction protocols (Young, 1945). However, some biologist supported the existence of Schmidt-Lantermann incisures as naturally occurring structures of albeit undetermined role (Nageotte, 1922; Cajal, 1928). With the advent of electron microscopy, it became apparent that Schmidt Lantermann insures consist of circular cytoplasmic dilation of the dense line, separated from the compact myelin by tight junctions, that connect the outer abaxonal aspect of the Schwann cell to its adaxonal compartment. While their speculated cytoplasmic origin was not conclusively demonstrated, Hall and William (1970) showed the existence of Schmidt-Lanterman incisures in vivo in the undisturbed sciatic nerve of a living mouse. To date it is believed that far from being static structures, Schmidt-Lanterman incisures, are extraordinarily dynamic and are influenced by dramatic events such as regeneration, re-myelination or development of the myelinated fiber (Hiscoe, 1947, Hall and William, 1970, Ghabriel and Allt, 1980). It was reported that new Schmidt-Lanterman incisures can be added/removed from the internodal myelin regions, or they can become focal points for Wallerian degeneration and ovoid formation following proximal nerve injury (Ghabriel and Allt, 1979a,b).

Considering that myelin lamellae surrounding the myelinated axon in a normal nerve represent a redoubtable barrier impermeable to diffusion, and in the regions of compacted myelin the myelinating cell's membranes are in close apposition, it becomes easily envisioned the role of Schmidt-Lanterman incisures as a conduit to and from the inner layers of myelin (Webster, 1965). Intracellular injections studies of tracer substances into the outer aspect of Schwann cells, revealed the existence of radial diffusion pathways (Singer et al., 1972, Hall and William, 1971). Therefore, it has been speculated that Schmidt-Lanterman incisures act as conduits for the transport of metabolites across the myelin sheath, an essential requirement for the synthesis and

maintenance of myelin (William and Hall, 1971a,b; Ghabriel and Allt, 1981).

The association of Cx32 mutations with CMTX syndrome (Bergoffen et al., 1993), combined with evidence that Cx32 myelin associated protein in PNS (Shcerer et al., 1995), led to subsequent immunohistochemically and electron microscopy studies revealing that Cx32 was predominantly located at the incisures and paranodal regions of myelinated axons in PNS (Scherer, 1999). The presence of apparently autologous gap junctions at Schmidt-Lanterman incisures was considered to be unusual at the time, as it was believed that connexin channels should be found only at specialized areas of cell-to-cell contact (for review see Arroyo and Scherer, 2000). This observation led to the hypothesis that Cx32 forms reflexive gap junctions between adjacent myelin layers to ensure cytoplasmic continuity across the myelin sheath. Such a reflexive coupling would create a conduit that would greatly reduce the distance required for diffusions of small molecules from the extracellular regions to the abaxonal domain of the Schwann cell (Balice-Gordon et al., 1998). Due to the unique geometry of Schwann cells, an unrolled myelin sheet surrounding a 7 μ axon would be approximately 4 mm long but only 2.3 μm thick (Friede and Bischhausen, 1980). It was estimated that the presence of a radial diffusion pathway across the myelin sheet would represent an important functional adaptation that would increase the diffusion rate by a factor of approximately 1700 (Balice-Gordon et al., 1998).

The presence of Schmidt-Lanterman incisures in CNS myelin has been firmly established, however debate still exists whether these structures are ubiquitous or they exist exclusively in large myelinated CNS fibers (Bunge et al., 1960; Hirano and Dembitzer, 1967; Blakemor, 1969; Hildebrand et al., 1993).

Overview of this project.

It is becoming apparent that the ability to form GJIC is not an isolated quality, restricted to a selected group of neural cells, but a wide-spread method of intercellular communication exhibited by virtually every cell type in the brain (for review see Nagy et al., 2003). In the last 10 years, accumulating evidence supports the emerging belief that cellular coupling in CNS is a complex event where each cell type exhibits selectivity with respect to cellular coupling partnership and connexin expression (Nagy and Rash, 2000; Nagy et al., 2003a). First, it has been established that connexin expression is segregated to distinct cell types in CNS, with astrocytes expressing Cx26, Cx30, Cx43 and oligodendrocytes expressing Cx32 (Yamamoto et al., 1990a,b; Dahl et al., 1996; Wolburg and Rohlmann, 1995; Ochalski et al., 1997; Kunzelmann et al., 1999; Nagy et al., 1999; Scherer et al., 1995; Li et al., 1997; Rash et al., 2000, 2001). Second, extensive high resolution investigative methods such as FRIL and thin-section EM corroborate evidence that astrocytes are involved in extensive homologous coupling with each other (A/A gap junctions), and are also involved in heterologous coupling with oligodendrocytes (A/O gap junctions). Moreover, it is believed that intercellular communication between oligodendrocytes occurs in an indirect fashion, by an astrocyte intermediary (Ochalski et al., 1997; Nagy et al., 1997, 1999, 2002; Rash et al., 2001). However, the existence of autologus coupling between oligodendrocytic processes as well as radial gap junction mediated interconnections of the concentric layers of myelin along myelinated fibers remains a controversial issue. Finally, despite the presence of Cx43 at A/O junctions, it is known that oligodendrocytic Cx32 is capable of forming permissive junctions only with Cx26 and Cx30 and not with Cx43 (White and Bruzzone, 1996).

Recently it has been reported that Cx29, a newly identified connexin, is highly associated with myelin and is expressed by oligodendrocytes in CNS and Schwann cells in PNS (Sohl et al., 2001; Altevogt et al., 2002; Li et al., 2002; Nagy et al., 2003a,b). In a recent study Teubner et al. (2001) reported *in situ* hybridization results showing that Cx47 mRNA is highly expressed in neurons. The absence of supporting immunocytochemical evidence, prompted us to develop specific anti-Cx47 antibodies that would allow a detailed study of Cx47 expression in CNS. The presence of additional connexins, Cx29 and/or Cx47, on the oligodendrocytic side of A/O gap junctions may clarify some previously unanswered questions.

Project1: The inability of Cx43 and Cx32 to form functional GJIC, yet the strong localization of Cx43 around oligodendrocytic somata, raised the possibility that oligodendrocytes express more than one connexin species. In this project, we first hypothesized that the newly identified Cx29 may be a candidate in coupling partnership with astrocytic Cx43. An extensive study was taken to determine the exact cellular localization of Cx29 in both developing and adult brain. The localization of the two oligodendrocytic connexins, Cx29 (Sohl et al., 2001; Altevogt et al., 2002; Li et al., 2002) and Cx32 was investigated in relationship with each other, as well as in relation to the astrocytic connexins Cx30 and Cx43. As a result of the limited colocalization of Cx29 with Cx30 and Cx43 both on the oligodendrocytic somata and along myelinated fibers, it was determined that Cx29 is not extensively involved in A/O gap junction formation in either developing or adult brain.

Project 2: An important controversial issued in connexin research remains whether Cx32 is expressed solely by oligodendrocytes, or as previously reported, wheather it is also expressed by neurons (Nadarajah and Parnavelas, 1999). In this study, Cx32 immunolabeling patterns and anti-Cx32 antibody specificity was investigated in wild type (WT) and Cx32 knockout (KO) mice. While Cx26, Cx30 and Cx43 are involved in A/A GJIC, only Cx26 and Cx30 have the ability to form functional A/O GJIC with oligodendrocytic Cx32. Therefore, we hypothesized that in the absence of Cx32 in Cx32 KO mice, the distribution pattern of the astrocytic connexins on the oligodendrocytic somata is affected in a fashion directly related to the astrocytic connexins involvement in functional A/O GJIC with Cx32. We investigated the association of Cx30 with Cx32, and whether the profile of astrocytic and oligodendrocytic connexins is altered in the absence of Cx32 in Cx32-defficient mouse brain. Contrary to previous reports (Teubner et al., 2001), we determined that Cx47 is an oligodendrocytic connexins, and that its robust expression does not appear to be affected by the absence of Cx32 in Cx32-KO mice. An important hypothesis to be tested in this project was that oligodendrocytic Cx47 exhibits a degree of colocalization with the astrocytic Cx43, sufficient to suggest that Cx43 and Cx47 are potential candidates in A/O GJIC formation.

Contribution for this project.

The present project is the result of the combined effort of our lab over a two year span. My direct contribution to the project:

- An important contributing factor to the success of this project was the developing process, in collaboration with Zymed Inc, of highly specific polyclonal antibodies directed against Cx29 and Cx47. This process involved extensive and exhaustive antibody selection and testing. Taking to consideration that the use of double and triple immunolabeling protocols was often used in our investigation, special attention was accorded to factors such as cross-reaction with existing antibodies, the development of suitable protocols that would allow optimum immunocytochemical detection of connexins, testing various fixation methods for brain tissue, as well as modifications of existing immunochemistry protocols for immunofluorescence labeling. At different stages during this project we encountered various technical problems such as: antibody cross-reaction, reduced immunostaining signal, unsuitable standard fixation protocols of neonatal and adult animals. I was responsible for finding and developing new protocols and technical solutions that would allow the circumvention of the above mentioned problems. These protocols were essential for obtaining optimal immunolabeling efficiency according to my judgment, and allowed tests of our hypothesis that Cx29 and Cx32 are not expressed by mutually exclusive subsets of oligodendrocytes as described in the literature, but rather are nearly entirely co-expressed by this cells.
- The advent of confocal microscopy has allowed a high level of image resolution, previously impossible to attain with standard transmitted light microscopy. However, the technicalities involved in acquiring and processing the data are highly complex and require extensive training and practice. I was directly responsible for all aspects of confocal image analysis, from production of tissue, immunolabeling slides to final image capture and processing. In direct collaboration with my advisor Dr. J. Nagy, I selected the confocal and light microscopy imagery to be included in each plate. Otherwise I was entirely responsible for producing and editing of all double labeled and triple labeled confocal plates (approximately 90% of microscopical imagery).
- The use of transgenic Cx32 KO animals represented an important tool extensively used during this project. The project commenced with the perfusion-fixation and dissection of Cx32 KO as well as of WT animals. I was directly responsible for the fixation perfusion of most animals, tissue sectioning and management of collected samples needed for future use. Initially these

animals were to establish without doubt previous demonstrations from this lab that Cx32 is heavily distributed along myelinated fibers, which was met with skepticism in the CNS gap junction field. Results from Cx32 KO mice, showing absence of Cx32 along myelinated fibers confirmed the previous results from this lab.

- Early during the project, I discovered that the distribution of Cx30 around oligodendrocytic somata in Cx32 KO mice drastically differs from the wild type counterpart. While such evidence was readily noticed during microscopical investigation, it soon become apparent that a more accurate method was needed to quantify the observed finding and to test the hypothesis based on this qualitative observation: The elimination of the Cx32 in oligodendrocytes directly affects the distribution of its astrocytic connexin coupling partner (Cx30) at the astro/oligodendrocytic gap junctions. Thus, I undertook in quantitative analysis of Cx30 puncta around oligodendrocytes in WT and Cx32-KO mice, and subsequent statistical analysis of the acquired data and confirmed the above hypothesis.
- Other aspects of the present project are structured on anatomical and immunocytochemical studies that by their nature are not easily quantifiable. Such observations require extensive knowledge of neuroanatomy and morphology in the context of connexin expression. During the course of this study, I have acquired the ability to interpret data obtained and consequently design and organize new experiments. The culmination of this project is the production of the manuscripts present in this thesis, to which I contributed in the form of writing the Methods and Discussion sections of the initial draft that was subsequently split into two manuscripts. Finally, I then assisted in the production and submission of the final version of the two manuscripts.

All aspect pertaining to western-blot procedures and biochemical analysis used for this were conducted by fellow graduate students Bruce Lynn and Carl Olson.

V. PROJECT 1: Connexin29 and connexin32 at oligodendrocyte/astrocyte gap junctions and in myelin of mouse CNS

James I. Nagy, Andrei V. Ionescu, Bruce D. Lynn and John E. Rash

Journal of Comparative Neurology, submitted

ABSTRACT

The cellular localization, relationship to other glial connexins (Cx30, Cx32, Cx43) and developmental expression of connexin29 (Cx29) was investigated in mouse central nervous system (CNS) using an anti-Cx29 antibody. Cx29 was enriched in subcellular fractions of myelin, and immunofluorescence for Cx29 was localized to oligodendrocytes and myelinated fibers throughout brain and spinal cord. Oligodendrocyte somata displayed minute Cx29-immunopositive puncta around their periphery, as well as intracellularly. In developing brain, Cx29 levels increased during the first few postnatal weeks and were highest in adult brain. Immunofluorescence labeling for Cx29 in oligodendrocyte somata was intense at early ages and was dramatically shifted in localization primarily to myelinated fibers in mature CNS. Labeling for Cx32 also was localized in oligodendrocyte somata and myelin, and was absent in Cx32 knockout mice. Cx29 and Cx32 were minimally co-localized on oligodendrocytes somata and partially co-localized along myelinated fibers. At gap junctions on oligodendrocyte somata, Cx43/Cx32 and Cx30/Cx32 were strongly associated, but there was minimal association of Cx29 and Cx43. Cx32 was very sparsely associated with astrocytic connexins along myelinated fibers. With Cx26, Cx30 and Cx43 expressed in astrocytes and Cx29, Cx32 and Cx47 expressed oligodendrocytes, the number of connexins localized to gap junctions of glial cells is now raised to six. The results suggest that Cx29 in mature CNS contributes minimally to gap junctional intercellular communication at oligodendrocyte cell bodies, but rather is targeted to myelin where it, along with Cx32, may contribute to connexin-mediated communication between adjacent layers of uncompacted myelin.

INTRODUCTION

Cells in the CNS communicate directly via gap junctions at close appositions between plasma membranes, providing channels for movement of ions and small molecules from cell to cell. It appears that virtually every neural cell type in brain has the capacity for gap junctional intercellular communication (GJIC), and evidence for several levels of complexity in this process is beginning to emerge. Each cell type exhibits selectivity with respect to cellular coupling partners and to connexin coupling partners (Nagy and Rash, 2000; Nagy et al., 2003a). Extensive homologous coupling occurs between astrocytes (A/A gap junctions), and widespread heterologous coupling also occurs between astrocytes and oligodendrocytes (A/O gap junctions), but little if any homologous coupling occurs between oligodendrocytes (Mugnaini, 1986; Rash et al., 1997, 2000; Nagy et al., 2003a). At least ten members of the family of connexin (Cx) proteins that form gap junctions in mammalian tissues are expressed in the CNS, and individual cells and gap junctions often contain two or more different connexins (Nagy et al., 1999; Severs, 1999; Nagy and Rash, 2000; Nagy and Dermietzel, 2000). It is now established that A/A junctions contain Cx26, Cx30 and Cx43, while A/O junctions contain these connexins on the astrocyte side, and Cx32 on the oligodendrocyte side (Dermietzel et al., 1989; Yamamoto et al., 1990a,b; Dahl et al., 1996; Wolburg and Rohlmann, 1995; Ochalski et al., 1997; Kunzelmann et al., 1999; Nagy et al., 1999; Scherer et al., 1995; Li et al., 1997; Rash et al., 2000, 2001).

Multiple connexin expression in each of a pair of gap junctionally coupled cells introduces the possibility of heterotypic channel formation between different connexins, some heterotypic combinations of which are functionally permissive, while others are not (White and Bruzzone, 1996). This suggests a diversity of functional GJIC depending on the connexins expressed by cells and the differential permeability of channels formed by the different connexins (Veenstra, 1996). The organization of heterologous gap junctions of oligodendrocytes with astrocytes in the CNS is not yet clear. While Cx32 and Cx43 are reported to be non-permissive for gap junction channel formation, Cx43 as well as Cx30 and Cx26 are nevertheless incorporated into gap junction plaques on the astrocyte side of A/O junctions on oligodendrocyte somata (Ochalski et al., 1997; Nagy et al., 1997, 1999, 2002; Rash et al., 2001). The presence of Cx43 at A/O junctions suggests that it may couple to other connexins in oligodendrocytes. Coupling partner candidates include Cx29 and Cx47, both of which are highly expressed in neural tissues and are localized to oligodendrocytes (Sohl et al., 2001; Altevogt et al., 2002; Li et al., 2002; Nagy and

Rash, 2003a,b). In addition, Cx32 in the CNS is densely localized nearly continuously along myelinated fibers (Li et al., 1997), thus differing from Cx32 localization in myelin of peripheral nerve, where it is highly concentrated at nodes of Ranvier and Schmidt-Lanterman incisures. In CNS myelin, Cx32 may form gap junctions with astrocytic processes that abut myelinated fibers, as has been described to occur in the CNS (Waxman and Black, 1984; Ochalski et al., 1997), or it may form autologous gap junctions between successive layers of cytoplasmic pockets to allow radial GJIC, as has been proposed to occur in peripheral nerve (Balice-Gordon et al., 1998).

In the present study, the expression and cellular localization of Cx29 in adult and developing mouse CNS was investigated by western blotting, light microscopy and confocal laser scanning immunofluorescence using a well characterized anti-Cx29 antibody (Li et al., 2002). In addition, the cellular localization of Cx29 and Cx32 was examined in relation to the astrocytic connexins Cx30 and Cx43, and the previously reported detection of Cx32 densely distributed along myelinated fibers (Li et al., 1997) was re-investigated using wild type (WT) and Cx32 knockout (KO) mice.

MATERIALS AND METHODS

Antibodies, animals and western blotting

The anti-connexin antibodies used in this study, together with source and citations reporting their specificity characteristics, are listed in Table 1. The anti-Cx29 antibody used has been characterized with respect to specificity of Cx29 detection in sciatic nerve and in HeLa cells transfected with Cx29 cDNA (Li et al., 2002). This antibody was developed and supplied by Zymed Laboratories Inc (South San Francisco, CA), and the peptide sequence within Cx29 against which the antibody was raised is proprietary. Polyclonal anti-Cx43 antibody 18A and monoclonal anti-Cx32 7C7 were generously provided by E.L. Hertzberg. For immunolabeling markers of oligodendrocytes and myelin, additional antibodies employed included monoclonal anti-2,'3'-cyclic nucleotide 3'-phosphodiesterase (CNPase) (Sternberger Monoclonals, Baltimore, MD), polyclonal anti-CNPase (provided by Dr. P.E. Braun, McGill University, Montreal, Quebec), and monoclonal anti-myelin associated glycoprotein (MAG) (Chemicon International, Temecula, CA).

A total of 72 adult male CD1 mice (30-40 g), including 25 at various developmental ages, and 4 adult male Sprague-Dawley rats (300-350 g) were obtained from Central Animal Services at

the University of Manitoba, and were treated according to approved protocols of the Central Animal Care Committee. In addition, Cx32 KO C57BL/6 mice were provided by K. Willecke (Bonn, Germany) and, together with wild-type (WT) C57BL/6 mice, were bred at Colorado State University according to standard protocols. A total of 8 WT and 9 KO animals were used.

For biochemical analyses, adult mice were decapitated, brain and spinal cord were removed, and various regions of brain were dissected and stored at -80°C until use. Tissues were similarly dissected from mice at postnatal ages of 1, 7, 14 and 20 days. Whole brains pooled from 6 mice (repeated twice) were taken for subcellular fractionation by discontinuous sucrose density gradient ultracentrifugation as previously described (Li et al., 1997; Lynn et al., 2001). The material obtained included a combined synaptosomal and mitochondrial fraction (P2), microsomal/plasma membrane fraction (P3), a soluble fraction, a synaptosomal fraction and a myelin fraction. Western blotting of Cx29 and Cx32 by sodium dodecylsulfate polyacrylamide gel electrophoresis (SDS-PAGE) was conducted as previously described (Li et al., 1997; 2002; Lynn et al., 2001). For regional analysis of Cx29 expression and comparisons of Cx29 levels in subcellular fractions, lanes were loaded with equal protein from homogenates of brain regions or subcellular fractions.

LM immunofluorescence

Mice were deeply anesthetized with equithesin (3 ml/kg; Scadding, 1981) and transcardially perfused with 3 ml of prefixative consisting of cold (4°C) 0.1 M sodium phosphate buffer (PB), pH 7.4, containing 0.9% saline (PBS), 0.1% sodium nitrite and heparin (1 unit/ml). This was followed by perfusion with 20, 40 or 60 ml of cold 0.16 M sodium phosphate buffer, pH 7.6, containing 4% formaldehyde and 0.2% picric acid. For protocols involving post-fixation, brains were removed, sectioned into transverse blocks 2 mm thick, placed into perfusion fixative for 1.5 hours, and then stored at 4°C in cryoprotectant (50 mM PB, 10% sucrose and 0.2% sodium azide) for a minimum of 48 hours before sectioning. For protocols avoiding post-fixation, fixative was flushed from animals by perfusion with 10 ml of PB, pH 7.4 containing 10% sucrose. Brains were removed, blocked and stored in cryoprotectant as above. For developmental studies, mouse pups at postnatal days 8, 14 and 20 were perfused as above except with solution volumes adjusted for body weight. Brains from 2 day old mice were immersion fixed for 2-4 hours in cold 0.16 M sodium phosphate buffer, pH 7.6, containing 4% formaldehyde and 0.2%

picric acid. Optimal immunohistochemical labeling for Cx29 was achieved by perfusion with 40 to 60 ml of fixative, with little discernable difference in labeling with or without postfixation. Optimal immunolabeling for Cx32 was obtained by perfusion with 20 to 40 ml of fixative without post-fixation. Immunolabeling for Cx30 and Cx43 was equally robust with all of the above fixation protocols.

Ten micron transverse sections were cut on a cryostat, collected on gelatinized glass slides and stored at -34 °C. Following storage, sections on slides were washed extensively in 50 mM Tris-HCl containing 1.5% sodium chloride (TBS) and 0.3% Triton X-100 (TBST). All sections were incubated with primary and secondary antibodies diluted in TBST containing 4% normal goat serum. Anti-connexin antibodies were used at the dilutions indicated in Table 1. Monoclonal anti-CNPase was diluted 1:5000, polyclonal CNPase was diluted 1:500, and anti-MAG was diluted 1:500. Sections processed for double immunofluorescence labeling were simultaneously incubated with two different primary antibodies for 24 hours at 4°C. Sections were then washed for 1 hour in TBST and incubated simultaneously with two appropriate secondary antibodies for 1.5 hours at room temperature. A similar protocol was used for triple immunofluorescence labeling. Secondary antibodies were fluorescein isothiocyanate (FITC)-conjugated horse anti-mouse IgG (Vector Laboratories, Burlingame, Ca.) diluted 1:100, Cy3-conjugated donkey anti-rabbit IgG (Jackson ImmunoResearch Labs, West Groove, PA) diluted 1:200, Cy3-conjugated goat anti-mouse IgG (Jackson ImmunoResearch Labs) diluted 1:200, AlexaFluor488 $F(ab')_2$-conjugated goat anti-rabbit (Molecular Probes, Eugene, OR) diluted 1:1000, Cy5-conjugated donkey anti-mouse IgG (Jackson Immunoresearch Labs) diluted 1:200, and Cy3-conjugated donkey anti-goat IgG (Jackson ImmunoResearch Labs) diluted 1:200. After incubation with secondary antibodies, sections were washed for 20 minutes in TBST, followed by two 20 minute washes in TBS, and then coverslipped with antifade medium. In control procedures, omission of one or the other of the two primary antibodies with inclusion of both secondary antibodies produced no inappropriate labeling (i.e. secondary anti-rabbit recognition of mouse monoclonal primary or secondary anti-mouse recognition of rabbit polyclonal primary), indicating lack of cross reactions between antibodies.

Images were acquired on a Zeiss Axioskop2 fluorescence microscope and Olympus Fluoview IX70 confocal microscope with krypton/argon laser. For confocal analysis, double-labeled sections were scanned twice using single laser excitation for one or the other fluorochrome.

Triple labeling was also conducted by single scans of sections for each fluorochrome. Digital images were acquired at sufficient magnification to discern individual immunolabeled puncta. Images were captured using AxioVision 3.0.6 software and assembled in either Photoshop 6.0 or Corel Draw 8. Minimal adjustment to brightness and contrast were required.

RESULTS

Cx29 expression in adult brain

Regional Cx29 expression in adult mouse CNS analyzed by western blotting is shown in Fig. 1A. In all areas examined, Cx29 was detected as a monomer form at 31-33 kDa and a presumptive dimer at 51 kDa. A protein of unknown identity was detected at 38-39 kDa in some brain regions, but may represent a breakdown product of dimeric Cx29. Although not quantified, Cx29 levels were highest in caudal CNS structures, including brainstem, cerebellum and spinal cord, moderate in thalamus and hypothalamus and lowest in cerebral cortex and hippocampus, indicating greater Cx29 expression in progressively more caudal CNS areas. Subcellular localization of Cx29, determined by western blotting of brain subcellular fractions, indicated that the myelin fraction contained the greatest abundance of Cx29 (Fig. 1B). Levels were low in the mixed mitochondrial/synaptosomal fraction (P2), barely detectable in the microsomal (P3) and pure synaptosomal fractions, and undetectable in the soluble fraction, where anti-Cx29 recognized instead a protein of unknown identity migrating slightly faster than the Cx29 dimer. Designation of the 51 kDa immunoreactive protein as dimeric Cx29 is supported by the enrichment of this band in the myelin fraction comparable to that of Cx29 monomer.

In view of anatomical results indicating Cx29 expression by oligodendrocytes (see below), together with documented expression of Cx32 by these cells, the detection and immunoblotting profile of Cx29 was compared with that of Cx32 in brain tissue from WT and Cx32 KO animals (Fig. 1C). In subcellular fractions of myelin, Cx29 and Cx32 appeared as distinctly different bands, with Cx29 migrating slightly slower than Cx32, indicating that anti-Cx29 does not cross react with Cx32 and, conversely, anti-Cx32 does not cross react with Cx29. In homogenates of thalamus probed with anti-Cx32 antibody 7C7, Cx32 was detected in tissue from WT mice and was absent in Cx32 KO mice, confirming Cx32 recognition by this antibody. Similar results were obtained with the other antibodies listed in Table 1. In homogenates of thalamus probed with anti-Cx29 antibody, Cx29 was detected in both WT and Cx32 KO mice, further indicating

that the immunoreactive band designated Cx29 does not represent a cross reaction with Cx32. Comparable levels of Cx29 were observed in WT and Cx32 KO tissue, suggesting that deletion of the Cx32 gene had little effect on Cx29 expression. Detection of the epitope against which the anti-Cx29 antibody was raised is shown by western blotting, with and without antibody preadsorption with peptide immunogen (Fig. 1D). Antibody preadsorption eliminated both the monomer and dimer immunoreactive bands in homogenates of thalamus and the myelin subcellular fraction.

Cx29 localization in adult brain

Immunohistochemical labeling for Cx29 in various areas of the CNS is shown in Figure 2. In most regions of mouse CNS, intense Cx29-immunoreactivity was localized to fibers and fiber tracts. As illustrated in sections of olfactory bulb (Fig. 2A,B) and cerebral cortex (Fig. 2C,D), double immunofluorescence for the myelin and oligodendrocyte marker CNPase combined with Cx29 revealed nearly identical patterns of fiber labeling. Localization of Cx29 along fibers often matched that of CNPase (Fig. 2E,F), suggesting association of Cx29 with myelin. Although only evident at higher magnification, CNPase-immunopositive oligodendrocyte cell bodies displayed faint Cx29 immunofluorescence (Fig. 2E,F). No evidence was found for Cx29 labeling associated with neuronal or astrocyte cell bodies in any brain region examined, nor was labeling associated with leptomeningeal, vascular or ependymal structures. Immunofluorescence for Cx29 was most intense in white and gray matter of the thalamus (Fig. 2G), globus pallidus (Fig. 2I), spinal cord (Fig. 2J) and brainstem (not shown), all of which contain dense concentrations of myelinated fibers. Regions with a paucity of labeling for CNPase, such as the striatum (Fig. 2I) and superficial layers (lamina II) of the spinal cord dorsal horn (Fig. 2J; CNPase not shown), also displayed sparse labeling for Cx29. All labeling was eliminated after preadsorption of anti-Cx29 antibody with cognate peptide, as illustrated in thalamus (Fig. 2H). Comparisons of Cx29-immunoreactivity in mouse and rat CNS, shown in sections through the dentate gyrus of the hippocampus, indicated that Cx29 labeling along fibers in mouse brain (Fig. 2K) was also evident in rat brain (Fig. 2L).

An exception to Cx29 association with CNPase-positive fibers and oligodendrocyte somata occurred in the cerebellum. Although CNPase/Cx29 co-localization was observed in cerebellar white matter and the granule cell layer, the molecular layer was devoid of labeling for CNPase

(Fig. 2M), but displayed dense, punctate labeling with the anti-Cx29 antibody (Fig. 2N). The association of this labeling with either astrocytes, Bergmann glial cells or neurons in the cerebellar molecular layer remains to be determined. In western blots of the cerebellum compared with other brain regions, the anti-Cx29 antibody failed to detect any additional bands that would suggest cross reaction with a cerebellar protein not present elsewhere in brain. However, we cannot exclude the possibility of such a cross reaction.

Cx29 in developing brain

The developmental profile of Cx29 expression was examined by western blotting of tissue homogenates from cerebral cortex, thalamus and brainstem at various postnatal ages. Blots are shown at optimal exposure time to film (Fig. 3, left column), as well as after film over-exposure (Fig. 3, right column) to adequately illustrate the comparatively wide range of expression levels in different regions and at different ages. Cx29 was barely detectable at postnatal day 7 in all regions examined, even at long film exposure. At postnatal day 14, Cx29 levels were moderate in brainstem and undetectable in thalamus and cerebral cortex at normal film exposure, but faintly present in the latter two regions after long exposure. From day 20 to adult, levels increased in each area, with an overall caudal-rostral pattern in onset time and relative abundance of Cx29.

Examination of Cx29 in combination with CNPase in mice at various ages indicated first appearance of Cx29 at about postnatal day 8 in the corpus callosum, which contained some labeled fibers and oligodendrocytes (Fig. 4A,B). No labeling was evident elsewhere in brain. By postnatal day 14, numerous Cx29-positive oligodendrocytes were observed in most brain areas, as shown by CNPase/Cx29 double-labeling in cerebral cortex (Fig. 4C,D). Many oligodendrocyte somata at this age were much more intensely labeled for Cx29 than in adult brain, and each soma appeared to be associated with a surrounding field of weakly labeled fibers (Fig. 4D). Similar results were obtained at postnatal day 20, except that fewer oligodendrocyte cell bodies were intensely labeled, and labeling associated with myelinated fibers was increased. In adult brain, a few oligodendrocyte somata per section displayed intense labeling (not shown) comparable to that seen during the second postnatal week. Faint, presumably non-specific labeling of neuronal nuclei occurred in some preparations of CNS tissues from younger animals (Fig. 4D,F). Although most oligodendrocyte somata were intensely labeled for CNPase at postnatal day 14 and 20, a small proportion exhibited weak labeling at the latter age, as shown in

hypothalamus (Fig. 4E). It appeared that weak labeling for CNPase was accompanied by intense labeling for Cx29 (Fig. 4F) and, conversely, diminished labeling for Cx29 was accompanied by the typically intense labeling for CNPase seen in adult brain.

Confocal imaging of double-labeling for CNPase and Cx29 at postnatal day 14 clearly demonstrated intense intracellular labeling for Cx29 within oligodendrocyte cell bodies and in their processes surrounding individual cells (Fig. 4G). At this age, Cx29 immunofluorescence could occasionally be followed continuously from cell bodies to several initial processes and along fibers forming Cx29-positive arbors around oligodendrocytes (Fig. 4H).

Cx29 co-localization with CNPase and MAG

Confocal immunofluorescence was used to examine co-localization of Cx29 with the oligodendrocyte markers CNPase and MAG. Anti-CNPase and anti-MAG antibodies produced robust labeling of fibers and oligodendrocyte somata throughout the CNS. CNPase was diffusely localized in cells, while MAG was granular (Fig. 5). In double-labeled sections, Cx29 along fibers and in oligodendrocyte somata was co-localized with CNPase, as shown in thalamus (Fig. 5A) and cerebral cortex (Fig. 5B), and with MAG, as shown in cerebral cortex (Fig. 5C-E). By single scan imaging, Cx29 was distributed around the periphery of oligodendrocyte cell bodies, where it appeared either as continuous labeling or as fine puncta associated with the plasma membrane (Fig. 5, A2,B2,E2). Labeling for Cx29 was also observed intracellularly where it had a granular appearance (Fig. 5E2), and displayed partial association with granules labeled for MAG (Fig. 5E). Cx29 exhibited greater co-localization with MAG along fibers (Fig. 5D).

Cx29 co-localization with Cx32

Confocal double immunofluorescence labeling for Cx32 and Cx29 was used to determine the extent of co-localization between Cx29 and Cx32. Both connexins were present on large and small diameter fibers. Labeling for Cx29 along fibers showed considerable, but not total overlap with labeling for Cx32 (Fig. 6A). Large diameter fibers were often more heavily labeled for Cx32 than Cx29, despite the surrounding presence of smaller diameter fibers that were intensely labeled for Cx29, suggesting that the occurrence of differential labeling was not an artifact of tissue fixation conditions. Immunofluorescence for Cx32 was seen as relatively large puncta decorating oligodendrocyte somata and extending for short distances along their initial processes

(Fig. 6B1). Very little Cx32 was discernable intracellularly in these somata. This is in contrast to the much smaller Cx29 puncta associated with these cells, the virtual absence of Cx29 along their initial processes, and the abundance of Cx29 intracellularly (Fig. 6B2). Overlays of double labeling indicated that fine Cx29 puncta around the periphery of oligodendrocytes were frequently co-localized with the larger Cx32 puncta (Fig. 6B3). The distribution of Cx32 and Cx29 along individual fibers exhibited various patterns, but was often punctate (Fig. 6C,E) or intermittent, spanning the width of fibers (Fig. 6D). Cx32 and Cx29 were partially co-localized at these sites. Co-localization along medium and small fibers was also evident, but was more variable with one or the other connexin predominating. Confocal analysis of triple immunofluorescence labeling for Cx29, Cx32 and CNPase in brain sections was conducted to confirm that cells exhibiting co-expression of Cx32 (Fig. 6F1) and Cx29 (Fig. 6F2) were oligodendrocytes as revealed by their labeling for CNPase (Fig. 6F3), and overlap of labeling in merged images (Fig. 6F4).

Cx29 and Cx32 in relation to astrocytic connexins

Confocal analysis of astrocytic Cx43 and Cx30 in relation to Cx32 and Cx29 at gap junctions formed by oligodendrocytes is shown in Figures 7. Immunofluorescence for Cx43 throughout brain appears as densely distributed puncta, most of which represents labeling of gap junctions between astrocytes (Yamamoto et al., 1990a,b). However, a small percentage of these puncta were co-associated with punctate labeling for Cx32 on oligodendrocyte cell bodies and their processes, as shown in hypothalamus (Fig. 7A) and thalamus (Fig. 7B). These sites of co-association correspond to gap junctions between astrocytic Cx43 and oligodendrocytic Cx32, as previously reported (Rash et al., 2001). Confocal immunofluorescence of astrocytic Cx30 and oligodendrocytic Cx32 revealed similar co-association of punctate labeling for these two connexins on oligodendrocyte cell bodies (Fig. 7C), consistent with the ultrastructural co-localization of Cx30 and Cx43 at astrocyte gap junctions with oligodendrocytes (Rash et al., 2001). Labeling of cells for CNPase and Cx30 confirmed that Cx30-positive puncta decorated the surface of oligodendrocytes (Fig. 7D). In contrast, confocal analysis of double labeling for Cx43 and Cx29 in numerous brain areas examined, and illustrated in the globus pallidus (Fig. 7E) and hypothalamus (Fig. 7F), revealed only minor co-association of the two connexins at sites along the periphery of oligodendrocyte somata.

Confocal double labeling was undertaken to determine the degree to which Cx32 along myelinated fibers was associated with Cx43 and Cx30 in astrocytic processes that form gap junctions at abutments with myelinated fibers. As illustrated in cerebral cortex (Fig. 7G) and thalamus (Fig. 7H), fields with relatively dense Cx43-positive puncta and robust labeling for Cx32 along myelinated fibers showed only occasional overlap of labeling for the two connexins along fibers. Similarly, in areas with dense labeling for Cx30, such as thalamus (Fig. 7I) and habenula (Fig. 7J), labeling for Cx32 along myelinated fibers displayed only minor overlap with Cx30-immunopositive puncta. Thus, unlike Cx32 associated with oligodendrocyte somata, the bulk of Cx32 in oligodendrocyte processes that form myelin appears to have little association with astrocytic elements.

Cx32 localization to myelinated fibers in brain was confirmed using comparisons of Cx32 immunolabeling in WT and Cx32 KO mice. Anti-Cx32 antibody that showed an absence of Cx32 detection in brain of Cx32 KO mice by western blotting (Fig. 1C) produced robust labeling of CNPase-positive myelinated fibers throughout the brain of WT mice, as illustrated in the cerebral cortex (Fig. 8A). Authenticity of Cx32 labeling was indicated by the total absence of Cx32 immunoreactivity in a field of cerebral cortex containing dense labeling for CNPase in tissue from a Cx32 KO mouse (Fig. 8B). High magnification confocal micrographs of CNPase/Cx32 co-localization along myelinated fibers is shown in Figure 8C.

DISCUSSION

We have demonstrated that Cx29 is expressed by oligodendrocytes throughout the CNS and that it is localized to these cells and their myelinating processes in adult and developing brain. These results were corroborated by documenting Cx29 enrichment in subcellular fractions of myelin vs low levels in synaptosomal subfractions, which previously were reported to be enriched in astrocytic and neuronal connexins (Lynn et al., 2001). A similar localization of Cx32, including presence in oligodendrocyte somata, dense concentration along myelinated fibers and enrichment in myelin as previously reported (Li et al., 1997), was supported by the current demonstration of a total absence of immunofluorescence labeling and western blot detection of Cx32 in Cx32 KO mice. Despite their cellular co-expression, Cx29 was minimally co-localized with Cx32 on oligodendrocyte somata and only partly co-localized with Cx32 along myelinated fibers. The only departure from Cx29 localization exclusively in oligodendrocytes occurred in

the molecular layer of the cerebellum, which was devoid of labeling for CNPase but contained dense immunoreactivity with anti-Cx29 antibody. The identity of the protein detected in this cerebellar subregion and its subcellular localization remains to be determined.

In PNS, Cx29 localization described recently by Altevogt et al. (2002) is in agreement with our LM and FRIL observations of Cx29 in sciatic nerve (Li et al., 2002). In CNS, however, Altevogt et al. (2002) reported Cx29 and Cx32 expression in mutually exclusive subsets of oligodendrocytes in spinal cord and noted similar expression patterns in olfactory bulb, cerebrum, cerebellum and pons. In contrast, after examination of >50 oligodendrocytes per section encompassing many CNS regions, including spinal cord, in >100 sections taken from >20 brains, we found that virtually all CNPase-positive oligodendrocyte somata contained both Cx29 and Cx32. Altevogt et al. (2002) also reported Cx29 and Cx32 localization to mutually exclusive subsets of myelin sheaths in CNS, while our findings indicate partial co-localization of these connexins along many fibers. Reasons for these disparities may be due to differences in tissue preparation and differences in efficiency of connexin detection by different antibodies.

Connexins at astrocyte/oligodendrocyte junctions

It is becoming clear that gap junctions linking cells in the pan glial syncytium are composed of multiple connexins with selective cellular expression patterns; Cx26, Cx30 and Cx43 in astrocytes, and Cx32, Cx29 and Cx47 in oligodendrocytes (Nagy et al., 1997, 1999, 2000, 2001; Rash and Yasumura, 1999; Rash et al., 1997, 2001; Altevogt et al., 2002; Nagy et al., 2003a,b). The presence of six different connexins in macroglial cells raises questions concerning the extent to which GJIC within the syncytium is regulated by the organization of connexin coupling partners at A/O gap junctions. In particular, the non-permissiveness of Cx43 coupling with Cx32 (White and Bruzzone 1996), together with the present findings that Cx29 is very sparsely distributed on oligodendrocyte somata in adult brain and exhibits only minor co-localization with Cx43 on these somata, suggests little if any Cx32/Cx43 or Cx29/Cx43 coupling at A/O junctions. Further, it can be more generally inferred that Cx29 is minimally co-associated with astrocytic Cx26 and Cx30 at A/O gap junctions in adult brain. Oligodendrocytes were reported to express Cx45 (Dermietzel et al., 1997; Kunzelmann et al., 1997) and Cx43/45 coupling is permissive for functional channel formation (Bruzzone et al., 1996; White and Bruzzone, 1996). However, widespread expression of Cx45 in oligodendrocytes has not been documented. Astrocytic Cx43

at A/O junctions more likely couples with Cx47, which is highly expressed in oligodendrocytes and exhibits immunolabeling patterns similar to that of Cx32 on oligodendrocyte somata (Nagy et al., 2003a). This was further suggested in a recent study involving Cx32 KO mice, where astrocytic Cx26 and Cx30 were reduced and astrocytic Cx43 and oligodendrocytic Cx47 remained densely concentrated on oligodendrocyte somata despite the absence of Cx32 (Nagy et al., 2003b).

Cx29 expression during CNS development

Examination of Cx29 levels during development indicated a temporal and spatial expression pattern consistent with the known onset time and caudal to rostral progression of myelination along the neuraxis (Verity and Campagnoni, 1988). Unlike transiently elevated levels of several connexins during brain development (Prime et al., 2000), Cx29 protein continuously increased to maximum levels in adult CNS. The shift from robust immunolabeling for Cx29 in oligodendrocyte cell bodies at early ages to much lower levels in mature somata, together with increasing levels along myelinated fibers, indicates a primary function of Cx29 in mature myelin. Distinct patterns of labeling for Cx29 and Cx32 around oligodendrocytic somata and their differential detection intracellularly may reflect segregation of connexin trafficking in these cells. In studies of other cell types expressing two different connexins, it appears that intracellular trafficking routes from the endoplasmic reticulum to gap junctional plaques can occur via different pathways involving either a Golgi-microtubule transport system or a Golgi-independent process (George et al., 1999, Jordan et al., 1999, Martin et al. 2001; Lauf et al., 2002; Gaietta et al., 2002). Thus, Cx29 and Cx32 in oligodendrocytes may contain different subcellular targeting signals, as has been reported for other connexins (Martin et al., 2001), and may be packaged and transported differently. This is supported by our previous ultrastructural observations of an association of oligodendrocytic Cx32 with endoplasmic reticulum with no evidence of its intracellular vesicular localization (Li et al., 1997) and preliminary observations of Cx29 association with vesicular elements in these cells (A. Sik, unpublished observations). The lack of Cx29 detection in the initial processes of oligodendrocytes in adult brain, despite its presence in myelin, suggests the involvement of trafficking pathway resulting in transient epitope masking during exit of Cx29 from somal to fiber compartments. Alternatively, transit through initial processes may be very rapid, and low levels at these sites may preclude detection.

Connexins in myelin

One possible function for connexins in CNS myelin is gap junction formation between non-compacted cytoplasmic compartments at the outer loop of myelin and astrocytic elements that abut these internodal myelin compartments. The occurrence, if not the frequency, of such A/O gap junctions has been well documented (Luizzi and Miller, 1987; Massa and Mugnaini, 1982; Waxman and Black, 1984), and includes demonstrations of Cx43 on the astrocytic side of such junctions (Ochalski et al., 1997; Rash et al., 2001). Our results showing a paucity of Cx43 association with Cx32 along myelinated fibers suggests that A/O junctions along these fibers is unlikely to account for the abundance of oligodendrocytic connexins in myelin. An additional and/or alternative possibility involves Cx29 and Cx32 localization at paranodal loops and Schmidt-Lanterman incisures, as seen in peripheral nerves (Li et al., 2002; Altevogt et al., 2002). Incisures have been observed in vivo in nerves of living animals (Williams and Hall, 1970), and EM studies of PNS revealed that they consist of short, circumferential dilations of Schwann cell cytoplasm spanning the full breath of myelin along internodal regions (Hall and Williams, 1970; Ghabriel and Allt, 1981). Considering that myelin lamellae surrounding axons form impermeable barriers to diffusion of substances, it has been suggested that Schmidt-Lanterman incisures provide a route for metabolic support and maintenance of myelin sheaths (Webster, 1965; Williams and Hall, 1971a,b; Ghabriel and Allt, 1981). It has also been proposed that connexins at incisures form autologous or reflexive gap junctions between successive inner to outer cytoplasmic membranes, providing a pathway consisting of a series of gap junction channels for radial diffusion of ions and metabolites (Bergoffen et al., 1993; Scherer et al., 1995; Scherer, 1996; Bone et al., 1997; Balice-Gordon et al., 1998; Arroyo and Scherer, 2000).

The existence of Schmidt-Lanterman incisures within CNS myelin has been firmly established However, unlike the conical arrangement of successive radial cytoplasmic pockets at incisures in peripheral nerves, incisures in the CNS occur as series of pockets coursing radially in a zig-zag manner, do not always extend from the outermost to the innermost myelin lamella, and apparently are present only in the largest of central myelinated fibers (Bunge et al., 1960; Hirano and Dembitzer, 1967; Conradi, 1969; Hildebrand, 1971; Blakemore, 1969; Hildebrand et al., 1993). If Cx29 and Cx32 are concentrated at incisures in CNS, then differences in the central and peripheral organization of these structures may account for differences in connexin labeling

patterns observed in CNS compared with PNS myelin. Moreover, our observations of the presence of Cx32 and Cx29 along a large proportion of CNPase-positive fibers might have been interpreted as suggesting a wider occurrence of Schmidt-Lanterman incisures in the CNS than previously believed.

A more likely alternative is that Schmidt-Lanterman incisures may indeed be rare in the CNS as reported, and that Cx29 and/or Cx32 may only be partly localized to these structures in central myelin, as suggested by our observations. First, while many fibers contained both Cx29 and Cx32, some had a preponderance of one or the other connexin. Since all oligodendrocytes express both connexins, differential labeling of fibers for Cx29 and Cx32 is unlikely to be due to mutually exclusive expression of these connexins by subpopulations of oligodendrocytes, but rather to differential transport from somata to myelin. Second, the partial co-localization of Cx29 and Cx32 along individual fibers suggests some degree of functional independence of these proteins in myelin. And third, while MAG is highly concentrated at incisures in PNS, it does not appear to be enriched at these structures in CNS (Trapp et al., 1989), yet it exhibited co-localization with Cx29 and Cx32 in central myelin. These points taken together suggest targeting of one or both of these connexins to several subcellular compartments in CNS myelin, thus excluding their restricted localization to Schmidt-Lanterman incisures. The localization of connexins in CNS myelin sheaths remains to be determined EM methods, in particular whether gap junctions are present at incisures, whether Cx29 and Cx32 both contribute to the formation of such junctions, and whether these connexins have additional as yet undetermined functions, as previously discussed (Li at al., 2002).

ACKNOWLEDGEMENTS

We thank B. McLean and N. Nolette for excellent technical assistance. We also Dr. P.E. Braun for the generous gift of polyclonal anti-CNPase, Dr. E. L. Hertzberg for providing monoclonal anti-Cx32 antibody 7C7 and polyclonal antibody 18A, and Dr. K. Willecke for supplying Cx32 KO mice.

Table 1. Connexin antibodies used for western blotting and immunohistochemistry

Antibody	Type*	Epitope; Designation	Dilution	Reference; Source
Cx29	polyclonal	c-terminus; 34-4200	0.6 μg/ml	Li et al., 2002; Zymed
Cx30	polyclonal	c-terminus; 71-2200	2.5 μg/ml	Nagy et al., 1999; Zymed
Cx32	monoclonal	aa 235-246; 7C7	1:25	Li et al., 1997
Cx32	monoclonal	c-terminus; 35-8900	1 μg/ml	Zymed
Cx32	polyclonal	cytoplasmic loop; 71-0600	1.25 μg/ml	Li et al., 1997; Zymed
Cx32	polyclonal	c-terminus; 34-5700	2.5 μg/ml	Zymed
Cx32	polyclonal	c-terminus; sc-7258	2 μg/ml	Santa Cruz Biotech
Cx43	monoclonal	c-terminus; 35-5000	3.5 μg/ml	Zymed
Cx43	polyclonal	c-terminus; 71-0700	0.25 μg/ml	Li et al., 1998; Zymed
Cx43	monoclonal	aa 252-270; mab 3067	2 μg/ml	Chemicon
Cx43	polyclonal	aa 346-363; 18A	1:1000	Yamamoto et al., 1990a,b

*All monoclonal antibodies were raised in mouse. All polyclonal antibodies were raised in rabbit, except polyclonal anti-Cx32 sc-7258 which was raised in goat.

FIGURES

Fig. 1. Western blots of Cx29 and Cx32 in various neural tissues. In all blots, numbers at left correspond to molecular weight markers. **A:** Immunoblot showing regional levels of Cx29 in adult mouse brain. Monomeric and presumptive dimeric Cx29 are detected at 31-33 kDa and 51 kDa, respectively. **B:** Immunoblot showing Cx29 in soluble, microsomal membrane (P3), mitochondrial/synaptosomal (P2), myelin and synaptosomal subcellular fractions of adult brain. Cx29 is concentrated in the myelin fraction, and a protein of unknown identity at 48 kDa is detected in the soluble fraction. **C:** Immunoblots showing comparison of Cx29 and Cx32 migration profiles. Lanes loaded with protein from myelin fraction and from thalamus homogenate of WT and Cx32 KO mice were probed with the antibodies indicated. Cx29 and Cx32 appear as distinct bands, and Cx32 at 30-31 kDa in WT thalamus is absent in Cx32 KO thalamus. Anti-Cx29 antibody detects Cx29 as corresponding bands in WT and Cx32 KO thalamus. **D:** Immunoblots of the tissues indicated show elimination of Cx29 detection (lanes 2, 4) after preadsorption of anti-Cx29 antibody with cognate peptide.

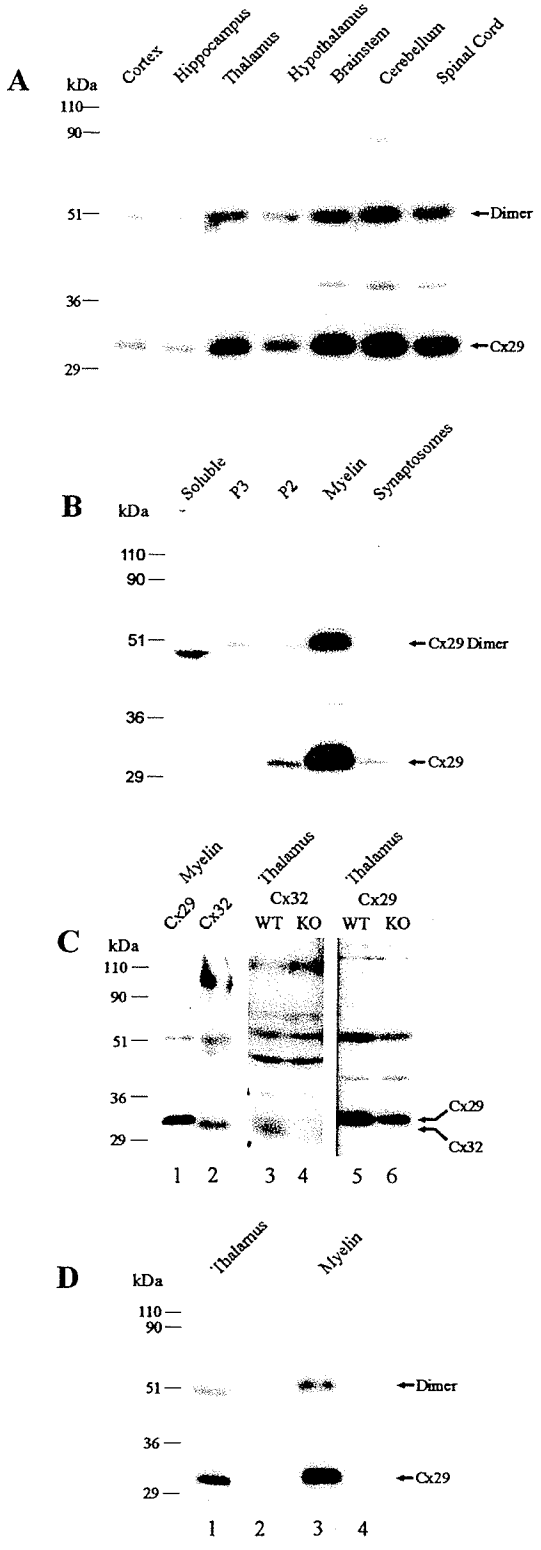
A
kDa
Cortex
Hippocampus
Thalamus
Hypothalamus
Brainstem
Cerebellum
Spinal Cord
110
90
51
36
29
Dimer
Cx29
B
kDa
Soluble
P3
P2
Myelin
Synaptosomes
110
90
51
36
29
Cx29 Dimer
Cx29
C
kDa
Myelin
Cx29
Cx32
Thalamus
Cx32
WT KO
Thalamus
Cx29
WT KO
110
90
51
36
29
Cx29
Cx32
1 2 3 4 5 6
D
kDa
Thalamus
Myelin
110
90
51
36
29
Dimer
Cx29
1 2 3 4

Fig. 1

Fig. 2. Immunofluorescence micrographs showing Cx29 localization in the CNS. **A-D:** Fields in olfactory bulb (A,B) and cerebral cortex (C,D) show overlapping distributions of fibers double-labeled for CNPase (A,C, arrows) and Cx29 (B,D, arrows). **E,F:** Magnification of cerebral cortex showing co-localization of CNPase (E) and Cx29 (F) along myelinated fibers (arrows) and oligodendrocyte somata (arrowheads). **G,H:** Area in thalamus (dorsal to the left) showing labeling for Cx29 (G) and elimination of labeling after preadsorption of anti-Cx29 with cognate peptide (H). **I:** Field at the border between striatum (Str) and globus pallidus (GP) showing Cx29 in fiber bundles, and in fibers scattered in neuropil of the GP. **J:** Lumbar spinal cord showing Cx29 in white matter and in myelinated fibers coursing through gray matter (arrows). **K,L:** Dentate gyrus of the hippocampus showing comparison of labeling for Cx29 in sections from mouse (K) and rat (L) brain. **M,N:** Field in a cerebellar folia showing co-localization of CNPase (M) and Cx29 (N) along myelinated fibers (arrows) in white matter and in the granule cell layer (GCL). Dense immunoreactivity with anti-Cx29 is also seen in the molecular layer (ML), which is devoid of CNPase-positive fibers. Scale bar: 100 μm (E,F, shown in F; all others shown in N).

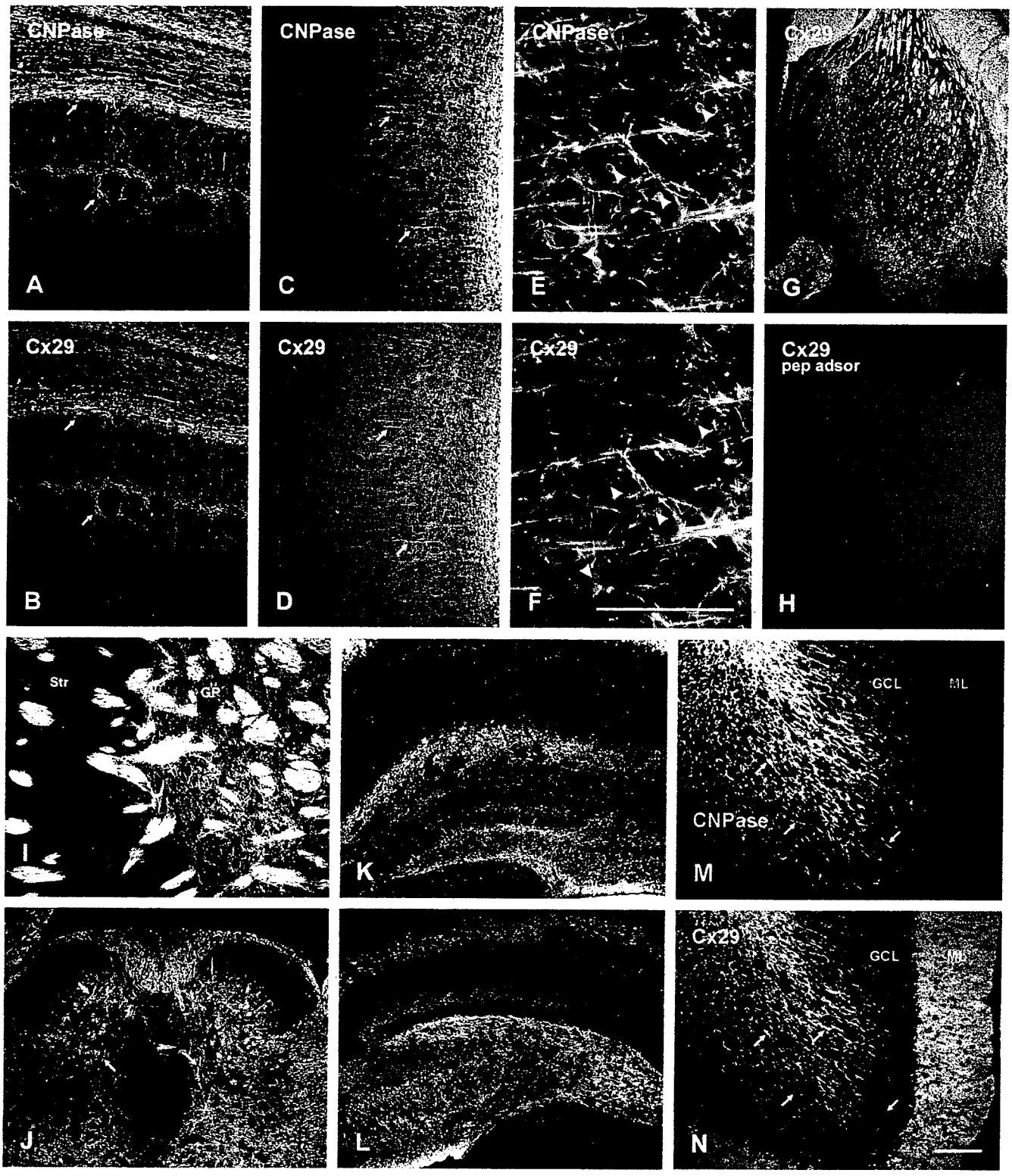
CNPase
A
CNPase
C
CNPase
E
Cx29
G
Cx29
B
Cx29
D
Cx29
F
Cx29
pep adsor
H
Str
GP
I
K
GCL
ML
CNPase
M
J
L
Cx29
GCL
ML
N

Fig. 2

Fig. 3. Western blots showing Cx29 levels in cerebral cortex (A), thalamus (B) and brainstem (C) during development. Lanes were loaded with equal protein from homogenates of structures at the postnatal ages in days (d) indicated. For comparison of levels, blots are shown after exposure to film for short (left blot for each structure) and long (right blot for each structure) duration. Cx29 levels are highest in adult brain, with increasing expression in each area during development.

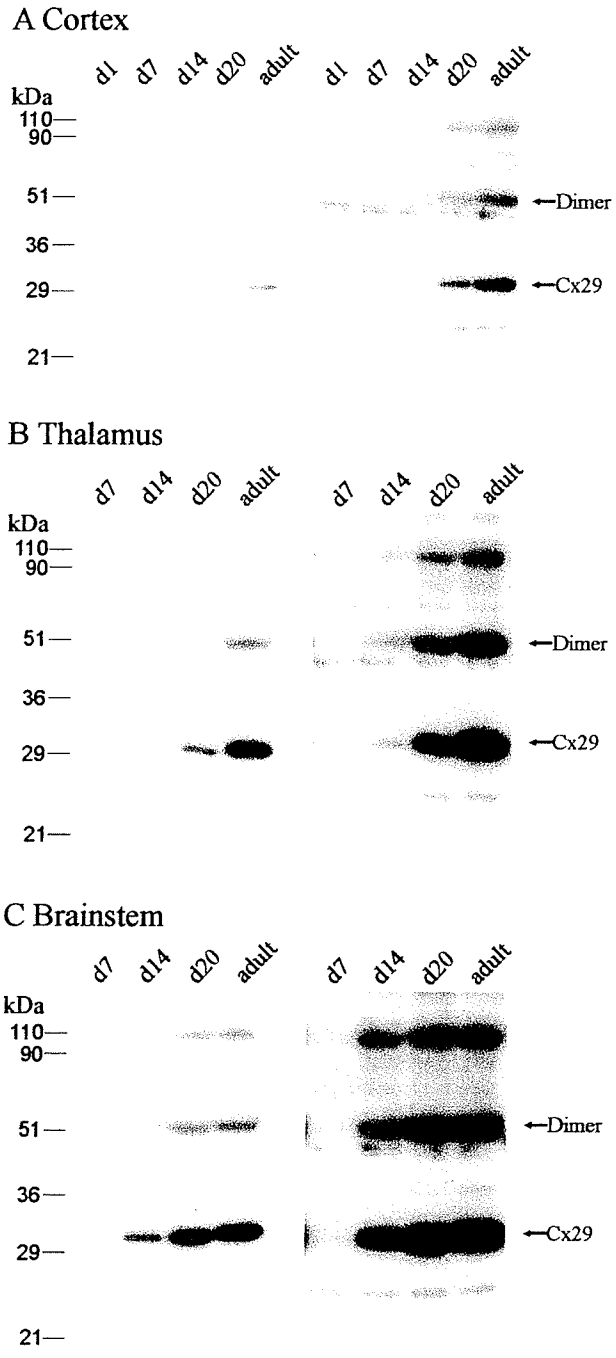
A Cortex
d1
d7
d14
d20
adult
d1
d7
d14
d20
adult
kDa
110
90
51
36
29
21
Dimer
Cx29
B Thalamus
d7
d14
d20
adult
d7
d14
d20
adult
kDa
110
90
51
36
29
21
Dimer
Cx29
C Brainstem
d7
d14
d20
adult
d7
d14
d20
adult
kDa
110
90
51
36
29
21
Dimer
Cx29

Fig. 3

Fig. 4. Immunofluorescence micrographs illustrating developmental profiles of Cx29. **A,B:** Double labeling in a field of corpus callosum at postnatal day 8 showing CNPase-positive fibers (A, arrows) and oligodendrocyte somata (A, arrowheads) labeled for Cx29 (B). **C-F:** Double-labeling for CNPase (C,E) and Cx29 (D,F) in a field of cerebral cortex (C,D) at postnatal day 14 and hypothalamus (E,F) at postnatal day 20. CNPase-positive fibers are sparsely labeled for Cx29 (arrows), while oligodendrocyte cell bodies (arrowheads) are intensely labeled for Cx29, but occasionally exhibit weak labeling for CNPase (E, double arrowheads). **G,H:** Confocal double immunofluorescence of fields in cerebral cortex at postnatal day 14 showing co-localization of labeling for CNPase (G1,H1) and Cx29 (G2,H2) around an oligodendrocyte (A, arrows), and several Cx29-positive processes emanating from a Cx29-positive oligodendrocyte somata (B, arrows). Scale bars: A-F, 100 μm; G,H, 20 μm.

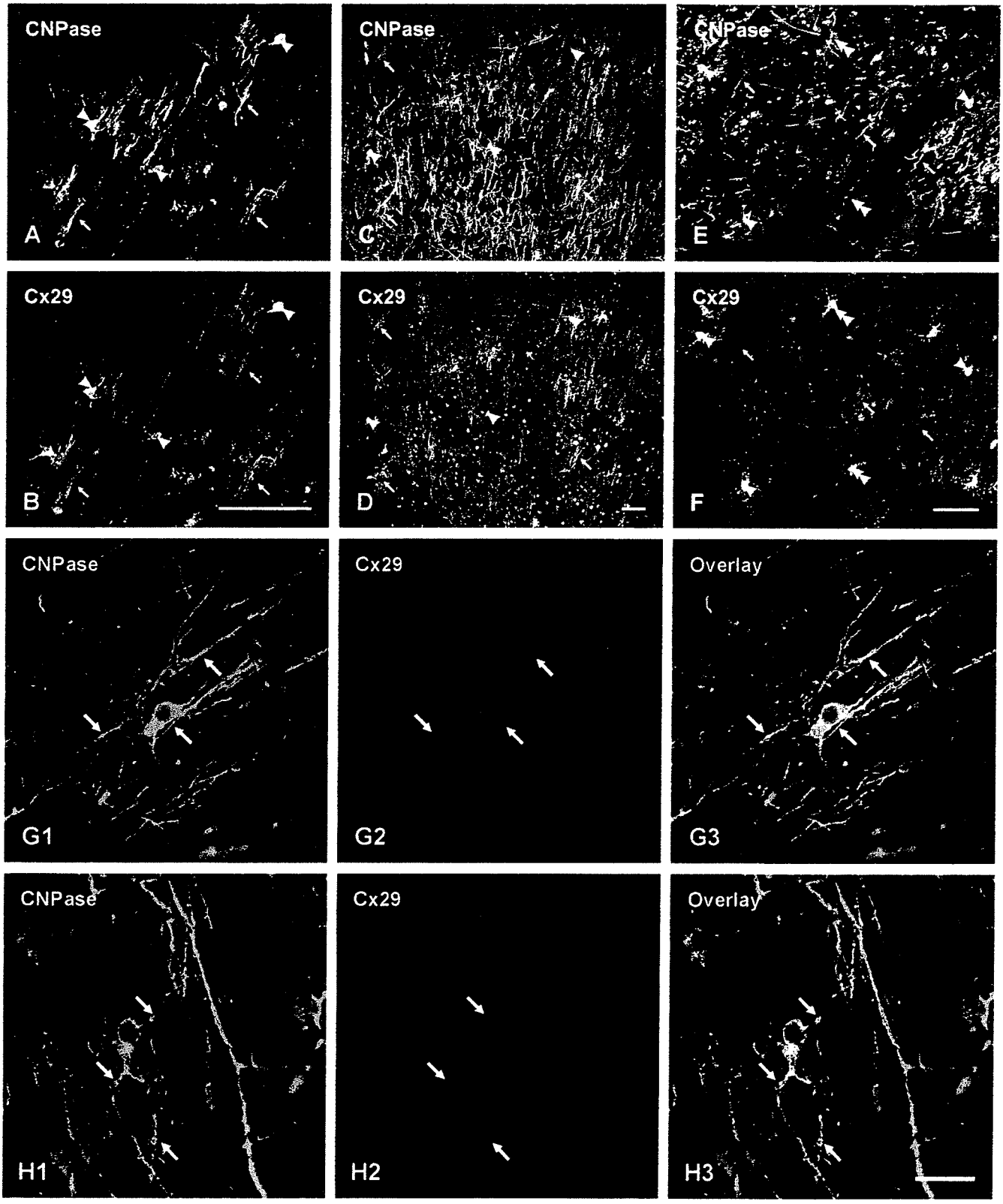
CNPase
A
CNPase
C
CNPase
E
Cx29
B
Cx29
D
Cx29
F
CNPase
G1
Cx29
G2
Overlay
G3
CNPase
H1
Cx29
H2
Overlay
H3

Fig. 4

Fig. 5. Confocal immunofluorescence showing association of Cx29 with the oligodendrocyte markers CNPase and MAG. **A,B:** Fields in ventroanterior thalamic nucleus (A) and in cerebral cortex (B) double-labeled for CNPase (A1,B1) and Cx29 (A2,B2). CNPase-positive fibers (arrows) and oligodendrocyte cell bodies (arrowheads) are immunopositive for Cx29 (yellow in image overlays, A3,B3). **C-E:** The same fields (C1,C2; D1,D2; and E1,E2) in cerebral cortex double-labeled for MAG and Cx29 as indicated. Low and high magnifications show substantial co-localization of MAG and Cx29 along myelinated fibers (arrows) and partial co-localization in oligodendrocyte somata (E, arrowhead) as shown by yellow in image overlays (C3,D3,E3). Scale bars: A-C, 20 μm; D,E, 2.5 μm.

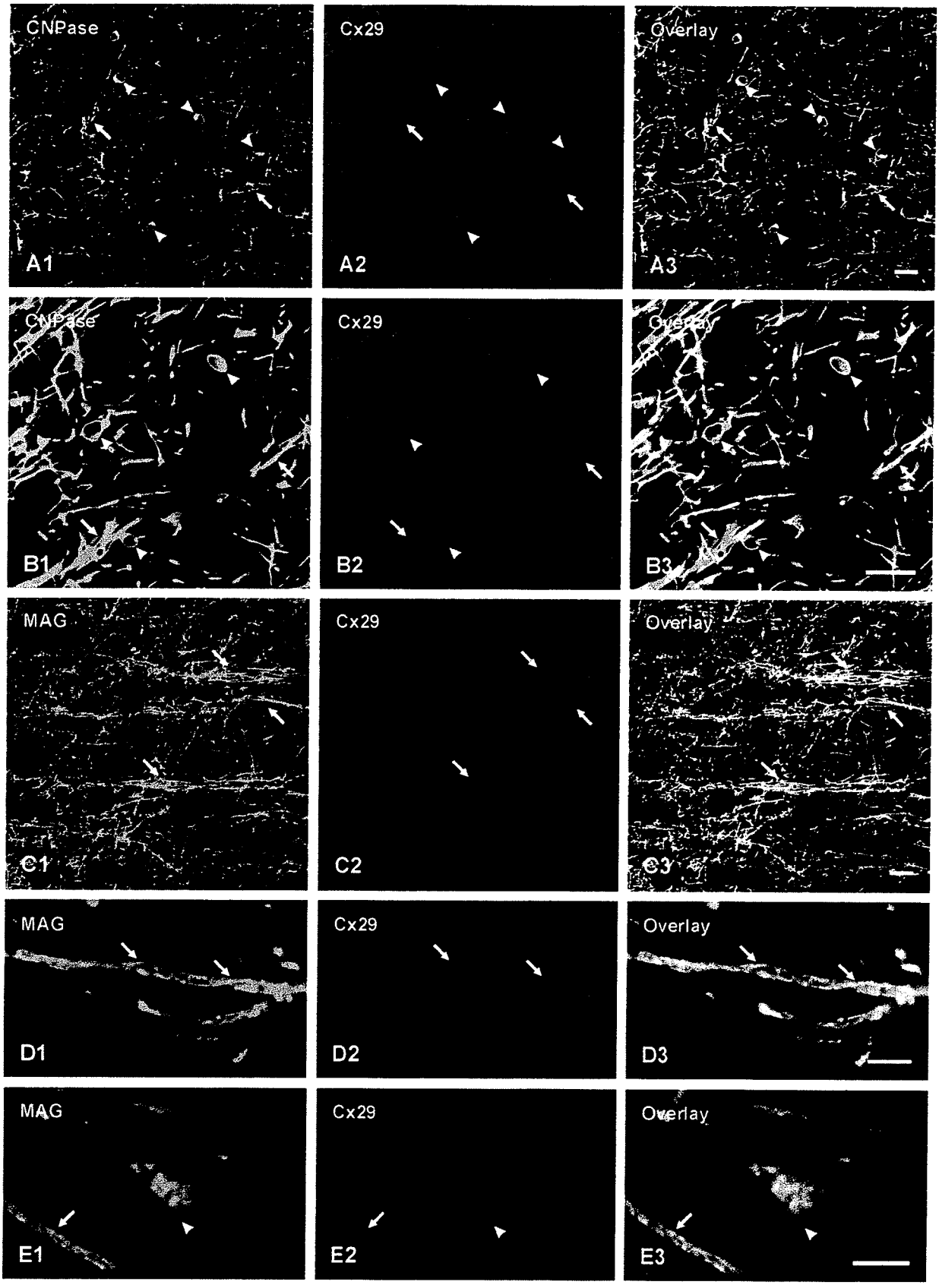
CNPase
Cx29
Overlay
A1
A2
A3
CNPase
Cx29
Overlay
B1
B2
B3
MAG
Cx29
Overlay
C1
C2
C3
MAG
Cx29
Overlay
D1
D2
D3
MAG
Cx29
Overlay
E1
E2
E3

Fig. 5

Fig. 6. Confocal immunofluorescence co-localization of Cx29 with Cx32 in adult brain. Each column of images in A to E illustrates a field double-labeled for Cx32 (green) and Cx29 (red), with co-localization appearing as yellow in image overlays. **A:** Low magnification in a field of thalamus showing Cx32 co-localization with Cx29 along myelinated fibers (arrows) and oligodendrocyte cell bodies (arrowheads). **B:** Oligodendrocyte somata in thalamus displaying punctate labeling for Cx32 (B1, arrowheads), finer punctate labeling for Cx29 intracellularly and at cell periphery (B2, arrowheads), and partial co-localization of the two connexins (B3). **C-E:** Labeling for Cx32 and Cx29 along myelinated fibers in cerebral cortex (C,D) and thalamus (E) appears as puncta (C,E, arrows) or intermittent stands (D, arrowheads), which exhibit partial co-localization (C3,D3,E3). **F:** Confocal triple-immunofluorescence showing that cells immunolabeled for Cx32 (F1, arrows) and Cx29 (F2, arrows) are CNPase-positive (F3, arrows), as seen in overlay of images (F4). Scale bars: A, 20 μm; B, 10 μm; C-E, (shown in C3), 5 μm; F, 5 μm.

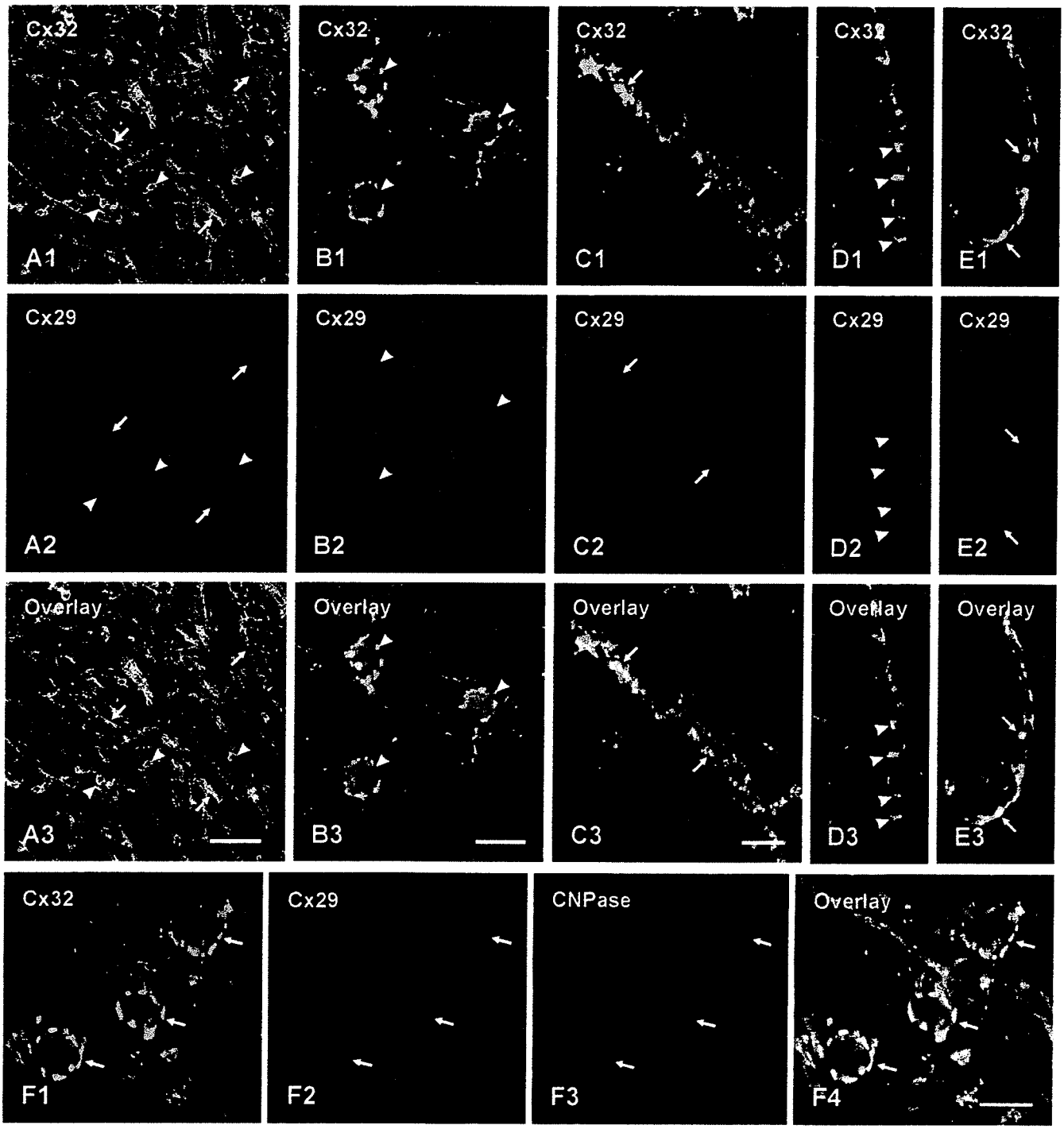
Cx32
A1
Cx32
B1
Cx32
C1
Cx32
D1
Cx32
E1
Cx29
A2
Cx29
B2
Cx29
C2
Cx29
D2
Cx29
E2
Overlay
A3
Overlay
B3
Overlay
C3
Overlay
D3
Overlay
E3
Cx32
F1
Cx29
F2
CNPase
F3
Overlay
F4

Fig. 6

Fig. 7. **A-C:** Confocal double immunofluorescence of Cx43 and Cx30 with Cx32 in adult brain. In fields of hypothalamus (A) and thalamus (B, shown only by overlay), some Cx43-positive puncta are co-associated with Cx32 on oligodendrocytes and their initial processes (A,B, arrows). In a field of cerebral cortex (C), intense punctate labeling for Cx30 (C1, arrows) is co-associated with Cx32 (C2, arrows) on oligodendrocyte somata (C3, overlay). **D:** Confocal double labeling showing Cx30 association with CNPase-positive oligodendrocyte in cerebral cortex (arrows) as seen by yellow in overlay. **E,F:** Confocal double labeling of Cx43 and Cx29 in adult brain. In fields of globus pallidus (E) and hypothalamus (F, shown only by overlay), minimal co-association of Cx43-positive puncta is seen with Cx29 on oligodendrocyte somata (arrows). **G-J:** Confocal double immunofluorescence labeling of astrocytic Cx43 (green) and Cx30 (green) in relation to labeling of Cx32 (red) along myelinated fibers. Overlay images of fields in cerebral cortex (G) and thalamus (H) show limited co-association of Cx43-positive puncta with Cx32-positive fibers (arrows). Overlay images of fields in thalamus (I) and habenula (J) show sparse co-association of Cx30-positive puncta with Cx32 along fibers (arrows). Scale bars: 5 μm.

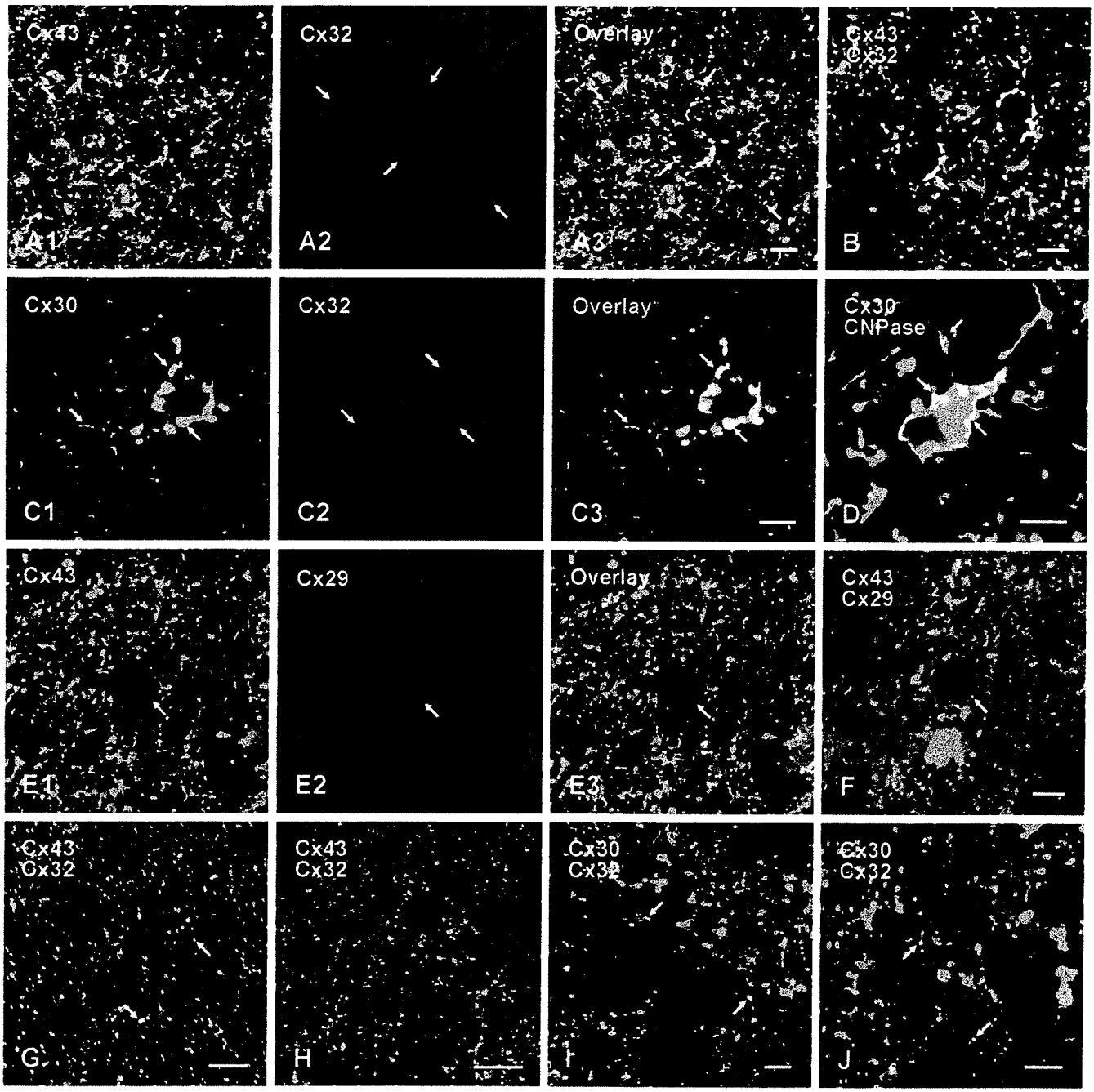
Cx43
A1
Cx32
A2
Overlay
A3
Cx43
Cx32
B
Cx30
C1
Cx32
C2
Overlay
C3
Cx30
CNPase
D
Cx43
E1
Cx29
E2
Overlay
E3
Cx43
Cx29
F
Cx43
Cx32
G
Cx43
Cx32
H
Cx30
Cx32
I
Cx30
Cx32
J

Fig. 7

Fig. 8. Immunofluorescence micrographs of Cx32 associated with myelinated fibers in mouse cerebral cortex. **A:** Low magnification of a cortical field from a WT mouse double-labeled for CNPase (A1) and Cx32 (A2) with co-localization shown in overlay (yellow in A3). **B:** A cortical field from a Cx32 KO mouse double-labeled for CNPase (B1) and Cx32 (B2) showing absence of Cx32 with consequent absence of yellow in overlay (B3). **C:** Confocal double immunofluorescence of a field in WT mouse showing CNPase-positive fibers (C1) labeled for Cx32 (C2) as seen by overlay (C3). Scale bars: A,B, 200 μm; C, 5 μm.

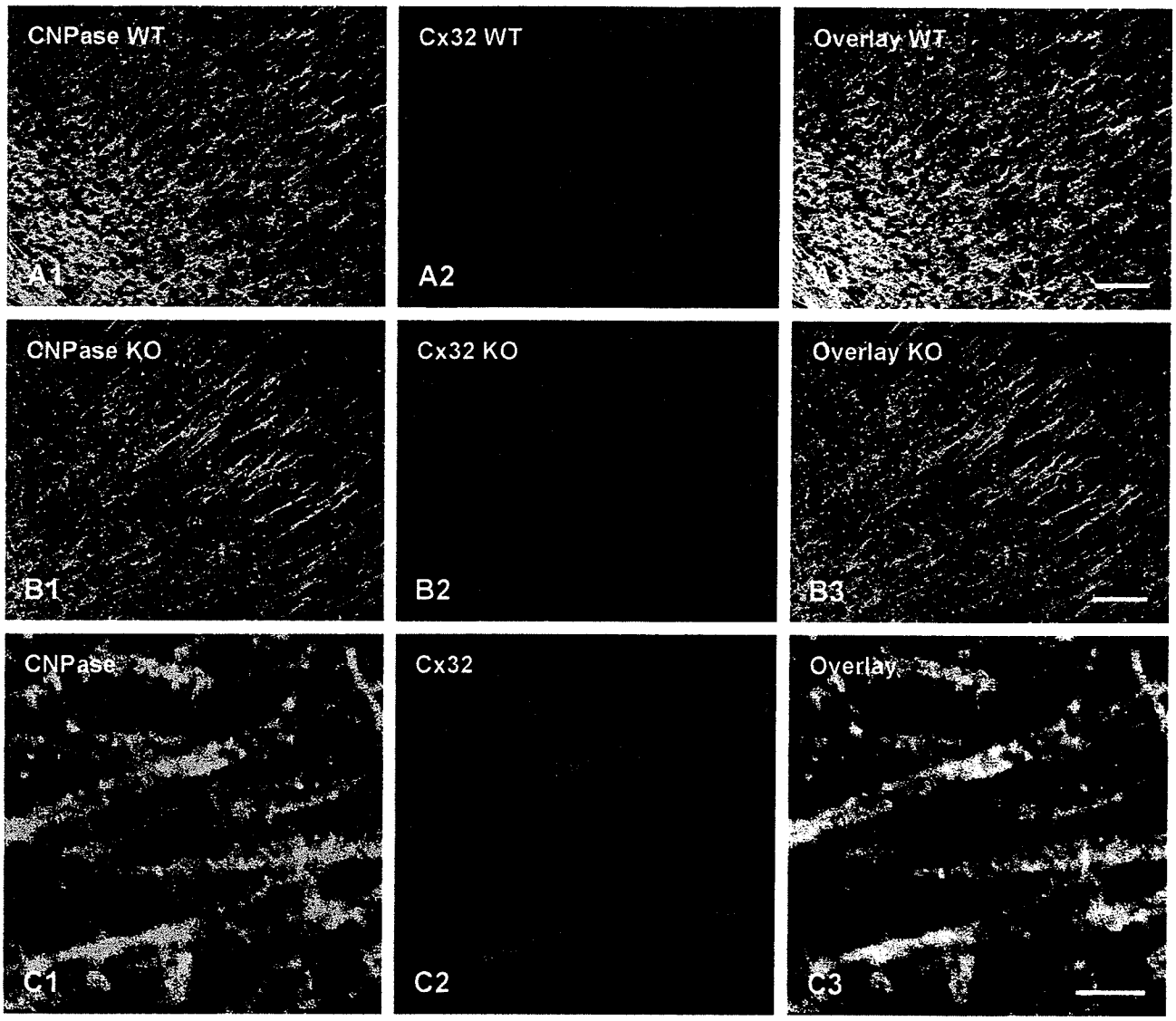
CNPase WT
Cx32 WT
Overlay WT
A1
A2
CNPase KO
Cx32 KO
Overlay KO
B1
B2
B3
CNPase
Cx32
Overlay
C1
C2
C3

Fig. 8

VI. PROJECT 2: Coupling of Astrocyte Connexins Cx26, Cx30, Cx43 to Oligodendrocyte Cx29, Cx32, Cx47: Implications From Normal and Connexin32 Knockout Mice

J. I. Nagy, A.-V. Ionescu, B. D. Lynn, and J. E. Rash

Glia, submitted

ABSTRACT

Oligodendrocytes in vivo form heterologous gap junctions with astrocytes, and these oligodendrocyte/astrocyte (O/A) gap junctions contain multiple connexins (Cx) including Cx26, Cx30 and Cx43 on the astrocyte side, and Cx32, Cx29 and Cx47 on the oligodendrocyte side. We investigated connexin associations at A/O gap junctions on oligodendrocytes in normal and Cx32 knockout (KO) mice. Immunoblotting and immunolabeling by several different antibodies indicated the presence of Cx32 in liver and brain of normal mice, but the absence of Cx32 in liver and brain of Cx32 KO mice, thereby confirming specificity and efficacy of the antibodies, as well as allowing the demonstration of Cx32 expression by oligodendrocytes. Oligodendrocytes throughout brain were decorated with numerous Cx30-positive puncta, which also were immunolabeled for both Cx32 and Cx43. In Cx32 KO mice, astrocytic Cx30 association with oligodendrocyte somata was nearly absent, Cx26 was partially reduced, and Cx43 was present in abundance. In normal and Cx32 KO mice, oligodendrocyte Cx29 was sparsely distributed, whereas Cx47-positive puncta were densely localized on oligodendrocyte somata. These results demonstrate that astrocyte Cx30 and oligodendrocyte Cx47 are widely present at A/O gap junctions. Immunolabeling patterns for these six connexins in Cx32 KO brain have implications for deciphering the organization of heterotypic connexin coupling partners at A/O junctions. The persistence and abundance of Cx43 and Cx47 at these junctions after Cx32 deletion, together with the paucity of Cx29 normally present at these junctions, suggests Cx43/Cx47 coupling at A/O junctions. Reductions in Cx30 and Cx26 after Cx32 deletion suggest that these astrocytic connexins likely form junctions with Cx32 and that their incorporation into A/O gap junctions is dependent on the presence of oligodendrocytic Cx32.

INTRODUCTION

Neurons, astrocytes and ependymocytes in the CNS form extensive homologous gap junctions (e.g., astrocyte-to-astrocyte, A/A junctions), whereas oligodendrocytes form only heterologous gap junctions with astrocytes (A/O junctions), but also form autologous junctions between myelin layers. Few if any gap junctions occur between two oligodendrocytes; however, oligodendrocytes indirectly communicate with each other through gap junctions with astrocyte "intermediaries" (Mugnaini, 1986; Wolburg and Rohlmann, 1995; Rash et al., 1997, 2001). Several different members of the connexin (Cx) family of proteins (Willecke et al., 2002) contribute to gap junctional intercellular communication (GJIC) at the gap junctions linking each macroglial cell type. These include Cx26, Cx30 and Cx43 in astrocytes (Yamamoto et al., 1990a,b; Nagy et al., 1997, 1999, 2001), and Cx29, Cx32 and Cx47 in oligodendrocytes (Dermietzel et al., 1997; Kunzelmann et al., 1997; Altevogt et al., 2002; Nagy et al., 2003a,b). A related but controversial issue is whether Cx32 is expressed exclusively by oligodendrocytes as reported by us (Li et al., 1997; Rash et al., 2001), or whether Cx32 is additionally expressed by neurons as reported by others (reviewed in Nagy et al., 2003a). Thin-section electron microscopy (EM) and freeze-fracture replica immunogold labeling (FRIL) studies have indicated that the three astrocytic connexins Cx26, Cx30 and Cx43 are each incorporated not only into individual A/A junctions, but also into the astrocyte side of A/O junctions (Nagy et al., 1999; Rash et al., 2001). Although relationships between Cx30 and oligodendrocytes has yet to be examined by light microscopy (LM), punctate labeling for astrocytic Cx26 and Cx43 was demonstrated around oligodendrocyte somata, and this labeling was co-associated with oligodendrocytic Cx32 (Rash et al., 2001; Nagy et al., 2001). Because the set of connexins in astrocytes is completely different from the set of connexins in oligodendrocytes, connexon channels at A/O gap junctions are necessarily heterotypic, meaning that heteromers of connexins forming connexons in astrocytes couple with entirely different connexin constituents in oligodendrocytes. Some connexin coupling pairs are permissive for the formation of functional GJIC channels (e.g., Cx30/Cx32), while others are not (Cx43/Cx32) (White and Bruzzone, 1996). Nevertheless, the specific connexin pairing combinations that occur at A/O junctions are completely unknown.

The aims of this study were three-fold. First, immunolabeling patterns of Cx32 in wild type (WT) and Cx32 knockout (KO) mice were investigated to confirm specificities of anti-Cx32 antibodies, as well as to confirm positive Cx32 localization in CNS of WT animals. Second, the

relative association of astrocyte Cx30 with oligodendrocyte Cx32 was investigated by LM. Third, we investigated whether the profile of astrocytic and oligodendrocytic connexins at A/O junctions is altered in Cx32 knockout (KO) mice (Nelles et al., 1996).

MATERIALS AND METHODS

Animals, Antibodies and Immunoblotting

A total of 25 normal male CD1 mice, 8 male WT C57BL/6 mice, and 9 male C57BL/6 Cx32 KO mice (the latter kindly provided by Dr. K. Willecke, University of Bonn, Germany) were used in this study. The WT and KO C57BL/6 animals were bred according to standard protocols at Colorado State University. Liver and brain from 3 WT and 4 KO mice were taken for western blotting analyses by methods previously described (Li et al., 1997, 1998, 2002; Rash et al., 2001). The remaining mice were used for anatomical studies.

The anti-connexin antibodies used, their sources and reference citations to previous characterizations are listed in Table 1. Monoclonal and polyclonal anti-Cx32 antibodies directed against different sequences in Cx32 were tested. Antibodies used as markers of oligodendrocytes included monoclonal anti-2,'3'-cyclic nucleotide 3'-phosphodiesterase (CNPase) (Sternberger Monoclonals, Baltimore, MD), and polyclonal anti-CNPase (Gravel et al., 1994), kindly provided by Dr. P. E. Braun (McGill University, Montreal, Canada).

LM Immunohistochemistry

Mice were deeply anesthetized with equithesin (3 ml/kg) (Scadding, 1981) and perfused transcardially with 3 ml of "prefixative" solution consisting of cold (4°C) 0.1 M sodium phosphate buffer (PB), pH 7.4, containing 0.9% NaCl (PBS), 0.1% sodium nitrite and heparin (1 unit/ml). This was followed by perfusion with 20 ml of cold 0.16 M sodium phosphate buffer, pH 7.6, containing 4% formaldehyde and 0.2% picric acid, which was followed by perfusion with 10 ml of PB, pH 7.4 containing 10% sucrose. Brains were removed and stored at 4°C for 48 hr in cryoprotectant consisting of 50 mM PB and 10% sucrose.

Cryostat tissue sections (10 μm thick) were obtained and collected on gelatinized glass slides and processed for immunofluorescence. All antibodies were diluted in 50 mM Tris-HCl, pH 7.4, containing 1.5% NaCl (TBS), 0.3% Triton X-100 (TBST) and 4% normal goat serum (NGS), and all washes were performed in TBST. For single labeling, sections were incubated for 24 hr at

4°C with either monoclonal mouse anti-Cx32 (7C7, derived from culture supernatant) diluted 1:25, monoclonal mouse anti-Cx32 (35-8900) diluted 1:400, monoclonal anti-Cx32 (13-8200) diluted 1:500, polyclonal rabbit anti-Cx32 (71-0600) diluted 1:100, or rabbit anti-Cx32 (34-5700) diluted 1:100. After primary antibody incubations, sections were washed for 1 hr in TBST and then incubated for 1.5 hr at room temperature with either fluorescein isothiocyanate- (FITC-) conjugated horse anti-mouse IgG (Vector Laboratories, Burlingame, CA) diluted 1:100, Cy3-conjugated goat anti-mouse (Jackson ImmunoResearch Labs, West Groove, PA) diluted 1:200, or Cy3-conjugated donkey anti-rabbit (Jackson ImmunoResearch Labs) diluted 1:200.

Sections processed for double immunofluorescence labeling of Cx32 and Cx30 were incubated for 24 hr at 4°C with monoclonal mouse anti-Cx32 (7C7 or 35-8900) as described above, plus polyclonal rabbit anti-Cx30 (71-2200) diluted 1:100. Alternatively, sections were incubated simultaneously with polyclonal rabbit anti-Cx32 (34-5700) as described above, and monoclonal anti-Cx30 (33-2500) diluted 1:500. Sections were then washed in TBST for 1 hr at room temperature and incubated simultaneously with appropriate combinations of (FITC)-conjugated horse anti-mouse IgG diluted 1:100, Alexa Fluor-conjugated goat anti-rabbit $F(ab')_2$ (Molecular Probes, Eugene, OR) diluted 1:1000, or Cy3-conjugated goat anti-mouse or donkey anti-rabbit IgG (Jackson ImmunoResearch Labs) diluted 1:200. The same protocol was followed for double immunofluorescence labeling of Cx30 and Cx43 using polyclonal rabbit anti-Cx30 diluted 1:100 and monoclonal mouse anti-Cx43 (33-5000) diluted 1:150. Sections were then incubated with appropriate combinations of secondary antibodies, as described above.

Sections processed for double immunofluorescence labeling of CNPase with either Cx26, Cx29, Cx30, Cx32, Cx43 or Cx47 were incubated for 24 hr at 4°C with monoclonal mouse anti-CNPase diluted 1:5000, and simultaneously with either polyclonal rabbit anti-Cx26 (51-2800) diluted 1:200, rabbit anti-Cx29 (34-4200) diluted 1:400, rabbit anti-Cx30, rabbit anti-Cx32 (71-0600 or 34-5700), rabbit anti-Cx43 diluted as above, or rabbit anti-Cx47 (36-4700) diluted 1:400. Additional sections were incubated with polyclonal rabbit anti-CNPase diluted 1:1000 and simultaneously with either monoclonal mouse anit-Cx26 (33-5800) diluted 1:200, monoclonal anti-Cx32 (7C7 or 35-8900), or monoclonal mouse anti-Cx43 all diluted as above. Sections were then washed and incubated simultaneously with Cy3-conjugated donkey anti-rabbit IgG and FITC-conjugated horse anti-mouse IgG, as described above. All sections were washed for 20 min in TBST, followed by two 20 min washes in 50 mM Tris-HCl buffer, pH 7.4, and

coverslipped with antifade medium. Control procedures were conducted by omission of one or the other of the primary antibodies with inclusion of both of the secondary antibodies. No labeling occurred with secondary antibodies that corresponded to the omitted primary antibody.

Fluorescence was examined on a Zeiss Axioskop2 fluorescence microscope and an Olympus Fluoview IX70 confocal microscope. For confocal analysis, double-labeled sections were scanned twice using single laser excitation for one or the other fluorochrome. Images were acquired by single scan of sections at sufficient magnification to discern individual immunolabeled puncta. Images were captured using Axiovision 3.0 (Carl Zeiss Canada, Toronto, Ca) software, assembled according to appropriate size and adjusted for contrast based on elimination of "empty" pixels in either Photoshop 6.0 or Corel Draw 8.

Data Analysis

To determine quantitatively the density of Cx30-positive puncta on the astrocytic side of A/O junctions on oligodendrocyte somata in brains of WT and Cx32 KO mice, the numbers of immunofluorescent puncta on CNPase-positive oligodendrocytes were counted in four different brain regions including cerebral cortex, globus pallidus, ventral lateral nucleus of the thalamus and hypothalamus. Counting was performed under immunofluorescence microscopy at 40X magnification in a grid-like fashion that allowed examination of consecutively adjacent areas in a non-overlapping pattern. A conservative approach was taken such that only clearly distinguishable and distinct puncta were counted at a single optimal focal plane on individual oligodendrocyte soma. Data were collected from groups of 3 WT and 3 Cx32 KO mice, and statistically analyzed by Students' t test. The mean number of Cx30-positive puncta (± SEM) surrounding oligodendrocytes in each brain region in each animal was obtained by pooling counts from both sides of the brain for each brain region examined. The total number of oligodendrocytes examined in each brain area in a total of 14 sections from the 3 WT and 3 KO animals is indicated in Table 2. The frequency distribution of the number of Cx30-positive puncta per oligodendrocyte in cortex and globus pallidus was derived by pooling data from 3 WT animals, and plotted by binning puncta numbers into 12 groups ranging from 0 to 22 puncta.

RESULTS

Cx32 and Cx47 Detection in WT and KO Mice

Five anti-Cx32 antibodies used for immunoblotting of WT mouse liver (and rat liver shown with two of the antibodies for comparison) detected monomeric Cx32 migrating at 30-32 kDa. In contrast no detection of Cx32 was observed in Cx32 KO mice (Fig. 1A). In addition, four of the antibodies detected dimeric Cx32 migrating at 49-52 kDa in normal mouse liver, and this dimer was absent in liver of KO animals. Detection of the dimer form in rat liver was variable. Using two of the anti-Cx32 antibodies, western blotting of brain tissue revealed Cx32 in thalamus of WT, but not in thalamus of Cx32 KO animals (Fig. 1B,C). Dimeric Cx32 was either not detected or was obscured by co-migrating non-specific bands. Other non-specific bands are of unknown identity, and possible relationships of these bands to immunofluorescence images are described below. Western blotting of various brain regions from WT mice (Fig. 1D) with anti-Cx47 antibody (directed against a nineteen animo acid sequence in the carboxy terminus of Cx47) revealed a band migrating at 50-52 kDa in 9% polyacrylamide gels. Analysis on 12.5% gels gave a similar apparent molecular weight (Fig. 1E), but Cx47 was resolved as a closely migrating doublet of bands, possibly reflecting different post-translational modification states of Cx47, as has been observed with Cx43 in brain (Li et al., 1998). There were no detectable differences in migration profiles or relative levels of Cx47 in CNS tissues of WT vs Cx32 KO mice (Fig. 1E).

Immunolabeling for Cx32 in liver of WT and Cx32 KO mice is shown in Fig. 2A-D. With all five antibodies (data from 13-8200 not shown), non-specific background immunoreactivity was low and clear punctate labeling was seen around hepatocytes in WT liver, whereas Cx32 labeling was absent in liver of Cx32 KO mice. Similar dense, punctate labeling for Cx26 was evident around hepatocytes in liver of WT mice, but labeling for Cx26 was barely detectable in liver of Cx32 KO animals (not shown), confirming previous reports (Nelles et al., 1996).

LM immunofluorescence was conducted to confirm that Cx32 is expressed by oligodendrocytes in the WT stain of C57BL/6 mice, as reported in other mouse stains (Li et al., 1997; Rash et al., 2001). Double-labeling revealed that cells immunopositive for the oligodendrocyte marker CNPase (Fig. 2E1) were consistently labeled for Cx32 (Fig. 2E2). Cx32 in brain was also associated with myelin of CNPase-positive fibers (Fig. 2), which accounts for additional Cx32-immunoreactivity not associated with oligodendrocyte somata in fields labeled for Cx32. A similar pattern of labeling around oligodendrocytes was obtained with each of the

five anti-Cx32 antibodies. The authenticity of this labeling was tested in Cx32 KO mice. Fields of brain demonstrating the presence of CNPase-positive oligodendrocyte cell bodies and myelinated fibers (Fig. 2F1) exhibited total absence of labeling of somata and myelinated fibers (Fig. 2F2) with all five Cx32 antibodies. In WT mice, widespread Cx32 labeling of oligodendrocyte somata is illustrated in a field of hypothalamus (Fig. 2G1). In KO mice, the absence of Cx32 labeling is illustrated in similar areas of hypothalamus (Fig. 2G2).

Despite the occasional presence of non-specific bands observed on western blots of brain tissue with some anti-Cx32 antibodies, all Cx32 immunolabeling was absent in brain of Cx32 KO mice with antibodies 7C7, 35-8900 and 34-5700. However, in addition to labeling of oligodendrocytes, antibody 13-8200 gave intense, diffuse labeling throughout brain, and antibody 71-0600 labeled fine varicose axons in restricted brain regions (e.g. amygdala), neither of which were eliminated in Cx32 KO animals, indicating cross reactions with other proteins. Thus, use of the latter two antibodies for immunohistochemical studies involving CNS tissues requires caution. In addition, a difficulty was encountered with monoclonal anti-Cx30 (33-2500). While single immunolabeling with this antibody produced robust detection of Cx30 in brain, double-labeling with accompanying controls revealed that monoclonal anti-Cx30 not only was detected by anti-mouse secondary antibodies, but also by Cy3-, FITC- and AlexaFuor-conjugated anti-rabbit antibodies (Jackson ImmunoResearch Labs; Molecular Probes). This cross species reactivity precludes use of Ab33-2500 for double labeling with rabbit primary antibodies.

Connexin Localization in WT Mice

Laser scanning confocal immunofluorescence, undertaken to confirm Cx32 localization to oligodendrocytes in C57BL/C6 mice, revealed numerous Cx32-positive puncta around oligodendrocyte cell bodies and their initial processes (Fig. 3A). A similar pattern of labeling around oligodendrocytes was obtained with each of the five anti-Cx32 antibodies, four of which were used in subsequent confocal LM studies, with exclusion of 13-8200.

To establish widespread astrocytic Cx30 association with oligodendrocytic Cx32 by LM, as reported in restricted brain regions examined by EM (Rash et al., 2001), confocal analysis was conducted after double-labeling for these two connexins in brain sections from WT C57BL/6 mice. In cerebral cortex, Cx30 labeling was widespread, reflecting primarily the distribution of A/A gap junctions. However, a small fraction of Cx30-positive puncta overlapped with Cx32-

positive puncta (Fig. 3B) in a manner reflecting the distribution pattern of Cx32 associated with CNPase (Fig. 3A). Similar results were obtained in many brain regions examined including globus pallidus (Fig. 3C), ventrolateral thalamic nucleus (Fig. 3D) and ventroanterior thalamus nucleus (Fig. 3E), where only the overlays of double labeling for Cx30 and Cx32 are shown. In fields labeled for Cx32, immunoreactivity that was not localized to oligodendrocyte somata was associated with CNPase-positive myelinated fibers (Fig. 3A). Double labeling for Cx43 and Cx30 also showed co-localization of these two connexins on the surface of oligodendrocytes (Fig. 3F), consistent with previous demonstrations of Cx43 association with Cx32 on these cells (Rash et al., 2001). Similar results were obtained in brain sections of CD1 mice (not shown).

Connexin Localization in Cx32 KO Mice

The deployment of astrocytic Cx30, Cx43 and Cx26 to the surface of oligodendrocytes was examined in Cx32 KO and compared with their distributions in WT mice. In cerebral cortex and many subcortical regions of WT brain, oligodendrocytes were conspicuous in sections labeled for Cx30 by virtue of their dense decoration with Cx30-positive puncta (Fig. 4A). Immunofluorescence of oligodendrocyte-associated Cx30 puncta was usually more intense than the more widely distributed Cx30 puncta that presumably were localized to gap junctions between astrocytes (Nagy et al., 1999, 2001; Rash et al., 2001). In similar fields of cerebral cortex and other regions of Cx32 KO brain, oligodendrocytes were virtually devoid Cx30-positive puncta (Fig. 4B). Confocal analysis of cerebral cortex confirmed that CNPase-positive cells in cerebral cortex of WT mice were decorated by Cx30-positive puncta (Fig. 4C), while CNPase-positive cells in cerebral cortex of Cx32 KO mice displayed vastly reduced labeling for Cx30 (Fig. 4G). Similar results were obtained in other brain regions of WT and Cx32 KO mice including globus pallidus (Fig. 4D,H), ventrolateral thalamic nucleus (Fig. 4E,I) and hypothalamus (Fig. 4F,J).

Frequency distributions of the percentage of CNPase-positive oligodendrocytes displaying puncta on their surface at a single focal plane in fields of cerebral cortex and globus pallidus is shown in Fig. 5. The data shown is an underestimate of the number of puncta per oligodendrocyte, as out-of-focus puncta on cells were not counted. Nevertheless, these images indicate that oligodendrocytes displayed a wide range of Cx30 puncta, with most oligodendrocyte images having 7-8 puncta in a single focal plane. In four brain areas examined

quantitatively and within the limit of LM resolution, Cx30-labeled puncta on CNPase-positive oligodendrocytes were reduced by 90% in Cx32 KO compared with WT mice (Table 2).

The density and distribution of Cx43-positive puncta on CNPase-positive oligodendrocytes in cerebral cortex of WT mice (Fig. 6A) was similar to that in Cx32 KO mice (Fig. 6E). Although not quantified, similar results were obtained in other brain areas including striatum, globus pallidus and ventroanterior thalamic nucleus, as shown by overlay of double-labeled images of these areas of WT (Fig. 6B-D) and KO (Fig. 6F-H) animals. The distribution of Cx47 around CNPase-positive oligodendrocyte somata and their initial processes throughout CNS of WT mice was very similar to that of Cx32 in cerebral cortex (Fig. 6I) and other brain regions examined (Fig. 6J-L). Preliminary FRIL and thin-section EM results indicate Cx47 localization on the oligodendrocyte side of gap junctions that these cells form with astrocytes (unpublished observations). In Cx32 KO mice, no change in the distribution of Cx47-positive puncta around oligodendrocytes was evident in cerebral cortex (Fig. 6M) or other brain areas (Fig. 6N-P).

Analysis of double-labeling for CNPase and Cx26 in various subcortical brain areas revealed oligodendrocytes displaying numerous Cx26-positive puncta on their surface in WT mice (Fig. 7A), with patterns similar to that of Cx30 and Cx43, whereas CNPase-positive cells exhibited reduced Cx26-positive puncta in Cx32 KO mice (Fig. 7B). Although not quantitatively analyzed, this result was representative of hundreds of CNPase-positive oligodendrocytes examined in 5 WT and 5 KO mice. The expression and localization of Cx29 in oligodendrocytes (described in detail elsewhere, Nagy et al., 2003a) was dissimilar to the appearance of labeling for Cx32 and Cx47 associated with oligodendrocytes in that Cx29 immunofluorescence appeared as much finer puncta localized to the somatic plasma membrane, with some labeling evident intracellularly, and was rarely observed on initial processes in adult animals. No differences in Cx29-immunoreactivity around oligodendrocytes were evident from comparisons of CNPase/Cx29 double-labeling in brains of WT (Fig. 7C) and Cx32 KO (Fig. 7D) animals.

DISCUSSION

The present results demonstrate that several of the anti-Cx32 antibodies utilized immunohistochemically (7C7, 35-8900, 34-5700) detect exclusively Cx32 in the CNS, whereas other antibodies have additional cross reactivities (13-8200, 71-0600). Three of the antibodies produced labeling associated with oligodendrocytes in WT mice, and no residual labeling

associated with glia or neurons was seen in Cx32 KO mice. Cx30 was shown to be heavily distributed around oligodendrocyte somata, where it was invariably co-localized with astrocytic Cx43 and co-associated with oligodendrocytic Cx32. Comparisons of astrocytic connexins at the surface of oligodendrocytes in WT and Cx32 KO mice indicated that Cx26 and Cx30 were reduced, while Cx43 appeared to be unaffected. Deletion of Cx32 had little effect on Cx29 and Cx47 in oligodendrocytes. These results were consistently obtained after examination of hundreds of oligodendrocytes in dozens of brain sections from over thirty animals subjected to various fixation conditions.

Our findings may be viewed in light of knowledge concerning compatibility of connexin coupling partners. Following identification of Cx43 expression in astrocytes (Dermietzel et al., 1989; Yamamoto et al., 1990a,b) and Cx32 expression in oligodendrocytes (Scherer et al., 1995; Dermietzel et al., 1997; Kunzelmann et al., 1997; Li et al., 1997), the nature of gap junction channels between these two cell types remained uncertain because Cx43 and Cx32 were found to be non-permissive for forming functional GJIC channels (Swenson et al., 1989; Werner et al., 1989; Elfgang et al., 1995). This raised the possibility that these macroglial cells express other connexins. This conjecture was confirmed with the identification of Cx30 in astrocytes (Nagy et al., 1997, 1999; Kunzelmann et al., 1999), allowing for permissive coupling of oligodendrocytic Cx32 with astrocytic Cx30 (Dahl et al., 1996). However, the participation of yet other connexins in A/O gap junctions remained likely in view of observations that while gap junctions and GJIC occur between astrocytes and oligodendrocytes in white matter (Mugnaini, 1986; Rash et al., 1997; Pastor et al., 1998), Cx30 is not present in white matter astrocytes (Nagy et al., 1999), leaving Cx32 in white matter oligodendrocytes with an unidentified astrocytic connexin coupling partner. This difficulty was potentially overcome by recent reports of Cx26 expression by astrocytes and localization of Cx26 on the astrocyte side of A/O gap junctions (Mercier and Hatton, 2001; Nagy et al., 2001), together with compatibility of functional Cx26/Cx32 junction formation (White and Bruzzone, 1996). Still other combinations of coupling at these junctions were likely, as oligodendrocytes have recently been found to express Cx29 and Cx47 (Altevogt et al., 2002; Nagy et al., 2003a,b). Oligodendrocytes have also been reported to express Cx45 (Kunzelmann et al., 1997; Dermietzel et al., 1997). Though highly expressed in sciatic nerve (Altevogt et al., 2002; Li et al., 2002), Cx29 was sparse on oligodendrocyte somata, exhibited limited co-localization with Cx32 on these cells and failed to display the pattern of punctate

labeling characteristic of astrocytic Cx30 and Cx43 abutments on oligodendrocytes (Nagy et al., 2003a). Consequently, Cx29 is unlikely to play a major role in the formation of intercellular A/O gap junctions.

In heterologous gap junctions between cells expressing multiple connexins and having the capability of forming various combinations of heterotypic connexon channels, it is not evident *a priori* that a particular connexin, among several others on one side of a plaque, will fail to be incorporated into the plaque if its sole coupling partner, among several connexins on the other side, is absent. Gap junctions between astrocytes and oligodendrocytes provide a rare opportunity to address this issue in vivo because this is a heterologous coupling situation where the three connexins on one side differ completely from those on the other side, allowing eventual analysis of how each connexin deletion on one side of a junction affects the connexins on the other side. At A/O gap junctions in adult Cx32 KO mice, the present results indicate that Cx30 is vastly or completely reduced, and that Cx26 is partially reduced on the astrocyte side after elimination of Cx32 on the oligodendrocyte side, whereas astrocytic Cx43 and oligodendrocytic Cx29 and Cx47 appear unaffected. Thus, it may be speculated that the stability of particular connexins at A/O gap junctions requires specifically the presence of its coupling partner. Thus, we infer that at A/O junctions, Cx32 couples extensively or exclusively with Cx30, but may couple to a limited extent with Cx26. Conversely, the presence of a small amount of Cx26 immunoreactivity on the astrocyte side of A/O junctions in Cx32 KO mice may suggest that Cx26 couples to an additional connexin in oligodendrocytes, presumably Cx47 and perhaps minimally with Cx29 given the low levels of this connexin on oligodendrocyte somata in adult brain. The maintained presence of Cx43 on the astrocyte side of A/O junctions in Cx32 KO mice suggests that Cx43 does not couple with Cx32, consistent with the non-permissiveness of this combination (White and Bruzzone, 1996). Rather, Cx43 is presumed to couple with Cx47. The organization of gap junction channels within individual junctional plaques containing two or more different connexins on each side becomes potentially more complicated given the existence of heteromeric connexons (Brink et al., 1997; Diez et al., 1999) consisting of various proportions of different connexins. This complicating factor is supported by observations that coupling of heteromeric connexons may alter permselectivities (Bevans et al., 1998).

The influence of Cx32 deletion on connexin coupling between glial cells is relevant to considerations of X-linked Charco-Marie-Tooth disease, in which Cx32 mutations result in

peripheral neuropathy and in CNS alterations (Bergoffen, 1993; Bone et al., 1997; Bahr et al., 1999; Panas et al., 1998). Although it is not yet clear whether other glial connexins are able to compensate for functional loss of Cx32, our findings suggest that the high levels of Cx43/Cx47 may provide a mechanism for compensation. Conversely, the low levels of Cx29 on oligodendrocyte somata in both WT and Cx32 KO mice, suggests that little compensation may occur through pairing of oligodendrocyte Cx29 with astrocytic Cx26, Cx30 or Cx43. These results also indicate that cellular trafficking and targeting of Cx29 and Cx47 are essentially independent of Cx32 expression, although possible deleterious actions of mutated Cx32 on processing of these other two oligodendrocytic connexin remain to be investigated. It also remains to be determined whether Cx32 mutations impact on localization and function of Cx29 and Cx32 in regions of uncompacted, internodal CNS myelin, which contain an abundance of these connexins (Altevogt et al., 2002; Nagy et al., 2003a). Consideration of connexin compensation must also take into account the wide range in permselectivity of junctional channels formed by various connexin combinations (Veenstra, 1996). In gap junctions between cells expressing several connexins, the presence of junctions formed by the remaining connexin pairs after deletion of one connexin may not represent compensation because the deleted connexin may mediate passage of different substances than the remaining connexins. Developmental stage of connexin expression is an additional factor to consider. It has been reported, for example, that onset of Cx30 expression in brain occurs relatively late during development (Nagy et al., 1999; Kunzelmann et al., 1999), with Cx30 protein expression at post-natal day 20 in mice being minimal as compared with that seen in adult brain (Nagy et al., 1999). Thus, any deficits in function due to reduced pairing of Cx30/Cx32 at A/O junctions in Cx32 KO mice may not be evident until after CNS development is largely complete, and any damage resulting from (or compensation of) function by other connexins may not be occur until a similar late developmental stage.

ACKNOWLEDGMENTS

This work was supported by grants from the CIHR to J.I. Nagy, and by NIH grant NS-31027, NS-44010 and NS-44395 to J.E. Rash. We thank B. McLean, C. Olson and N. Nolette for assistance, Dr. K. Willecke for Cx32 KO mice and Dr. P.E. Braun for providing anti-CNPase.

Table 1. Connexin antibodies used for western blotting and immunohistochemistry

Antibody	Type	Epitope; Designation	Reference; Source
connexin26	monoclonal	c-terminus; 33-5800	Nagy et al., 2001; Zymed
connexin26	polyclonal	c-terminus; 51-2800	Nagy et al., 2001; Zymed
connexin29	polyclonal	c-terminus; 34-4200	Li et al., 2002; Zymed
connexin30	monoclonal	c-terminus; 33-2500	Rash et al., 2001; Zymed
connexin30	polyclonal	c-terminus; 71-2200	Nagy et al., 1999; Zymed
connexin32	monoclonal	aa 235-246; 7C7	Li et al., 1997
connexin32	monoclonal	c-terminus; 35-8900	Zymed
connexin32	monoclonal	cytoplasmic loop; 13-8200	Zymed
connexin32	polyclonal	cytoplasmic loop; 71-0600	Li et al., 1997; Zymed
connexin32	polyclonal	c-terminus: 34-5700	Zymed
connexin43	monoclonal	c-terminus; 35-5000	Zymed
connexin43	polyclonal	c-terminus; 71-0700	Li et al., 1998; Zymed
connexin43	polyclonal	aa 346-363; 18A	Yamamoto et al., 1990a,b
connexin47	polyclonal	c-terminus; 36-4700	Zymed

All antibodies were raised against peptides corresponding to connexin sequences. Monoclonal Cx32 antibody 13-8200 and polyclonal 71-0600 are directed against the same sequence in the cytoplasmic loop region of Cx32. Monoclonal 35-8900 and polyclonal 34-5700 are directed against the same sequence in the c-terminus region of Cx32. Zymed, Zymed Laboratories Inc., South San Francisco, CA.

Table 2. Counts of Cx30-immunoreactive puncta surrounding CNPase-positive oligodendrocyte somata in various brain regions of WT and Cx32 KO mice

Brain area	Wild Type	Cx32 KO
cerebral cortex	8.96 ± 0.29 (291)	1.25 ± 0.07 (305)*
globus pallidus	8.38 ± 0.34 (165)	1.09 ± 0.08 (173)*
VL thalamus	8.22 ± 0.42 (99)	0.78 ± 0.08 (153)*
hypothalamus	8.14 ± 0.31 (197)	0.81 ± 0.06 (185)*

Values indicate means +/- SEM of the numbers of Cx30-immunopositive puncta associated with the surface of individual oligodendrocytes each viewed at a single focal plane in the indicated brain regions of WT and Cx32 KO mice. Numbers in parentheses indicate the total number of oligodendrocyte somata examined in each brain region of 3 WT and 3 Cx32 KO mice. *Significantly different from WT, $p < 0.001$.

FIGURES

Fig. 1. **A:** Western blots of liver from WT and Cx32 KO mice probed with five different anti-Cx32 antibodies listed in Table 1 and indicated above each blot. Monomeric Cx32 is detected migrating at about 30-32 kDa in liver from WT mice (lanes 1, 3, 6, 9, and 11), but is absent in liver of Cx32 KO mice (lanes 2, 4, 7, 10 and 12). Detection of Cx32 in rat liver with two of the antibodies is shown for comparison (lanes 5 and 8). Four of the antibodies detect a dimeric Cx32 in WT mice (lanes 3, 6, 9 and 11), which is also absent in Cx32 KO mice (lanes 4, 7, 10 and 12). Some non-specific bands are evident, particularly with antibody 7C7, where detection of dimeric Cx32 is obscured by reaction with a similarly migrating protein. **B,C:** Western blots of brain homogenate from WT and Cx32 KO mice probed with anti-Cx32 antibodies indicated above each blot. Both antibodies detect Cx32 in brain of WT mice and show its absence in Cx32 KO mice. The higher molecular weight bands recognized are of unknown identity. **D:** Western blots of various CNS regions (thalamus, lane 1; spinal cord, lane 2; hypothalamus, lane 3; cerebellum, lane 4) (9% gels) probed with anti-Cx47 antibody 36-4700 show Cx47 migrating at about 50-52 kDa. **E:** A doublet of bands is recognized by anti-Cx47 antibody after separation of spinal cord protein on 12.5% gels, with no apparent difference in levels or migration profile in tissue from WT compared with Cx32 KO mice.

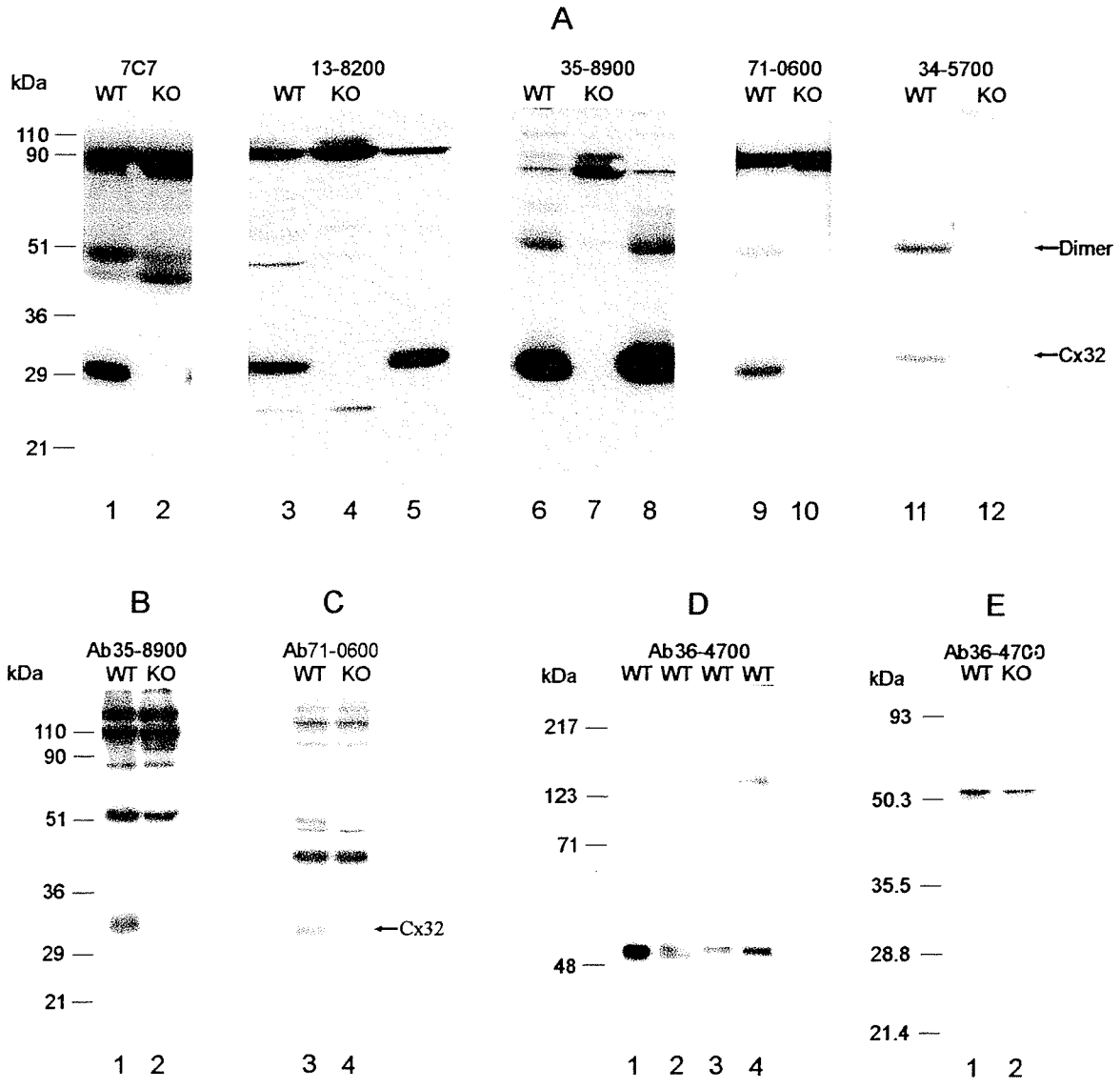
A
kDa
7C7
WT KO
13-8200
WT KO
35-8900
WT KO
71-0600
WT KO
34-5700
WT KO
110
90
51
36
29
21
←Dimer
←Cx32
1 2 3 4 5 6 7 8 9 10 11 12
B
Ab35-8900
WT KO
C
Ab71-0600
WT KO
←Cx32
1 2 3 4
D
Ab36-4700
WT WT WT WT
kDa
217
123
71
48
1 2 3 4
E
Ab36-4700
WT KO
kDa
93
50.3
35.5
28.8
21.4
1 2

Fig. 1

Fig. 2. **A-D:** Immunofluorescence labeling for Cx32 with various antibodies in liver of WT and Cx32 KO mice. A,B, 7C7; C,D, 71-0600. E,F, 34-5700; G,H, 35-8900. With each antibody, punctate labeling is seen around hepatocytes in liver of Cx32 WT mice, and a total absence of labeling is seen in liver of Cx32 KO mice. **E:** Immunofluorescence double-labeling in hypothalamus from a WT mouse showing oligodendrocyte cell bodies immunopositive for both CNPase (E1, arrows) and Cx32 (E2, arrows). **F:** A field in globus pallidus of a Cx32 KO mouse labeled for CNPase to identify oligodendrocytes (F1, arrows), and the same field labeled for Cx32 showing total absence of immunoreactivity (F2). **G:** Low magnification micrographs showing over sixty oligodendrocyte cell bodies labeled for Cx32 in hypothalamus of a WT mouse (G1, arrows), and a similar area in hypothalamus of a Cx32 KO mouse showing a total absence of labeling for Cx32 (F). Scale bars: A-C, 20 μm; D, 40 μm; E-F, 40 μm; G, 10 μm.

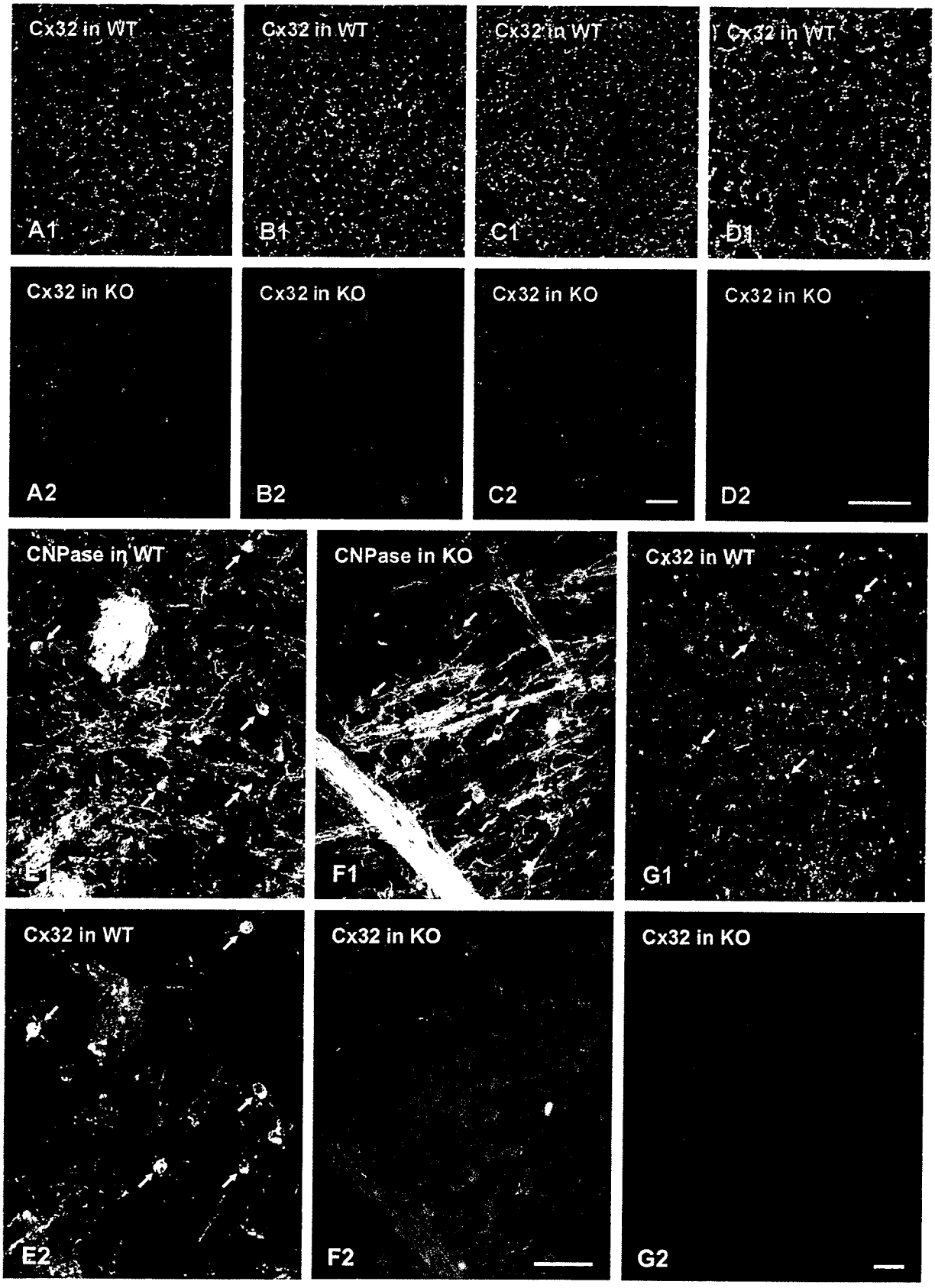
Cx32 in WT
A1
Cx32 in WT
B1
Cx32 in WT
C1
Cx32 in WT
D1
Cx32 in KO
A2
Cx32 in KO
B2
Cx32 in KO
C2
Cx32 in KO
D2
CNPase in WT
E1
CNPase in KO
F1
Cx32 in WT
G1
Cx32 in WT
E2
Cx32 in KO
F2
Cx32 in KO
G2

Fig. 2

Fig. 3. Laser scanning confocal immunofluorescence of connexin association with oligodendrocytes in various brain regions of WT mice. **A:** Confocal double-labeling in an area of the thalamus showing a CNPase-immunopositive oligodendrocyte (A1, arrowhead) with numerous Cx32-immunopositive puncta (A2, arrows) on the cell body and initial processes (yellow in overlay image, A3). **B:** Confocal double-labeling in the cerebral cortex showing Cx30-immunopositive puncta (B1, arrows) co-associated with Cx32-immunopositive puncta (B2, arrows) on an oligodendrocyte (yellow in overlay image, B3). **C-E:** Confocal micrographs showing Cx30 (green) co-association with Cx32 (red) as seen by yellow in overlay images from globus pallidus (C), ventrolateral thalamic nucleus (D) and ventroanterior thalamic nuclues (E). **F:** Double-labeling in cerebral cortex showing Cx43-immunopositive puncta (F1, arrows) co-localized with Cx30-immunopositve puncta (F2, arrows) on an oligodendrocyte (yellow in overlay image, F3). Scale bars: 5 μm.

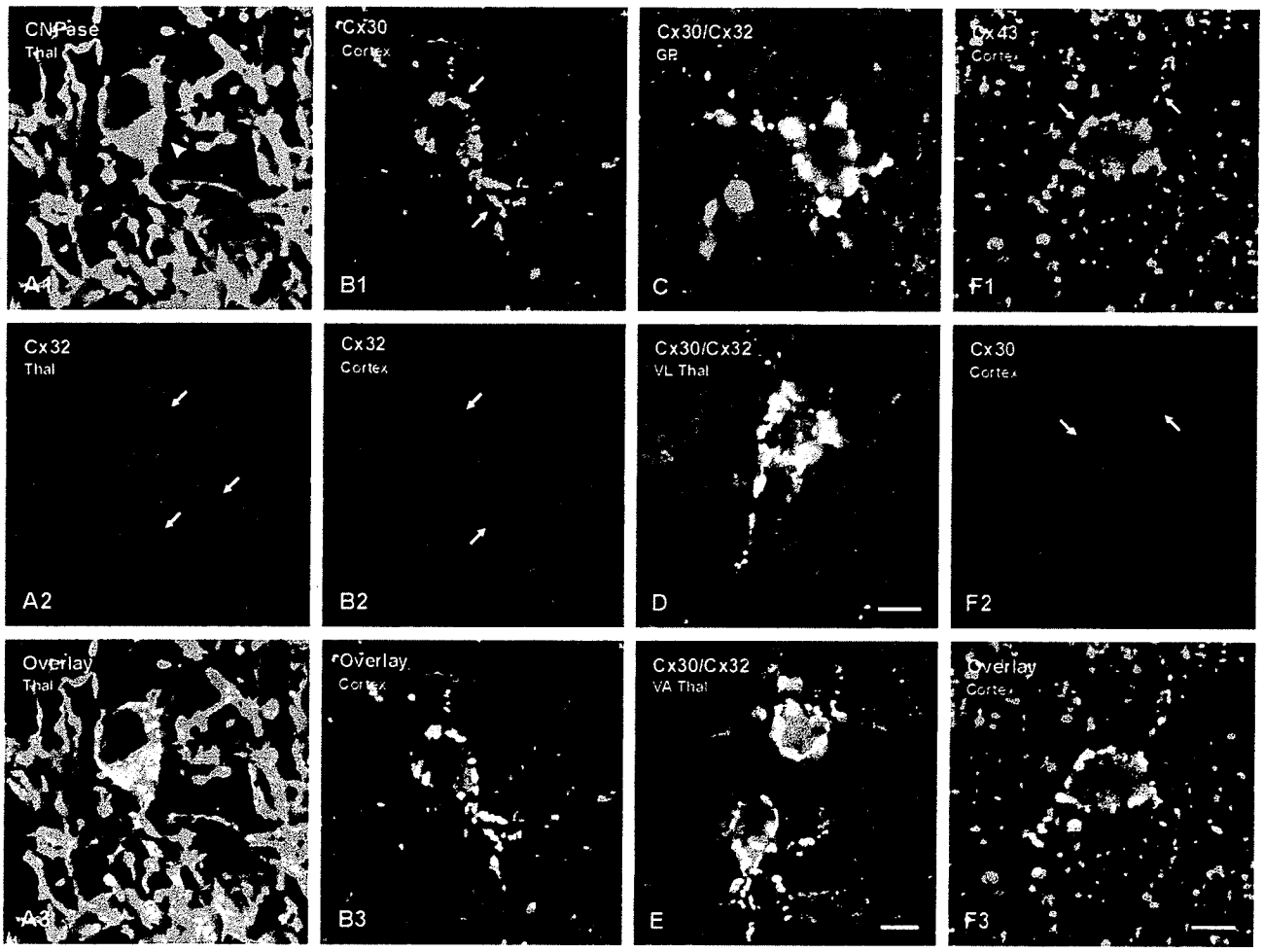
CNPase
Thal
A1
Cx30
Cortex
B1
Cx30/Cx32
GP
C
Cx43
Cortex
F1
Cx32
Thal
A2
Cx32
Cortex
B2
Cx30/Cx32
VL Thal
D
Cx30
Cortex
F2
Overlay
Thal
A3
Overlay
Cortex
B3
Cx30/Cx32
VA Thal
E
Overlay
Cortex
F3

Fig. 3

Fig. 4. Immunofluorescence micrographs showing Cx30 in brains of WT and Cx32 KO mice. **A,B:** A field in cerebral cortex of a WT mouse showing oligodendrocytes (A, arrows) densely surrounded by punctate labeling for Cx30, and a similar field in cortex of a Cx32 KO mouse showing absence of labeling for Cx30 on oligodendrocytes (B). Cx30-immunopositive puncta that are not associated with oligodendrocytes appear similar in WT and Cx32 KO mice. **C-J:** Laser scanning confocal immunofluorescence of Cx30 association with oligodendrocytes in various brain regions of WT and Cx32 KO mice. **C:** Confocal double-labeling in cerebral cortex of WT mouse showing two CNPase-positive oligodendrocytes (C1, arrowheads) each decorated with Cx30-positive puncta (C2, arrows) indicated by yellow in overlay image (C3). **D-F:** Confocal micrographs from WT mouse showing CNPase (green) co-association with Cx30 (red), as seen by yellow in overlay images from globus pallidus (D), ventrolateral thalamic nucleus (E) and hypothalamus (F). **G:** Confocal double-labeling in cerebral cortex of Cx32 KO mouse showing two CNPase-positive oligodendrocytes (G1, arrowheads) both lacking Cx30-positive puncta (G2, arrows) on their surfaces, as seen by absence of yellow in the overlay image (E3). **H-J:** Confocal micrographs from Cx32 KO mouse showing lack of CNPase (green) and Cx30 (red) co-association in globus pallidus (H), ventrolateral thalamic nucleus (I) and hypothalamus (J). Scale bars: A,B, 40 μm; C, 10 μm; D-J, 5 μm.

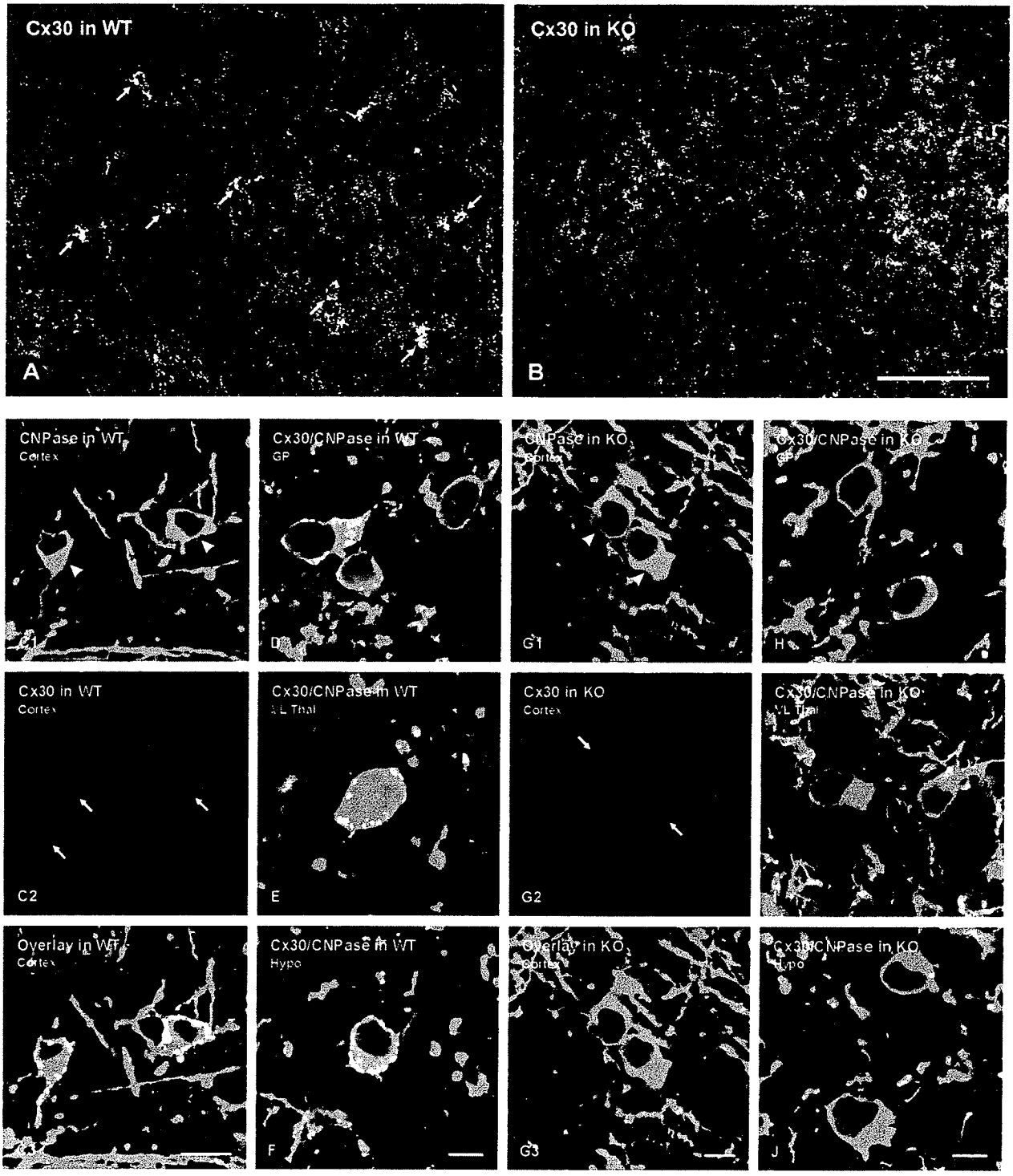
Cx30 in WT
A
Cx30 in KO
B
CNPase in WT
Cortex
C1
Cx30/CNPase in WT
GP
D
CNPase in KO
Cortex
G1
Cx30/CNPase in KO
GP
H
Cx30 in WT
Cortex
C2
Cx30/CNPase in WT
VL Thal
E
Cx30 in KO
Cortex
G2
Cx30/CNPase in KO
VL Thal
Overlay in WT
Cortex
Cx30/CNPase in WT
Hypo
F
Overlay in KO
Cortex
G3
Cx30/CNPase in KO
Hypo
J

Fig. 4

Fig. 5. Frequency distribution showing percentage of oligodendrocytes and the numbers of Cx30-immunopositive puncta surrounding oligodendrocytes in cerebral cortex and globus pallidus. Numbers of puncta were binned in pairs (1-2), (3-4) up to (21-22). Percentages are the mean +/- standard error from the total number of oligodendrocytes (indicated in Table 2) examined in three WT animals.

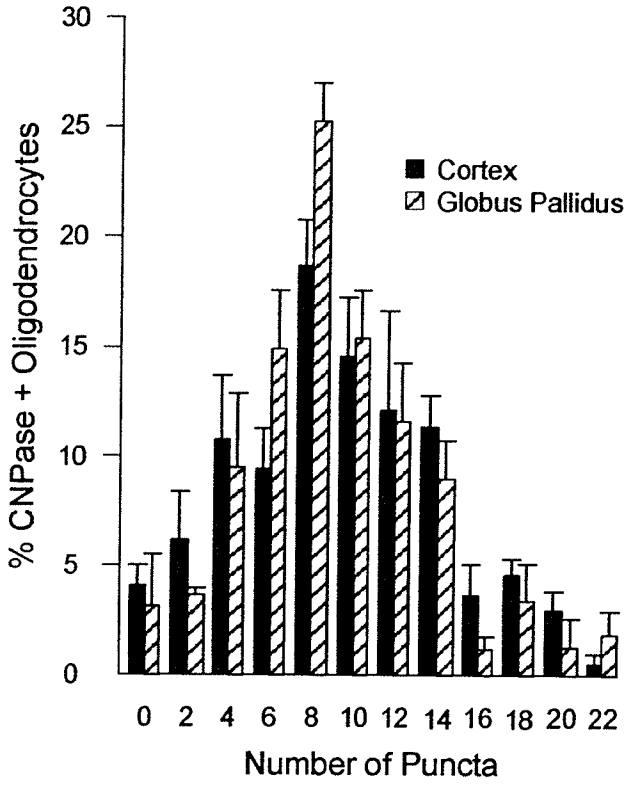
30
25
20
15
10
5
0
% CNPase + Oligodendrocytes
Cortex
Globus Pallidus
0 2 4 6 8 10 12 14 16 18 20 22
Number of Puncta

Fig. 5

Fig. 6. Laser scanning confocal immunofluorescence of Cx43 and Cx47 association with CNPase-labeled oligodendrocytes in various brain regions of WT and Cx32 KO mice. **A:** Confocal double-labeling in cerebral cortex of WT mouse showing two CNPase-positive oligodendrocytes (A1, arrowheads) with Cx43-positive puncta (A2, arrows) on the cell bodies (yellow in overlay image, A3). **B-D:** Confocal micrographs from WT mouse showing CNPase (green) co-association with Cx43 (red) as seen by yellow in overlays from striatum (B), globus pallidus (C) and ventroanterior thalamic nucleus (D). **E:** Confocal double-labeling in cerebral cortex of Cx32 KO mouse showing CNPase-positive oligodendrocyte (E1, arrowheads) with Cx43-positive puncta (E2, arrows) on its surface (yellow in overlay, E3). **F-H:** Confocal micrographs from Cx32 KO mouse showing CNPase (green) co-association with Cx43 (red), as seen by yellow in overlays from striatum (F), globus pallidus (G) and ventroanterior thalamic nucleus (H). **I:** Confocal double-labeling in cerebral cortex of WT mouse showing a CNPase-positive oligodendrocyte (I1, arrowhead) with Cx47-positive puncta (I2, arrows) on the cell body (yellow in overlay, I3). **J-L:** Confocal micrographs from WT mouse showing CNPase (green) co-association with Cx47 (red), as seen by yellow in overlays from striatum (J), thalamus (K) and hypothalamus (L). **M:** Confocal double-labeling in cerebral cortex of Cx32 KO mouse showing a CNPase-positive oligodendrocyte (M1, arrowhead) with Cx47-positive puncta (M2, arrows) on its surface (yellow in overlay, E3). **N-P:** Confocal micrographs from Cx32 KO mouse showing CNPase (green) co-localization with Cx47 (red), as seen by yellow in overlays from striatum (N), thalamus (O) and hypothalamus (P). Scale bars: A-C, 10 μm; D-H, (shown in D,H), 5 μm; I-N, (shown in N), 5 μm; O,P, 5 μm.

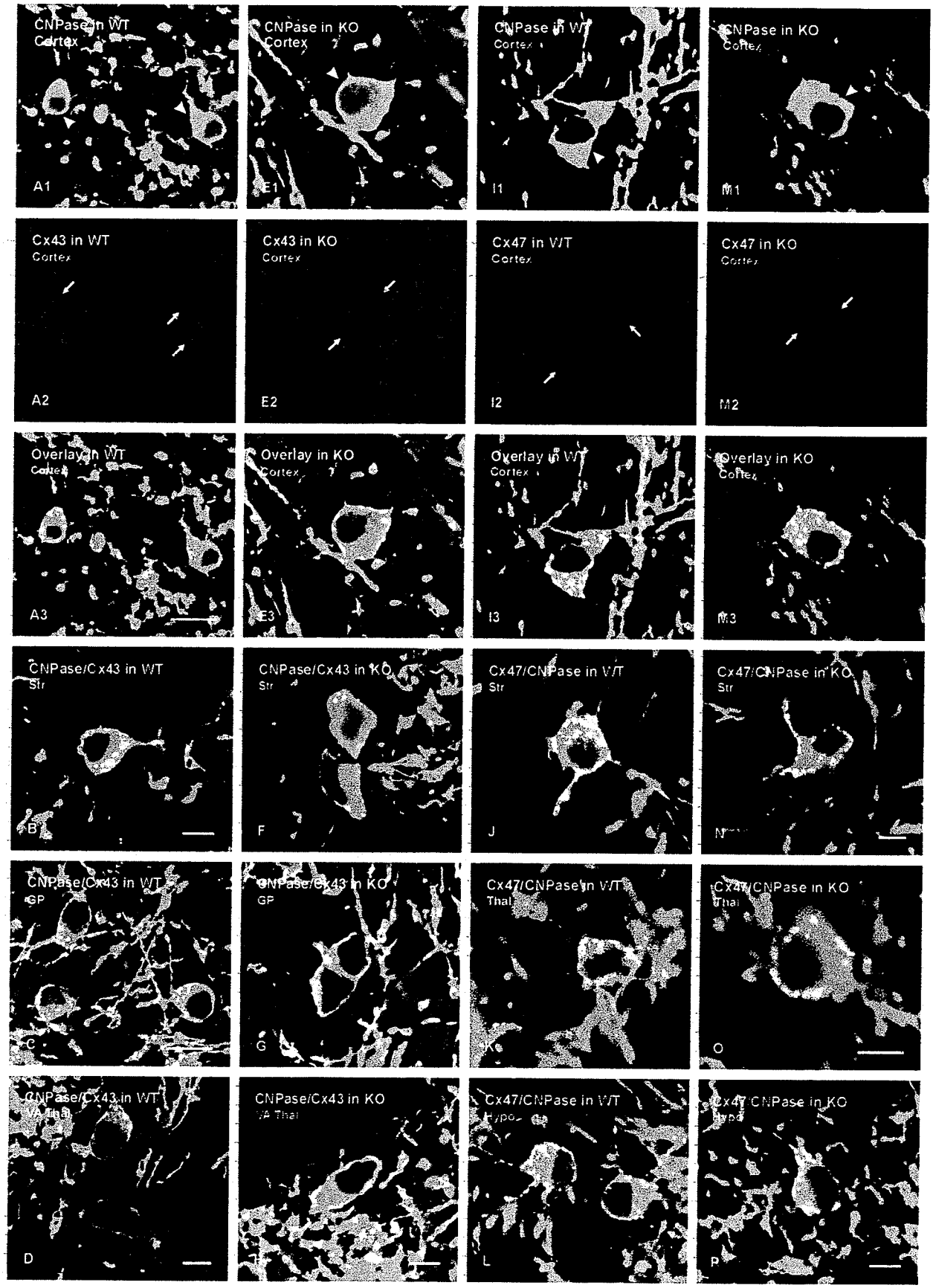
CNPase in WT
Cortex
A1
CNPase in KO
Cortex
E1
CNPase in WT
Cortex
I1
CNPase in KO
Cortex
M1
Cx43 in WT
Cortex
A2
Cx43 in KO
Cortex
E2
Cx47 in WT
Cortex
I2
Cx47 in KO
Cortex
M2
Overlay in WT
Cortex
A3
Overlay in KO
Cortex
E3
Overlay in WT
Cortex
I3
Overlay in KO
Cortex
M3
CNPase/Cx43 in WT
Str
B
CNPase/Cx43 in KO
Str
F
Cx47/CNPase in WT
Str
J
Cx47/CNPase in KO
Str
N
CNPase/Cx43 in WT
GP
C
CNPase/Cx43 in KO
GP
G
Cx47/CNPase in WT
Thal
K
Cx47/CNPase in KO
Thal
O
CNPase/Cx43 in WT
VA Thal
D
CNPase/Cx43 in KO
VA Thal
H
Cx47/CNPase in WT
Hypo
L
Cx47/CNPase in KO
Hypo
P

Fig. 6

Fig. 7. **A-B:** Laser scanning confocal immunofluorescence showing CNPase-positive oligodendrocytes in globus pallidus (A1,B1, arrowheads), and numerous Cx26-positive puncta on the surface of these cells in WT (A2, arrows), but not KO (B2, arrows) mice as seen by yellow in corresponding overlay images (A3,B3, arrows). **C,D:** Laser scanning confocal immunofluorescence showing CNPase-positive oligodendrocytes in cerebral cortex (C1,D1, arrowheads), and similar appearence of Cx29 (C2,D2, arrows) associated with these cells in WT and Cx32 KO mice as seen by yellow in corresponding overlay images (C3,D3, arrows). Scale bars: A,C,D, 10 μm; B, 5 μm.

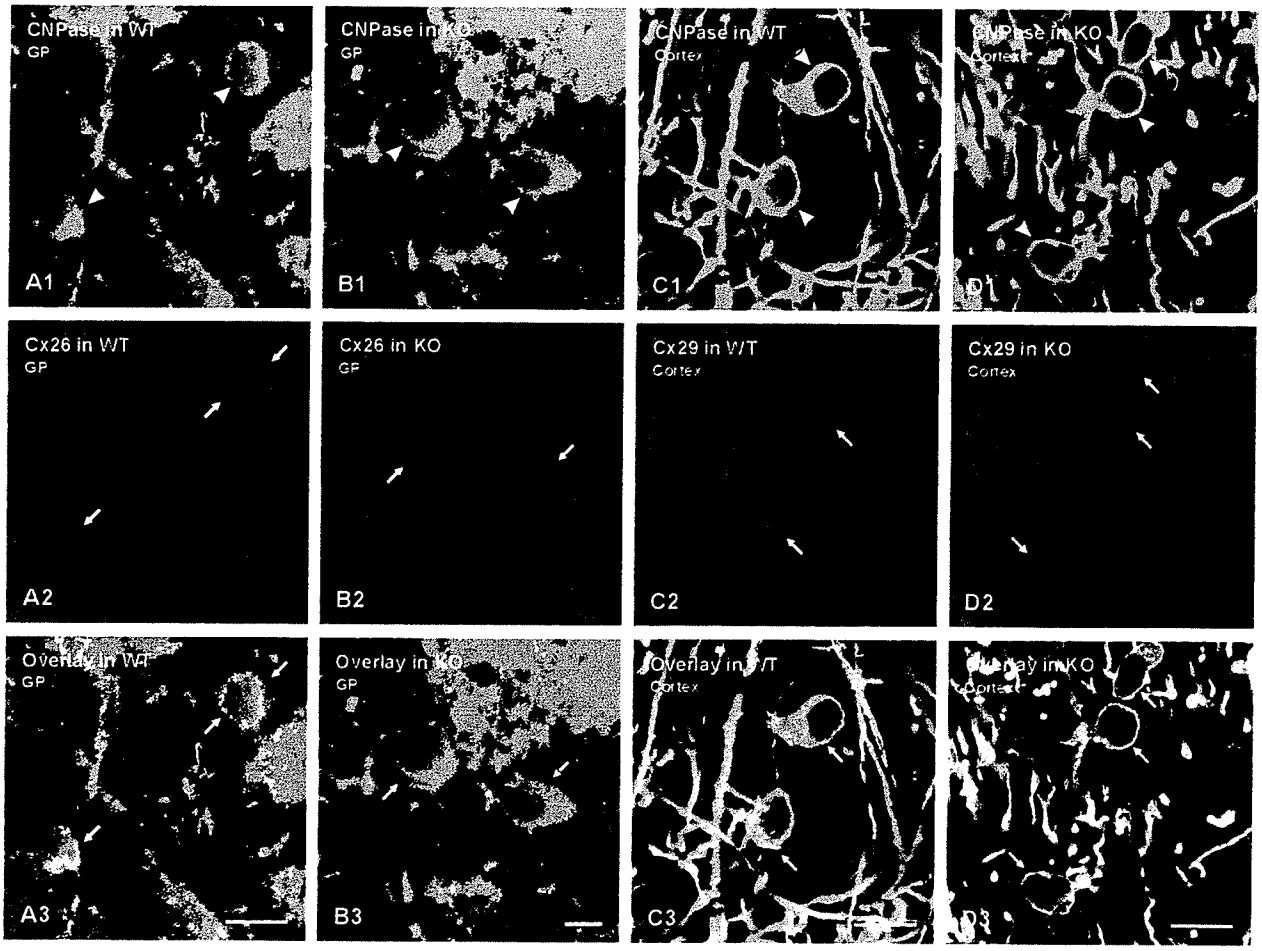
CNPase in WT
GP
A1
CNPase in KO
GP
B1
CNPase in WT
Cortex
C1
CNPase in KO
Cortex
D1
Cx26 in WT
GP
A2
Cx26 in KO
GP
B2
Cx29 in WT
Cortex
C2
Cx29 in KO
Cortex
D2
Overlay in WT
GP
A3
Overlay in KO
GP
B3
Overlay in WT
Cortex
C3
Overlay in KO
Cortex
D3

Fig. 7

Table 1. Connexin antibodies used for western blotting and immunohistochemistry

Antibody	Type	Epitope; Designation	Reference; Source
connexin26	monoclonal	c-terminus; 33-5800	Nagy et al., 2001; Zymed
connexin26	polyclonal	c-terminus; 51-2800	Nagy et al., 2001; Zymed
connexin29	polyclonal	c-terminus; 34-4200	Li et al., 2002; Zymed
connexin30	monoclonal	c-terminus; 33-2500	Rash et al., 2001; Zymed
connexin30	polyclonal	c-terminus; 71-2200	Nagy et al., 1999; Zymed
connexin32	monoclonal	aa 235-246; 7C7	Li et al., 1997
connexin32	monoclonal	c-terminus; 35-8900	Zymed
connexin32	monoclonal	cytoplasmic loop; 13-8200	Zymed
connexin32	polyclonal	cytoplasmic loop; 71-0600	Li et al., 1997; Zymed
connexin32	polyclonal	c-terminus: 34-5700	Zymed
connexin43	monoclonal	c-terminus; 35-5000	Zymed
connexin43	polyclonal	c-terminus; 71-0700	Li et al., 1998; Zymed
connexin43	polyclonal	aa 346-363; 18A	Yamamoto et al., 1990a,b
connexin47	polyclonal	c-terminus; 36-4700	Zymed

All antibodies were raised against peptides corresponding to connexin sequences. Monoclonal Cx32 antibody 13-8200 and polyclonal 71-0600 are directed against the same sequence in the cytoplasmic loop region of Cx32. Monoclonal 35-8900 and polyclonal 34-5700 are directed against the same sequence in the c-terminus region of Cx32. Zymed, Zymed Laboratories Inc., South San Francisco, CA.

General discussion

The past few years were exciting and fruitful times for research and this work summarizes the effort of our lab in the field of connexins and gap junction biology. In partnership with Zymed Laboratories Inc., we developed specific antibodies to Cx29 and Cx47 giving us access to highly accurate tools that facilitated the study of gap junctions and their potential function in CNS and PNS. While Cx32 was previously demonstrated to be expressed exclusively by Schwann cells and oligodendrocytes (Rash et al., 1997), project 2 demonstrates that Cx32 is a myelin associated protein, and its expression by any other cell types in CNS remains highly unlikely. Also, in project 1 we confirm early reports that the newly cloned Cx29 is associated with myelin and it is expressed by oligodendrocytes in CNS and by Schawnn cells in peripheral nerves (Shol et al., 2001; Altevogt et al., 2002). Moreover, we strongly believe that Cx47, previously reported to be expressed in neurons, is an oligodendrocytic connexin (project 2). Evidence supporting the oligodendrocytic nature of Cx47 has recently became available, in study involving Cx47-nul mice (Odermatt et al., 2003). The expression of additional connexins by myelinating cells, combined with the relative functional and morphological neural integrity observed in CNS and PNS of Cx32 KO mice, raised the possibility of a functional redundant effect mediated by Cx29 or Cx47 in the absence of Cx32. In the light of our investigation (project 1 and 2), we reliably assert that astrocytes and oligodendrocytes express completely different subsets of connexins. Therefore the segregation of distinct connexins to specific cell types raises new questions regarding permissive gap junction coupling partnership. We proposed that Cx29 is an unlikely participant in A/O coupling and hence it is unable to fully compensate for the absence of Cx32 in myelinating cells (project 1). However the expression of Cx47 by oligodendrocytes (project 2) and its probable involvement in extensive A/O coupling with astrocytic Cx43 and Cx26 may be responsible for the relative protection from extensive neuronal damage of the PNS myelinated nerve fibers of Cx32 KO animals, as well as in humans afflicted with CMTX (Bergofen et al., 1993).

CMTX! The Cx32 connection...

Since it was discovered that mutations in Cx32 gene are associated with the X-linked form of CMT, at least 163 mutations have been identified (Nelis et al., 1999; Ressot et al., 2000). While most mutations result in expression of functionally incompetent channels, some mutations have

been associated with Cx32 gap junctions that display aberrant conduction properties (Ressot et al., 1998). This suggests that the total absence of channel communication is not a prerequisite for the development of CMTX (Bargiello et al., 1999). Also, it has been observed that in PC12 cells transfected with mutated forms of Cx32 gene, the trafficking pattern of Cx32 shows drastic disruptions (Matsuyama et al., 2001). In some instances Cx32 remains sequestered intracellularly to the extent that no Cx32 channel formation is possible (Matsuyama et al., 2001). Moreover, it has been determined that some mutated Cx32 genes can play a negative dominant effect on other expressing connexins, thus disrupting the potentially rescuing effect mediated by the viable coexpressing connexins (Bruzzone et al., 1994; Nicholson et al., 1999). Considering the extensive A/O coupling observed, it could be expected that disruption of the Cx32 gene may have a negative effects on neural physiology. However, while CMTX is synonymous with extensive motor and sensory peripheral neuropathy, the afflicted individuals are virtually asymptomatic with respect to CNS manifestations (Ressot and Bruzzone, 2000). While the exact mechanism of CMTX pathology remains elusive, it appears that Cx32 may play a different role in PNS myelinated fibers than along the oligodendrocytic wrapped axons of CNS. It has been proposed that Cx32 may form autologous gap junctions between successive Schmidt Lanterman incisures in peripheral nerves, and loss of Cx32 function may interfere with the radial diffusion pathway of ions and metabolites (Scherer et al., 1995). However, in a recent study, radial diffusion of dyes at incisure regions was not affected in Cx32 KO mice (Balice-Gordon et al., 1998). Taking into consideration the distinct morphology of myelin in CNS versus PNS, and the fact that Schwann cells are endowed with additional physiological roles resembling astrocytes, it is also plausible that the loss of Cx32 function may not be equally well compensated in PNS as in CNS.

It is believed that astrocytes are compartmentalized in the CNS according to local physiological and functional needs of the neural environment (Nagy et al., 2003c). Thus, distinct A/O partnership may exist according to anatomical location. As presented in project 2, we conclude that Cx32 partners with astrocytic Cx30 in gray matter, mostly at contact regions between astrocytes and oligodendrocytic somata, with little if any coupling along the CNS myelinated fibers. The presence of astrocytic Cx26 and Cx43 on the oligodendrocytic somata of Cx32 KO mice suggest that oligodendrocytic Cx47 may provide a partially functional redundancy in the absence of Cx32 in CNS. It is probable that distinct physiology in CNS and

PNS may play a role in CMTX symptomatic, however, another possibility would implicate extrinsic environmental factors as potential triggers in CMTX pathology. While nerves in CNS are relatively static structures, peripheral nerves are subjected to a considerable range of motion that involve drastic and sudden changes in nerve fiber geometry that must be well tolerated by a compact and relatively rigid myelin. Following the observation that Schmidt Lanterman incisures have a conical morphology and are present at periodic intervals along myelinated fibers, it has been proposed that incisures act as hydraulic devices that confer flexibility to an otherwise inelastic structure (Glees, 1943). This hypothesis is also supported by the observation that each incisure is able to accommodate up to 9% increase in length without sustaining damage to the myelin sheet (Friede and Samorajski, 1969). Bearing in mind that each internodal region contains many incisures and the overall elasticity of the internode is the additive function of individual incisures, the overall gain in flexibility is potentially huge (Fried and Samorajski 1969). Interestingly, humans afflicted with CMTX develop progressive peripheral neuropathies at approximately 10-12 years of age, at a time when the vast majority are fully functional and mobile individuals, thus suggesting a cumulative progression of damage (Ressot and Bruzzone, 2000).

Cx29! When is a gap junction more than just a channel?

The observation that functional abnormalities associated with CMTX remain segregated mostly to PNS, also raised the possibility that in CNS a compensation for Cx32 loss of function exists, presumably, by the presence of another oligodendrocytic connexin (Scherer et al., 1998). The recent cloning of Cx29 and the reported association of this novel connexin with oligodendrocytes and Schwann cells raised an exciting possibility. Specifically, that Cx29 may participate in A/O coupling in CNS, possibly partnering with Cx43. At the same time, in peripheral nerves Cx29 may only partially compensate for loss of Cx32, thus explaining the late onset of symptoms in CMTX. Previously our lab reported that Cx29 appears to be located at Schmidt Lanterman incisures in PNS myelin, suggesting the possible involvement of Cx29 in reflexive gap junction formations between concentric myelin layers. However the localization of Cx29 at incisures was not conclusively demonstrated by FRIL. In a recent study however, Altevogt et al. (2002), determined that Cx29 is unable to form functional homologous channels with itself, nor heterologous coupling with Cx32. Moreover, in CNS we reported minimal

colocalization of Cx29 on the oligodendrocytic somata and fibers with all astrocytic connexins, either during development or adult stage (project 1). The obvious change in distribution of Cx29 during CNS development, from cell bodies to fibers, as well as the predominant localization of Cx29 on small diameter fibers lead us to believe that Cx29 plays a role in myelin maintenance that is distinct from that of Cx32 (project 1).

It has been previously documented that heteromeric channels composed of two or more distinct connexins display physiological properties that differ from either homomeric "parent" channel (Valiunas et al., 2001). Therefore, the production of connexons of various connexin combinations would allow a cell to fine tune its channel gating properties according to its immediate physiological needs. While Cx29 does not appear to be involved in homotypic and heterotypic coupling, it has been shown that Cx29/Cx32 heteromeric channels are functional, and display unique and distinct electrophysiological properties (Altevogt et al. 2002). Thus, it is possible that oligodendrocytes modulate the gating properties of gap junctions along fibers by selective recruitment of Cx29 in heteromeric interactions. However, for such a mechanism to take place, an *a priori* requirement is that both connexins are trafficked along the same route, as heteromeric channels are assembled prior to connexon exit from Golgi network (Martin et al., 2001; Das Sarma et al., 2002).

What is next?

The discovery that CMTX is associated with Cx32 mutations has brought renewed interest to the importance of connexins in glial cell biology. The development of KO animals where different connexin genes have been disrupted provides a powerful tool that allows in depth studies on gap junction pathology. In this respect, it has been determined that Cx32 KO mice develop progressive weakness of the motor pathway, symptoms also characteristic of CMTX. However, out of 163 Cx32 gene mutations associated with CMTX, only one has been identified to be a deletion that completely eliminates the entire coding region of Cx32 gene (Ainsworth et al., 1998). While the vast majority of Cx32 gene mutations have been shown to be missense, resulting in non-conservative amino acid changes, nonsense and frame shift micro-deletions also have been reported (Bergofen et al., 1993; Silander et al., 1997). Considering the potential dominant negative effect of mutated Cx32 on the trafficking of other connexins, it is obvious that the pathology associated with abnormal Cx32 exceeds just the simple loss of functions.

Therefore, it is apparent that Cx32 KO animals may not be relevant research models for some forms of CMTX, and thus the use of knock-in mice where Cx32 gene is not just deleted but carries discrete mutations, would represent the next logical step in CMTX research. While the mutation of Cx32 gene does not seem to have a major deleterious effect on neural development (Ressot and Bruzzone. 2000), it is possible that defective forms of Cx29 may drastically affect the phenotype of the afflicted individuals to the point that such mutations are incompatible with life.

A controversial issue remains the proposition that neural cells are expressing different sets of connexins at different developmental stages, or following intense traumatic events (Dermietzel et al., 1989; Bruzzone and Ressot, 1997; Rozental et al., 2000). However, the exact mechanism responsible for the proposed phenotypic transition, as well as possible physiological implications is not well understood. The use of conditional transgenic mice that would allow researchers to specifically target a viable connexin gene and render it nonfunctional would greatly increase our understanding of this issue.

An intriguing aspect remains the observation that Cx29 may not participate in either reflexive gap junction formation, or in partnership with astrocytic connexons. This opens the possibility that Cx29 performs novel roles that are not necessarily congruent with traditional gap junction function. Further studies directed at the trafficking pathway of Cx29 would be necessary in order to investigate the proposed modulatory function of Cx29 on Cx32 gap junction formation, and the apparent size dependent distribution of Cx29 along myelinated fibers.

REFERENCES

Abrams CK, Oh S, Ri Y, Bargiello TA. (2000). Mutations in connexin 32: the molecular and biophysical bases for the X-linked form of Charcot-Marie-Tooth disease. *Brain Res Rev* 32(1):203-14

Adzhubei AA, Sternberger MJE. (1993). Left-handed polyproline II helices commonly occur in globular proteins. *J Mol Biol* 229:472-493

Ainsworth PJ, Bolton CF, Murphy BC, Stuart JA, Hahn AF. (1998). Genotype/phenotype correlation in affected individuals of a family with a deletion of the entire coding sequence of the connexin 32 gene. *Hum Genet* 103:242-244

Altevogt BM, Kleopa KA, Postma FR, Scherer SS, Paul DL. (2002). Connexin29 is uniquely distributed within myelinating glial cells of the central and peripheral nervous systems. *J Neurosci* 22:6458-6470.

Araque A, Parpura V, Sanzgiri RP, Haydon PG. (1999). Tripartite synapses: glia, the unacknowledged partner. *Trends Neurosci* 22:208-215

Arroyo EJ, Scherer SS. (2000). On the molecular architecture of myelinated fibres. *Histochem Cell Biol* 113:1-18.

Asklund T, Appelskog IB, Ammerpohl O, Langmoen IA, Dilber MS, Aints A, Ekstrom TJ, Almqvist PM. (2003). Gap junction-mediated bystander effect in primary cultures of human malignant gliomas with recombinant expression of the HSVtk gene. *Exp Cell Res* 284(2):183-93

Bahr M, Andres F, Timmerman V, Nelis ME, Van Broeckhoven C, Dichgans J. (1999). Central visual, acoustic and motor pathway involvement in Charcot-Marie-Tooth family with an asn205ser mutation in the connexin32 gene. *J Neurol Neurosurg Psych* 66:202-206.

Baker TS, Caspar DLD, Hollingshead CJ, Goodenough DA. (1983). Gap junctions structures. IV. Asymmetric features revealed by low-irradiation microscopy. *J.Cell Biol.* 96:204-216

Balice-Gordon RJ, Bone LJ, Scherer SS. (1998). Functional gap junctions in the Schwann cell myelin sheath. *J Cell Biol* 142:1095-1104.

Barr L, Dewey MM, Berger W. (1965). Propagation of action potentials and the structure of the nexus in cardiac muscle. *J. Gen. Physiol.* 48:792-823

Barr ML, Kiernan JA. (1993). The human nervous system. *An anatomical viewpoint 6th edition* (JB Lippincott Company) pp.28-33

Batias C, Defamine N, Lablack A, Thepot D, Fenichel P, Segretain D, Pointis G. (1999). Modified expression of testicular gap junction connexin 43 during normal spermatogenic cycle and in altered spermatogenesis. *Cell and Tissue Res.* 298:113-121

Baumann N, Pham-Dinh D. (2001). Biology of oligodendrocyte and myelin in the mammalian central nervous system. *Physiol Rev* 81(2):871-927

Baux G, Simonneau M, Tauc L, Segundo JP. (1978). Uncoupling of electrotonic synapses by calcium. *Proc Natl Acad Sci USA* 75(9):4577-81

Beardslee MA, Laing JG, Beyer EC, Saffitz JE. (1999). Rapid turnover of connexin43 in the adult rat heart. *Circ Res* 83(6):629-35

Bennett MVL, Goodenough DA. (1978) Gap junctions, electrotonic coupling and intercellular communication. *Neurosci Res Prog Bull* 16:376-486

Bennett MVL. (1977). Electrical transmission: a functional analysis and comparison with chemical transmission. *In: Handbook of Physiology, Section I; The nervous system,* Vol. 1, Cellular Biology of Neurons, Part 1 (ER Kandel, ed) pp. 357-416

Bennett MV, Barrio LC, Bargiello TA, Spray DC, Hertzberg E, Saez JC. (1991). Gap junctions: new tools, new answers, new questions. *Neuron* 6:305-320

Bennett MV, Verselis VK. (1992). Biophysics of gap junctions. *Semin Cell Biol* 3(1):29-47

Bennett MV. (2000). Electrical synapses, a personal perspective (or history). *Brain Res Brain Res Rev* 32:16-28

Bergoffen J, Scherer SS, Wang S, Oronzi-Scott M, Bone L, Paul DL, Chen K, Lensch MW, Chance P, Fischbeck K. (1993). Connexin mutations in X-linked Charcot-Marie-Tooth disease. *Science* 262:2039-2042

Bevans CG, Kordel M, Rhee SK, Harris AL. (1998). Isoform composition of connexin channels determines selectivity among second messengers and uncharged molecules. *J Biol Chem* 273:2808-2816.

Beyer EC, Paul DL, Goodenough DA. (1987). Connexin43: a protein from rat heart homologous to a gap junction protein from liver. *J Cell Biol* 105:2621-2629

Beyer EC, Veenstra RD. (1994). In Perachcia, C. ed. *Handbook of membrane channels*, Academic Press, London. pp. 379-401

Bierhuizen MF, van Amersfoorth SC, Groenewegen WA, Vliex S, Jongsma HJ. (2000). Characterization of the rat connexin40 promoter: two Sp1/Sp3 binding sites contribute to transcriptional activation. *Cardiovasc Res* 46:511-22

Bittman K, Owens DF, Kriegstein AR, LoTurco JJ. (1997). Cell coupling and uncoupling in the ventricular zone of developing neocortex. *J Neurosci* 17:7037-7044

Blakemore WF. (1969). Schmidt-Lanterman incisures in the central nervous system. *J Ultrastra Res* 29:496-498.

Bone LJ, Deschênes SM, Balice-Gordon RJ, Fischbeck KH, Scherer SS. (1997). Connexin 32 and X-linked Charcot-Marie-Tooth disease. *Neurobiol Dis* 4:221-230.

Bonner PH. (1989). Correlation of development stage and gap junction formation between chick embryo neurons and cloned skeletal muscle myoblasts. *Exp Cell Res* 181(1):205-16

Brink, PR, Dewey MM. (1980). Evidence for fixed charge in the nexus. *Nature (London)* 285:101-102

Brink PR, Cronin K, Banach K, Peterson E, Westphale EM, Seul KH, Ramanan SV, Beyer EC. (1997). Evidence for heteromeric gap junction channels formed from rat connexin43 and connexin37. *Am Physiol Soc* 273:C1386-C1396.

Bruzzone R, White TW, Paul DL. (1995). Connections with connexins: the molecular basis of direct intercellular signaling. *Eur J Biochem* 238:1-27

Bruzzone R, White TW, Paul DL. (1996). Connections with connexins: the molecular basis of direct intercellular signaling. *Eur J Biochem* 238:1-27.

Bruzzone R, Ressot C. (1997). Connexins, gap junctions and cell-cell signalling in the nervous system. *Eur J Neurosci* 9:1-6

Bukauskas FF, Elfgang C, Willecke K, Weingart R. (1995). Heterotypic gap junction channels (connexin26 – connexin32) violate the paradigm of unitary conductance. *Pflügers Arch.* 429:870-872

Bukauskas FF, Peracchia C. (1997). Two distinct gating mechanisms in gap junction channels: CO_2- sensitive and voltage-sensitive. *Biophys J* 72:2137-2142

Bukauskas FF, Angele AB, Verselis VK, Bennett MV (2002). Coupling asymmetry of heterotypic connexin 45/ connexin 43-EGFP gap junctions: properties of fast and slow gating mechanisms. *Proc Natl Acad Sci U S A* 14;99(10):7113-8; Erratum in: *Proc Natl Acad Sci U S A* 23;99(15):10228

Bunge RP, Bunge MB, Ris R. (1960). Electron microscopic study of demyelination in an experimentally induced lesion in adult cat spinal cord. *J Biophys Biochem Cytol* 7:685-696.

Burt JM. (1989). Uncoupling of cardiac cells by doxyl stearic acids specificity and mechanism of action. *Am J Physiol* 256(4 Pt 1):C913-C924

Burt JM, Spray DC. (1989). Volatile anesthetics block intercellular communication between neonatal rat myocardial cells. *Circ Res* 65:829-837

Butt AM, Ransom BR. (1993). Morphology of astrocytes and oligodendrocytes during development in the intact rat optic nerve. *J Comp Neurol* 338:141-158

Cajal SRV. (1928). Degeneration and regeneration of the nervous system Vol. 1 and 2. Oxford University Press. London.

Carroll WM, Jennings AR. (1994). Early recruitment of oligodendrocyte precursors in CNS demyelination. *Brain* 117:563-78

Cascio M, Gogol E, Wallace BA. (1990). The secondary structure of gap junctions. Influence of isolation methods and proteolysis. *J Biol Chem* 265(4):2358-64

Caspar DL, Goodenough DA, Makowski L, Phillips. WC. (1977). Gap junction structures. I. Correlated electron microscopy and x-ray diffraction. *J Cell Biol* 74:605-628

Chang Q, Gonzalez M, Pinter MJ, Balice-Gordon RJ. (1999). Gap junctional coupling and patterns of connexin expression among neonatal rat lumbar spinal motor neurons. *J Neurosci* 19:10813-10828

Chang M, Werner R, Dahl G. (1996). A role for an inhibitory connexin in testis? *Dev* Biol 175:50-56

Chen H, Chopp M, Schultz L, Bodzin G, Garcia JH. (1993). Sequential neuronal and astrocytic changes after transient middle cerebral artery occlusion in the rat. *J Neurol Sci* 118:109-116

Christ GJ, Spray DC, El-Sabban M, Moore LK, Brink PR. (1996). Gap junctions in vascular tissues. Evaluating the role of intercellular communication in the modulation of vasomotor tone. *Circ Res* 79:631-646

Cohen GB, Ren R, Baltimore D. (1995). Modular binding domains in signal transduction proteins. *Cell* 80:237-248

Condorelli DF, Parenti R, Spinella F, Trovato Salinaro A, Belluardo N, Cardile V, Cicirata F. (1998). Cloning of a new gap junction gene (Cx36) highly expressed in mammalian brain neurons. *Eur J Neurosci* 10:1202-1208

Condorelli DF, Belluardo N, Trovato-Salinaro A, Mudo G. (2000). Expression of Cx36 in mammalian neurons. *Brain Res Brain Res Rev* 32:72-85

Conradi S. (1969). Observations on the ultrastructure of the axon hillock and initial axon segment of lumbosacral motoneurons in the cat. *Acta Physiol Scand Suppl* 332:65-84.

Cottrell GT, Lin R, Warn-Cramer BJ, Lau AF, Burt JM. (2003). Mechanism of v-Src- and mitogen-activated protein kinase-induced reduction of gap junction communication. *Am J Physiol Cell Physiol* 284:C511-520

Dahl E, Manthey D, Chen Y, Schwarz H-J, Chang S, Lalley PA, Nicholson BJ, Willecke K. (1996). Molecular cloning and functional expression of mouse connexin30, a gap junction gene highly expressed in adult brain and skin. *J Biol Chem* 271:17903-17910.

Dahl GW, Werner R, Levine E, Rabadan-Diehl C. (1992). Mutational analysis of gap junction formation. *Biophys J* 62:172-182

Dahl GW, Nonner W, Werner R. (1994). Attempts to fefine functional domains of gap junction proteins with synthetic peptides. *Biophys J* 67:1816-1822

Das Sarma J, Meyer RA, Wang F, Abraham V, Lo CW, Koval M (2001). Multimeric connexin interactions prior to the trans-Golgi network. *J Cell Sci* 114(Pt 22):4013-24

De Maio A, Vega VL, Contreras JE. (2002).Gap junctions, homeostasis, and injury. *J Cell Physiol* 191(3):269-82

Dermietzel R, Traub O, Hwang TK, Beyer E, Bennett MVL, Spray DC, Willecke K. (1989). Differential expression of three gap junction proteins in developing and mature brain tissues. *Proc Nat Acad Sci USA* 86:10148-10152.

Dermietzel R, Spray DC. (1993). Gap junctions in the brain: where, what type, how many and why? *Trends Neurosci* 16:186-192

Dermietzel R, Farooq M, Kessler JA, Hertzberg EL, Spray DC. (1997). Oligodendrocytes express gap junction proteins connexin32 and connexin45. *Glia* 20:101-114.

Diez JA, Ahmad S, Evans WH. (1999). Assembly of heteromeric connexons in guinea-pig liver en route to the Golgi apparatus, plasma membrane and gap junction. *Eur J Biochem* 262:142-148.

Duffy HS, Delmar M, Spray DC. (2002). Formation of the gap junction nexus: binding partners for connexins. *J Physiol Paris* 96:243-249

Ek-Vitorin JF, Calero G, Morley GE, CoombsW, Taffet SM, Delmar M. (1996). pH regulation of connexin43: molecular analysis of the gating particle. *Biophys J* 71:1273-1284

Elfgang C, Eckert R, Lichtenberg-Frate H, Butterweck A, Traub O, Klein RA, Hulser DF, Willecke K. (1995). Specific permeability and selective formation of gap junction channels in connexin-transfected Hela cells. *J Cell Biol* 129:805-817.

Engelmann TW. (1875). Ueber die Leitung der Erregung im Herzmuskel. *Arch. Gesamate. Physiol* 11:465-480

Evans WH, Rahman S. (1989). Gap junctions and intercellular communication: topology of the major junctional protein of rat liver. *Biochem Soc Trans* 17(6):983-5.

Falk MM, Buehler LK, Kumar NM, Gilula NB. (1997). Cell-free synthesis and assembly of connexins into functional gap junction membrane channels. *EMBO* 16:2703-2716

Felix JA, Chaban VV, Woodruff ML, Dirken ER. (1998). Mechanical stimulation initiates intercellular Ca^{2+} signaling in intact tracheal epithelium maintained under normal gravity and simulated microgravity. *Am J Respir Cell Mol. Biol.* 18:602-610

Fernandez-Cobo M, Stewart D, Drujan D, De Maio A. (2001). Promoter activity of the rat connexin 43 gene in NRK cells. *J Cell Biochem* 81:514-22

Fischbeck KH, ar-Rushdi N, Pericak-Vance M, Rozear M, Roses AD, Fryns JP. (1986). X-linked neuropathy: gene localization with DNA probes. *Ann Neurol* 20(4):527-32

Flagg-Newton J, Loewenstein WR. (1979). Experimental depression of junctional membrane permeability in mammalian cell culture. A study with tracer molecules in the 300 to 800 dalton range. *J Membr Biol* 50:65-100

Foote CI, Zhou L Zhu, Nicholson BJ. (1998). The pattern of disulfide linkages in the extracellular loop regions of connexin 32 suggests a model of the docking interface of gap junctions. *J. Cell Biol* 140:1187-1197

Friede R, Samorajski T. (1969). The clefts of Schmidt-Lantermann: A quantitative electron microscopic study of their structure in developing and adult sciatic nerves of the rat. *Anat Rec* 165:89-102

Friede RL, Bischhausen R. (1980). The precise geometry of large internodes. *J Neurol Sci* 48(3):367-81

Fulton BP. (1997). Gap junctions in the developing nervous system. *Perspect Dev Neurobiol* 2(4):327-34

Gabriel HD, Jung D, Butzler C, Temme A, Traub O, Winterhager E, Willecke K. (1998). Transplacental uptake of glucose is decreased in embryonic lethal connexin26-deficient mice. *J Cell Biol* 140(6):1453-61

Gaietta G, Deerinck TJ, Adams SR, Bouwer J, Tour O, Laird DW, Sosinsky GE, Tsien RY, Ellisman MH. (2002). Multicolor and electron microscopic imaging of connexin trafficking. *Science* 296:503-507

Garbay B, Heape AM, Sargueil F, Cassagne C. (2000). Myelin synthesis in the peripheral nervous system. *Prog Neurobiol* 61(3):267-304.

Garcia JH, Yoshida Y, Chen H, Li Y, Zhang ZG, Lian J, Chen S, Chopp M. (1993). Progression from ischemic injury to infarct following middle cerebral artery occlusion in the rat. *Am J Pathol* 142:623-635

George CH, Kendall JM, Evans WH. (1999). Intracellular trafficking pathways in the assembly of connexins into gap junctions. *J Biol Chem* 274:8678-8685

Ghabriel MN, Allt G. (1979a). The role of Schmidt-Lanterman incisures in Wallerian degeneration. I. A quantitative teased fibre study. *Acta Neuropathol (Berl)* 48:93-93

Ghabriel MN, Allt G. (1979b). The role of Schmidt-Lanterman incisures in Wallerian degeneration. II. An electron microscopic study. *Acta Neuropathol (Berl)* 48:95-103

Ghabriel MN, Allt G. (1981). Incisures of Schmidt-Lanterman. *Prog Neurobiol* 17:25-58.

Gilula NB, Reeves OR, Steinbach A. (1972). Metabolic coupling, ionic coupling and cell contacts. *Nature* 235:262-265

Gilula NB. (1987). Topology of gap junction protein and channel function. *Ciba Found Symp* 125:128-139

Giepmans BN, Moolenaar WH. (1998). The gap junction protein connexin43 interacts with the second PDZ domain of the zona occludens-1 protein. *Curr Biol* 8:931-934

Glees P. (1943). Observations on the structure of the connective tissue sheath of coutaneous nerves. *J Anat.* 77:153-159

Goldberg GS, Lampe PD, Nicholson BJ. (1999). Selective transfer of endogenous metabolites through gap junctions composed of different connexins. *Nat Cell Biol* 1(7):457-9

Goodenough DA, Revel JP. (1970). A fine structural analysis of intercellular junctions in the mouse liver. *J Cell Biol* 45:272-290

Goodenough DA, Paul DL, Jesaitis L. (1998). Topological distribution of two connexin32 antigenic sites in intact and split rodent hepatocyte gap junctions. *J* Cell Biol. 107:1817-1824

Goodenough DA, Simon AM, Paul DL. (1999). Gap junctional intercellular communication in the mouse ovarian follicle. *Novartis Found Symp* 219:226-35; discussion 235-40

Goodenough DA, Goliger JA, Paul DL. (1996). Connexins, connexons, and intercellular communication. *Ann. Rev. Biochem.* 65:475:502

Gravel M, DeAngelis D, Braun PE. (1994). Molecular cloning and characterization of rat brain 2',3'-cyclic nucleotide 3'-phosphodiesterase isoform 2. *J Neurosci Res* 15:243-247

Green LM, LaBue M, Lazarus JP, Jennings JC. (1996). Reduced cell-cell communication in experimentally induced autoimmune thyroid disease. *Endocrinology* 137:2823-2832

Guthrie SC. (1984). Patterns of junctional communication in the early amphibian embryo. *Nature* 311:149-151

Guthrie SC, Gilula NB. (1989). Gap junctional communication and development. *Trends Neurosci* 12:12-16

Guthrie PB, Knappenberger J, Segal M, Bennett MV, Charles AC, Kater SB. (1999). ATP released from astrocytes mediates glial calcium waves. *J Neurosci* 19:520-528

Hahn AF, Brown WF, Koopman WJ, Feasby TE. (1990). X-linked dominant hereditary motor and sensory neuropathy. *Brain* 113 (Pt 5):1511-25

Hall SM, Williams PL. (1970). Studies of the incisures of Schmidt and Lanterman. *J Cell Sci* 6:767-791.

Hand GM, Müller DJ, Nicholson BJ, Engel A, Sosinsky GE. (2002). Isolation and characterization of gap junctions form tissue culture cells. *J Mol Biol* 315:587-600

Harding AE. (1995). From the syndrome of Charcot, Marie and Tooth to disorders of peripheral myelin proteins. *Brain* 118 (Pt 3):809-18

Hatton GI, Yang QZ, Cobbett P. (1987). Dye coupling among immunocytochemically identified neurons in the supraoptic nucleus: increased incidence in lactating rats. *Neuroscience* 21:923-930

Hatton GI. (2002). Glial-neuronal interactions in the Mammalian brain. *Adv Physiol Educ* 26(4):225-37

Haubrich S, Schwarz H-J, Bukauskas F, Lichtenberg-Frate H, Traub O, Weingart R, Willecke K. (1996). Incompatibility of connexin 40 and 43 hemichannels in gap junctions between mammalian cells is determined by intracellular domains. *MBC* 7:195-2006

Hiscoe HB. (1947). Distribution of nodes and incisures in normal and regenerated nerve fibers. *Anat Rec* 99:447-475

Hecht S, Schlaer S, Pirenne MH. (1942) Energy, Quanta and vision. *J Opt Soc America* 38:196-208

Hennemann H, Suchyna T, Lichtenberg-Frate H, Jungbluth S, Dahl E, Schwarz J, Nicholson BJ, Willecke K. (1992). Molecular cloning and functional expression of mouse connexin40, a second gap junction gene preferentially expressed in lung. *J Cell Biol* 117:1299-1310

Hertzberg EL. (1984). A detergent-independent procedure for the isolation of gap junctions from rat liver. *J Biol Chem* 259:9936-9943

Hertzberg EL, Disher RM, Tiller AA, Zhou Y, Cook RG. (1988). Topology of the Mr 27,000 liver gap junction protein. Cytoplasmic localization of amino- and carboxyl termini and a hydrophilic domain which is protease-hypersensitive. *J Biol Chem* 263:19105-19111

Hildebrand C. (1971). Ultrastructural and light-microscopic studies of the nodal region in large myelinated fibers of the adult feline spinal cord white matter. *Acta Physiol Scand Suppl* 364:43-79.

Hildebrand C, Remahl S, Persson H, Bjartmar C. (1993). Myelinated nerve fibers in the CNS. *Prog Neurobiol* 40:319-384.

Hirano A, Dembitzer HM. (1967). A structural analysis of the myelin sheath in the central nervous system. *J Cell Biol* 34:555-567.

Hirokawa N, Heuser J. (1982). The inside and outside of gap junction membranes visualized by deep etching. *Cell* 30:395-406

Hoh JH, Lal R, John SA, Revel J-P, Arnsdorf MF. (1991a). Atomic force microscopy and dissection of gap junctions. *Science* 235:1405-1408

Hoh JH, John SA, Revel JP. (1991b). Molecular cloning and characterization of a new member of the gap junction gene family, connexin-31. *J Biol Chem* 266:6524-6531

Hoh JH, Sosinsky GE, Revel J-P, Hansma PK. (1993). Structure of the extracellular surface of the gap junction by atomic force microscopy. *Biophys J* 65:149-163

Hossain MZ, Peeling J, Sutherland GR, Hertzberg EL, Nagy JI. (1994) Ischemia-induced cellular redistribution of the astrocytic gap junctional protein connexin43 in rat brain. *Brain Res* 652:311-322

Imanaga I, Kameyama M, Irasawa H. (1987). Cell-to-cell diffusion of fluorescent dyes in paired ventricular cells. *Am J Phsiol* 252:H223-H232

Ionasescu VV, Searby C, Ionasescu R, Neuhaus IM, Werner R. (1996). Mutations of the noncoding region of the connexin32 gene in X-linked dominant Charcot-Marie-Tooth neuropathy. *Neurology* 47(2):541-4

Ismailov II, Benos DJ. (1995). Effects of phosphorylation on ion channel function. *Kidney Int* 48(4):1167-79

Jacob A, Beyer EC. (2001). Mouse connexin45: genomic cloning and exon usage. *DNA Cell Biol* 20:11-19

John SA, Revel JP. (1991). Connexin integrity is maintained by non-covalent bonds: intramolecular disulfide bonds link the extracellular domains in connexin-43. *Biochm Biophys Res Comm* 178:1312-1318

Jongsma H.J, van Rijen HVM, Kwak BR, Chanson. (2001). Phosphorylation of Connexins: Consequences for Permeability, Conductance, and Kinetics of Gap Junction Channels. *Curr Top Memb Vol 49*

Jordan K, Salan JL, Dominquez M, Sia M, Hand A, Lampe PD, Laird DW. (1999). Trafficking, assembly, and function of a connexin Cx43-green fluorescent protein chimera in live mammalian cells. *Mol Biol Cell* 10:2033-2050

Kandler K, Katz LC. (1998). Coordination of neuronal activity in developing visual cortex by gap junction-mediated biochemical communication. *J Neurosci* 18:1419-1427

Kanemitsu MY, Loo LW, Simon S, Lau AF, Eckhart W. (1997). Tyrosine phosphorylation of connexin 43 by v-src is mediated by SH2 and SH3 domain interactions. *J. Biol. Chem.* 272:22824-22831

Kelsell DP, Dunlop J, Stevens HP, Lench NJ, Liang JN, Parry G, Mueller RF, Leigh IM. (1997). Connexin 26 mutations in hereditary non-syndromic sensorineural deafness. *Nature* 387(6628):80-83

Kettenmann H, Orkand RK, Schachner M. (1983). Coupling among identified cells in mammalian nervous system cultures. *J Neurosci* 3(3):506-516

Kirchhoff F, Dringen R, Giaume C. (2001). Pathways of neuron-astrocyte interactions and their possible role in neuroprotection. *Eur Arch Psychiatry Clin Neurosci* 251:159-69

Koval M, Harley JE, Hick E, Steinberg TH. (1997). Connexin46 is retained as monomers in a trans-Golgi compartment of osteoblastic cells. *J Cell Biol* 137:847-857

Kruger O, Plum A, Kim JS, Winterhager E, Maxeiner S, Hallas G, Kirchhoff S, Traub O, Lamers WH, Willecke K. (2000). Defective vascular development in connexin 45-deficient mice. *Development* 127:4179-4193

Kumar NM, Gilula NB. (1986). Cloning and characterization of human and rat liver cDNAs coding for a gap junction protein. *J Cell Biol* 103:767-776

Kumar NM, Gilula NB. (1996). The gap junction communication channel. *Cell* 843:381-388

Kunzelmann P, Blumcke I, Traub O, Dermietzel R, Willecke K. (1997). Coexpression of connexin45 and -32 in oligodendrocytes of rat brain. *J Neurocytol* 26:17-22

Kunzelmann P, Schröder W, Traub O, Steinhäuser C, Dermietzel R, Willecke K. (1999). Late onset and increasing expression of the gap junction protein connexin30 in adult murine brain and long-term cultured astrocytes. *Glia* 25:111-119

Kwak BR, van Veen TA, Analbers LJ, Jongsma HJ. (1995). TPA increases conductance but decreases permeability in neonatal rat cardiomyocyte gap junction channels. *Exp Cell Res* 220:456-63

Kwak BR, Jongsma HJ. (1996). Regulation of cardiac gap junction channel permeability and conductance by several phosphorylating conditions. *Mol Cell Biochem* 157:93-99

Laird DW, Castillo M, Kasprzak L. (1995). Gap junction turnover, intracellular trafficking, and phosphorylation of connexin43 in brefeldin A-treated rat mammary tumor cells. *J Cell Biol* 131(5):1193-203

Lal R, John SA, Laird DW, Arnsdorf MF. (1995). Heart gap junction preparations reveal hemiplaques by atomic force microscopy. *Am J Physiol* 268:C968-C977

Lampe PD, Lau AF. (2000). Regulation of gap junctions by phosphorylation of connexins. *Arch Biochem Biophys* 384(2):205-15

Lang LM, Beyer EC, Schwartz AL, Gitlin JD. (1991). Molecular cloning of a rat uterine gap junction protein and analysis of gene expression during gestation. *Am J Physiol* 260:E787-E793

Larsen WJ, Tung NH, Polking C. (1981). Responese fo granulose cell gap junctions to human chorionic gonadotropin (hCG) at ovulation. *Biol Reprod* 25:1119-1123

Lauf U, Giepmans BNG, Lopez P, Braconnot S, Chen S-S, Falk MM. (2002). Dynamic trafficking and delivery of connexons to the plasma membrane and accretion to gap junctions in living cells. *Proc Natl Acad Sci USA* 99:10446-10451.

Li JY, Boado RJ, Pardridge WM. (2001). Blood-brain barrier genomics. *J Cereb Blood Flow Metab* 21(1):61-8

Li J, Hertzberg EL, Nagy JI. (1997). Connexin32 in oligodendrocytes and association with myelinated fibres in mouse and rat brain. *J Comp Neurol* 379:571-591

Li WEI, Ochalski PAY, Hertzberg EL, Nagy JI. (1998). Immunorecognition, ultrastructure and phosphorylation status of astrocytic gap junctions and connexin43 in rat brain after cerebral focal ischemia. *Eur J Neurosci* 10:2444-2463

Li WE, Nagy JI. (2000). Activation of fibres in rat sciatic nerve alters phosphorylation state of connexin-43 at astrocytic gap junctions in spinal cord: evidence for junction regulation by neuronal-glial interactions.
Neuroscience 97:113-23

Li Xinbo, Lynn BD, Olson C, Meier C, Davidson KGV, Yasumura T, Rash JE, Nagy JI. (2002). Connexin29 expression, immunocytochemistry and freeze-fracture replica immunogold labeling (FRIL) in sciatic nerve. *Eur J Neurosci* 16:795-806

Lin JH, Yang J, Liu S, Takano T, Wang X, Gao Q, Willecke K, Nedergaard M. (2003). Connexin mediates gap junction-independent resistance to cellular injury. *J Neurosci* 23:430-441

Liu S, Taffet SM, Stoner L, Vallano ML, Jalife J. (1993). A structural bias for the unequal sensitivity of the major cardiac and liver gap junctions to intracellular acidification: the carboxyl terminal length. *Biophys J* 64:1422-1433

Loo LW, Berestecky JM, Kanemitsu MY, Lau AF. (1995). pp60src-mediated phosphorylation of connexin 43, a gap junction protein. *J Biol Chem* 270:12751-12761

Luizzi FJ, Miller RH. (1987). Radially oriented astrocytes in the normal adult rat spinal cord. *Brain Res* 403:385-388

Lynn BD, Rempel JL, Nagy JI. (2001). Enrichment of neuronal and glial connexins in the postsynaptic density subcellular fraction of rat brain. *Brain Res* 898:1-8

Martin PE, Blundell G, Ahmad S, Errington RJ, Evans WH. (2001). Multiple pathways in the trafficking and assembly of connexin 26, 32 and 43 into gap junction intercellular communication channels. *J Cell Science* 114:3845-3855

Martinez AD, Hayrapetyan V, Moreno AP, Beyer EC. (2002). Connexin43 and connexin45 form heteromeric gap junction channels in which individual components determine permeability and regulation. *Circ Res* 90(10):1100-7

Massa PT, Mugnaini E. (1982). Cell junctions and intramembrane particles of astrocytes and oligodendrocytes: a freeze-fracture study. *Neuroscience* 7:523-538.

Matsuyama W, Nakagawa M, Moritoyo T, Takashima H, Umehara F, Hirata K, Suehara M, Osame M. (2001). Phenotypes of X-linked Charcot-Marie-Tooth disease and altered trafficking of mutant connexin 32 (GJB1*). J Hum Genet* 46(6):307-13

Meda P, Chanson M, Pepper M, Giordano E, Bosco D, Traub O, Willecke K, el Aoumari A, Gros D, Beyer EC, Orci L, Spray D. (1991). In vivo modulation of connexin43 gene expression and junctional coupling for pancreatic β-cells. *Exp Cell Res* 192:469-480

Meier C, Petrasch-Parwez E, Habbes HW, Teubner B, Guldenagel M, Degen J, Sohl G, Willecke K, Dermietzel R. (2002). Immunohistochemical detection of the neuronal connexin36 in the mouse central nervous system in comparison to connexin36-deficient tissues. *Histochem Cell Biol* 117:461-71

Mercier F, Hatton GI. (2001). Connexin 26 and basic fibroblast growth factor are expressed primarily in the subpial and subependymal layers in adult brain parenchyma: Roles in stem cell proliferation and morphological plasticity? *J Comp Neurol* 431:88-104.

Milks LC, Kumar NM, Houghten R, Unwin N, Gilula NB. (1988). Topology of the 32-kd liver gap junction protein determined by site-directed antibody localizations. *EMBO J* 7:2967-2975

Morley GE, Taffet SM, Delmar M. (1996) Intramolecular interactions mediate the pH regulation of connexin43. *Biophys J* 70:1294-1302

Mugnaini E. (1986). Cell junctions of astrocytes, ependyma, and related cells in the mammalian central nervous system, with emphasis on the hypothesis of a generalized functional syncytium of supporting cells. In: Fedoroff S, Vernadakis A, editors. *Astrocytes, Vol. I. New York Academic Press*. p329-371.

Muller-Borer BJ, Johnson TA, Gettes LS, Cascio WE. (1995). Failure of impulse propagation in a mathematically simulated ischemic border zone: influence of direction of propagation and cell-to-cell electrical coupling. *J Cardiovasc Electrophysiol* 6(12):1101-12

Musil LS, Goodenough DA. (1993). Multisubunit assembly of an integral plasma membrane channel protein, gap junction connexin43, occurs after exit from the ER. *Cell* 74:1065-1077

Nageotte J. (1992). L'organisation de la matiere. *Librairie Felix Alcan* Paris

Nagy JI, Ochalski PAY, Li J, Hertzberg EL. (1997). Evidence for co-localization of another connexin with connexin-43 at astrocytic gap junctions in rat brain. *Neuroscience* 78:533-548.

Nagy JI, Patel D, Ochalski PAY, Stelmack GL. (1999). Connexin30 in rodent, cat and human brain: selective expression in gray matter astrocytes, co-localization with connexin30 at gap junctions and late developmental appearance. *Neuroscience* 88:447-468.

Nagy JI, Dermietzel R. (2000). Gap junctions and connexins in the mammalian central nervous system. In: Hertzberg EL, editor. *Advances in Molecular and Cell Biology, Vol. 30. Greenwich: JAI Press*. p323-396.

Nagy JI, Rash JE. (2000). Connexins and gap junctions of astrocytes and oligodendrocytes in the CNS. *Brain Res* Rev 32:29-44

Nagy JI, Li X, Rempel J, Stelmack G, Patel D, Staines WA Yasumura T, Rash JE. (2001). Connexin26 in adult rodent CNS: demonstration at astrocytic gap junctions and co-localization with connexin30 and connexin43. J Comp Neurol 441:302-323.

Nagy JI, Ionescu AV, Lynn BD, Rash JE. (2003a). On connexin29 and connexin32 expression in mouse CNS: Oligodendrocyte/astrocyte gap junction coupling relationships and connexin organization in myelin. Submitted to *J Comp Neurol.*

Nagy JI, Ionescu AV, Lynn BD, Rash JE. (2003b). Coupling of Astrocyte Connexins Cx26, Cx30, Cx43 to Oligodendrocyte Cx29, Cx32, Cx47: Implications From Normal and Connexin32 Knockout Mice. *Glia*, submitted.

Nagy JI, Dudek FE, Rash JE. (2003c). Update on connexins and gap junctions in neurons and glia in the nervous system. *Brain Res Rev* In Press.

Naus CC, Bechberger JF, Zhang Y, Venance L, Yamasaki H, Juneja SC, Kidder GM, Giaume C. (1997). Altered gap junctional communication, intercellular signaling, and growth in cultured astrocytes deficient in connexin43. *J Neurosci Res* 49:528-540

Nelis E, Haites N. Van Broeckhoven C. (1999). Mutations in the peripheral myelin genes and associated genes in inherited peripheral neuropathies. *Hum Mutat* 13:11–28.

Nelles E, Butzler C, Jung D, Temme A, Gabriel H-D, Dahl U, Traub O, Stumpel F, Jungermann K, J. Zielasek, Toyka KV, Dermietzel R, Willecke K. (1996). Defective propagation of signals generated by sympathetic nerve stimulation in the liver of connexin32-deficient mice. *Proc Natl Acad Sci USA* 93:9565-9570.

Neveu MJ, Hully JR, Babcock KL, Vaughan J, Hertzberg EL, Nicholson BJ, Paul DL, Pitot HC. (1995). Proliferation-associated differences in the spatial and temporal expression of gap junction genes in rat liver. *Hepatology* 22:202-212

Newman EA. (1995a). Membrane physiology of retinal glial (Muller) cells. *J Neurosci* 5:2225-2239

Newman EA. (1985b). Regulation of potassium levels by the glial cells in the retina. *Trends Neurosci.* 8:156-159

Nicholson SM, Ressot C, Gomes D, D'Andrea P, Perea J, Duval N, Bruzzone R. (1999). Connexin32 in the peripheral nervous system: functional analysis of mutations associated with X-linked Connexin32 in the peripheral nervous system: functional analysis of mutations and implications for the pathophysiology of the disease, *An NY Aca Sci* 883:168-85

Norenberg MD, Martinez-Hernandez A. (1979). Fine structural localization of glutamine synthetase in astrocytes of rat brain. *Brain Res* 161:303-310

Ochalski PAY, Frankenstein UN, Hertzberg EL, Nagy JI. (1997). Connexin43 in rat spinal cord: localization in astrocytes and identification of heterotypic astro-oligodendrocytic gap junctions. *Neuroscience* 76:931-945

Odermatt B, Wellershaus K, Wallraff A, Seifert G, Degen J, Euwens C, Fuss B, Büssow H, Schilling K, Steinhäuser C, Willecke K. (2003). Connexin 47 (Cx47)-Deficient Mice with Enhanced Green Fluorescent Protein Reporter Gene Reveal Predominant Oligodendrocytic Expression of Cx47 and Display Vacuolized Myelin in the CNS. *J Neurosci* 23: 4549-4559

Oh S, Ri Y, Bennett MVL, Trexler EB, Verselis VK, Bargiello TA. (1997). Changes in permeability caused by connexin 32 mutations underline X-linked Charcot-Marie-Tooth disease. *Neuron* 19:927-938

Pal JD, Liu X, Mackay D, Shiels A, Berthoud VM, Beyer EC, Ebihara L. (2000). Connexin46 mutations linked to congenital cataract show loss of gap junction channel function. *Am J Physiol Cell Physiol* 279(3):C596-C602

Panas M, Karadimas C, Avramopoulos D, Vassilopoulos D. (1998). Central nervous system involvement in four patients with Charcot-Marie-Tooth disease with connexin32 extracellular mutations. *J Neurol Neurosurg Psychiat* 65:947-948.

Pastor A, Kremer M, Möller T, Kettenmann H, Dermietzel R. (1998). Dye coupling between spinal cord oligodendrocytes: Differences in coupling efficiency between gray and white matter. *Glia* 24:108-120.

Paul DL. (1995). New functions for gap junctions. *Curr Opin Cell Biol* 7:665-672

Paul DL. (1986). Molecular cloning of cDNA for rat liver gap junction protein. *J Cell Biol* 103:123-134

Pekny M. (2001). Astrocytic intermediate filaments: lessons from GFAP and vimentin knock-out mice. *Prog Brain Res* 132:23-30

Peracchia C. (1980). Structural correlates of gap junction permeations. *Int Rev Cytol* 66:81-146

Perkins GA, Goodenough DA, Sosinsky GE. (1998). Formation of the gap junction intercellular channel requires a 30 degree rotation for interdigitating two apposing connexons. *J Mol Biol* 277(2):171-7

Perez J, Tranque PA, Naftolin F, Garcia-Segura LM. (1990). Gap junctions in the hypothalamic arcuate neurons of ovariectomized and estradiol-treated rats. *Neurosci Lett* 108:17-21

Phelan P, Bacon JP, Davies JA, Stebbings LA, Todman MG, Avery L, Baines RA, Barnes TM, Ford C, Hekimi S, Lee R, Shaw JE, Starich TA, Curtin KD, Sun YA, Wyman RJ. (1998). Innexins: a family of invertebrate gap-junction proteins. *Trends Genet* 14:348-349

Piechocki MP, Burk RD, Ruch RJ. (1999). Regulation of connexin32 and connexin43 gene expression by DNA methylation in rat liver cells. *Carcinogenesis* 20:401-406

Piechocki MP, Toti RM, Fernstrom MJ, Burk RD, Ruch RJ. (2000). Liver cell-specific transcriptional regulation of connexin32 *Biochim Biophys Acta*. 1491:107-122

Pixley SK, Kobayashi Y, de Vellis J. (1994). Monoclonal antibody to intermediate filament proteins in astrocytes. *J Neurosci Res* 12(4):525-41

Prime G, Horn G, Sutor B. (2000). Time-related changes in connexin mRNA abundance in the rat neocortex during postnatal development. *Dev Brain Res* 119:111-125.

Rahman S, Evans WH. (1991). Topography of connexin 32 in rat liver gap junctions: evidence of an intramolecular disulfide linkage connecting the two extracellular peptide loops. *J Cell Sci* 100:567-578

Rash JE, Duffy HS, Dudek FE, Bilhartz BL, Whalen LR, Yasumura T. (1997). Grid-mapped freeze-fracture analysis of gap junctions in gray and white matter of adult rat central nervous system, with evidence for a "panglial syncytium" that is not coupled to neurons. *J Comp Neurol* 388:265-292.

Rash JE, Yasumura T. (1999). Direct immunogold labeling of connexins and aquaporin4 in freeze-fracture replicas of liver, brain and spinal cord: factors limiting quantitative analysis. *Cell Tissue Res* 296:307-321.

Rash JE, Staines WA, Yasumura T, Patel D, Hudson CS, Stelmack GL, Nagy JI. (2000). Immunogold evidence that neuronal gap junctions in adult rat brain and spinal cord contain connexin36 but not Cx32 or Cx43. *Proc Nat Acad Sci USA* 97:7573-7578.

Rash JE, Yasumura T, Dudek FE, Nagy JI. (2001). Cell-specific expression of connexins and evidence of restricted gap junctional coupling between glial cells and between neurons. *J Neurosci* 21:1983-2000.

Ressot C, Gomes D, Dautigny A, Pham-Dinh D, Bruzzone R. (1998). Connexin32 mutations associated with X-linked Charcot-Marie-Tooth disease show two distinct behaviors: loss of function and altered gating properties. *J Neurosci* 18:4063-4075

Ressot C, Bruzzone R. (2000). Connexin channels in Schwann cells and the development of the X-linked form of Charcot-Marie-Tooth disease. *Brain Res Rev* 32:192-202

Revel JB, Karnovsky MJ. (1967). Hexagonal array of subunits in intercellular junctions of the mouse heart and liver. *J. Cell Biol* 33: C7-C12

Reyher CK, Lubke J, Larsen WJ, Hendrix GM, Shipley MT, Baumgarten HG. (1991).Olfactory bulb granule cell aggregates: morphological evidence for interperikaryal electrotonic coupling via gap junctions. *J Neurosci* 11(6):1485-95

Ripps H. (2002). Cell death in retinitis pigmentosa: gap junctions and the 'bystander' effect. *Exp Eye Res* 74(3):327-36

Robertson JD. (1963). The occurrence of a subunit pattern in the unit membranes of club endings in Mauthner cell synapses in goldfish brains. *J Cell Bio* 19:201-221

Robinson SR, Hampson EC, Munro MN, Vaney DI. (1993). Unidirectional coupling of gap junctions between neuroglia. *Science* 262:1072-1074

Rosenberg E, Spray DC, Reid LM. (1992). Transcriptional and posttranscriptional control of connexin mRNAs in periportal and pericentral rat hepatocytes. *Eur J Cell Biol* 59:21-26

Rozental R, Giaume C, Spray DC. (2000). Gap junctions in the nervous system. *Brain Res Brain Res Rev.* 32:11-15

Rubin JB, Verselis VK, Bennett MVL, Bargiello TA. (1992). A domain substitution procedure and its use to analyze voltage dependence of homotypic gap junctions formed by connexin 26 and 32. *Proc Natl Acad Sci USA* 89:3820-3824

Rutherford JG, Gwyn DG. (1977). Gap junctions in the inferior olivary nucleus of the squirrel monkey, Saimiri sciureus. *Brain Res* 128(2):374-8

Saez JC, Spray DC, Nairn AC, Hertzberg E, Greengard P, Bennett MV. (1986). cAMP increases junctional conductance and stimulates phosphorylation of the 27-kDa principal gap junction polypeptide. *Proc Natl Acad Sci U S A* 83:2473-2477

Saez JC, Berthoud VM, Kadle R, Traub O, Nicholson BJ, Bennett MV, Dermietzel R. (1991). Pinealocytes in rats: connexin identification and increase in coupling caused by norepinephrine. *Brain Res* 568:265-75

Sanderson MJ, Charles AC, Boitano S, Dirksen ER. (1994). Mechanism and function of intercellular calcium signaling. *Mol Cell Endocrinol* 98(2):173-187

Sandri C, Van Buren JM, Akert K. (1977). Membrane morphology of the vertebrate nervous system. A study with freeze-etch technique. *Prog Brain Res* 46:1-384

Scadding JW. (1981). Development of ongoing activity, mechanosensitivity, and adrenaline sensitivity in severed peripheral nerve axons. *Exp Neurol* 73:345-364.

Scherer SS, Deschenes SM, Xu Y-T, Grinspan JB, Fischbeck KH, Paul DL. (1995). Connexin32 is a myelin-related protein in the PNS and CNS. *J Neurosci* 15:8281-8294.

Scherer SS. (1996). Molecular specializations at nodes and paranodes in peripheral nerve. *Microsc Res Tech* 34:452-461.

Scherer SS, Xu YT, Nelles E, Fischbeck K, Willecke K, Bone LJ. (1998). Connexin32-null mice develop demyelinating peripheral neuropathy. *Glia* 24(1):8-20

Scherer SS. (1999). Nodes, paranodes, and incisures: from form to function. *Ann N Y Acad Sci* 883:131-42

Schlaepfer WW, Myers FK. (1973). Relationship of myelin internode elongation and growth in the rat sural nerve. *J Comp Neurol* 147:255-66

Scemes E. (2000). Components of astrocytic intercellular calcium signaling. *Mol Neurobiol* 22:167-79

Scott DA, Kraft ML, Carmi R, Ramesh A, Elbedour K, Yairi Y, Srisailapathy CR, Rosengren SS, Markham AF, Mueller RF, Lench NJ, Van Camp G, Smith RJ, Sheffield VC. (1998). Identification of mutations in the connexin 26 gene that cause autosomal recessive nonsyndromic hearing loss. *Hum Mutat* 11(5):387-94

Severs NJ. (1999). Cardiovascular disease. *Novartis Found Symp* 219:188-206.

Shiels A, Mackay D, Ionides A, Berry V, Moore A, Bhattacharya S. (1997). A missense mutation in the human connexin50 gene (GJA8) underlies autosomal dominant "zonular pulverulent" cataract, on chromosome 1q. *Am J Hum Genet* 62:526-532

Silander K, Meretoja P, Pihko H, Juvonen V, Issakainen J, Aula P, Savontaus M. (1997). Screening for connexin 32 mutations in Charcot-Marie-Tooth disease families with possible X-linked inheritance. *Hum Genet* 100:391-397

Singer M, Krishnan N, Fyfe DA. (1972). Penetration of ruthenium red into peripheral nerve fibers. *Anat Rec* 173:375-89

Simpson I, Rose B, Loewenstein WR. (1977). Size limit of molecules permeating the junctional membrane channels. *Science* 195:294-296

Skerrett M, Kasperek E, Aronowitz J, Cymes G, Nicholson BJ. (1998). Identification of amino acids that line the pore of gap junctions. *Supplement to MBC* 9 Abstract #541

Skerrett IM, Smith JF, Nicholson BJ. (2000). *Curr Topics in Memb. Biol.* 49:1-249-269

Sloper JJ. (1972). Gap junctions between dendrites in the primate neocortex. *Brain Res* 44(2):641-6

Skerrett IM, Aronowitz J, Shin JH, Cymes G, Kasperek E, Cao FL, Nicholson BJ. (2002). Identification of amino acid residues lining the pore of a gap junction channel. *J Cell Biol* 159:349-*360*

Skre H. (1974). Genetic and clinical aspects of Charcot-Marie-Tooth's disease. *Clin Genet* 6(2):98-118

Smit AB, Syed NI, Schaap D, van Minnen J, Klumperman J, Kits KS, Lodder H, van der Schors RC, van Elk R, Sorgedrager B, Brejc K, Sixma TK, Geraerts WP. (2001). A glia-derived acetylcholine-binding protein that modulates synaptic transmission. *Nature* 411:261-268

Söhl G, Eiberger J, Jung YT, Kozak CA, Willecke K. (2001). The mouse gap junction gene connexin29 is highly expressed in sciatic nerve and regulated during brain development. *Biol Chem* 382:973-978.

Sosinsky GE, Jesior JC, Caspar DLD, Goodenough DA. (1998). Gap junction structures VIII. Membrane cross-section. *Biophys J* 53:709-722

Sosinsky GE. (2000). Gap junction structure: New structures and insights. *Curr Topics in Memb. Biol.* 49:1-22

Spray DC, Stern JH, Harris AL, Bennett MV. (1982). Gap junctional conductance: comparison of sensitivities to H and Ca ions. *Proc Natl Acad Sci U S A* 79:441-445

Spray DC, Fujita M, Saez JC, Choi H, Watanabe T, Hertzberg E, Rosenberg LC, Reid LM. (1987). Proteoglycans and glycosaminoglycans induce gap junction synthesis and function in primary liver cultures. *J Cell Biol* 105:541-551

Spray DC, Dermietzel R. (1995). X-linked dominant Charcot-Marie-Tooth disease and other potential gap-junction diseases of the nervous system. *Trends Neurosci* 18:256-262

Spray DC, Duffy HS, Scemes E. (1999). Gap junctions in glia. Types, roles, and plasticity. *Adv Exp Med Biol* 468:339-359

Stagg RB, Fletcher WH. (1990). The hormone-induced regulation of contact-dependent cell-cell communication by phosphorylation. *Endocr Rev* 11(2):302-25

Stauffer KA, Kumar NM, Gilula NB, Unwin N. (1991). Isolation and purification of gap junction channels. *J Cell Biol* 115(1):141-50

Steinberg TH. (1998). Gap junction function: the messenger and the message. *Am J Pathol.* 152:851-854

Suchyna, T.M., Xu, X.L., Gao, F., Fourtner, C.R., and Nicholson, B.J. (1993). Identification of a proline residue as a transduction element involved in voltage gating of gap junctions *Nature* 365:847-849

Suchyna TM, Nitsche JM, Chilton M, Harris AL, Veenstra RD, Nicholson BJ. (1999). Different ionic selectivities for connexins 26 and 32 produce rectifying gap junction channels. *Biophys J* 77(6):2968-87

Suter U, Snipes GJ. (1995). Biology and genetics of hereditary motor and sensory neuropathies. *Annu Rev Neurosci* 18:45-75

Swenson KI, Jordan JR, Beyer EC, Paul DL. (1989). Formation of gap junctions by expression of connexins in Xenopus oocyte pairs. *Cell* 57:145-155.

ter Keurs HEDJ, Zhang YM. (1997). Triggered propagated contractions and arrhythmias caused by acute damage to cardiac muscle. In "*Discontinuous conduction in the heart*" (Spooner PM, Joyner RW, Jalife J, eds.) pp223-239. Futura Publishing Co Armonk NY

Teunissen BE, van Amersfoorth SC, Opthof T, Jongsma HJ, Bierhuizen MF. (2002). Sp1 and Sp3 activate the rat connexin40 proximal promoter. Biochem *Biophys Res Commun* 292:71-8

Thonnissen E, Rabionet R, Arbones ML, Estivill X, Willecke K, Ott T. (2002). Human connexin26 (GJB2) deafness mutations affect the function of gap junction channels at different levels of protein expression. *Hum Genet* 111:190-197

Toyofuku T, Yabuki M, Otsu K, Kuzuya T, Hori M, Tada M. (1998). Direct association of the gap junction protein connexin-43 with ZO-1 in cardiac myocytes. *J Biol Chem* 273(21):12725-31

Toyofuku T, Akamatsu Y, Zhang H, Kuzuya T, Tada M, Hori M. (2001). c-Src regulated the interaction between connexin-43 and ZO-1 in cardiac myocytes. *J. Biol. Chem.* 276-1780-1788

Trapp BD, Andrews SB, Cootauco C, Quarles R. (1989). The myelin-associated glycoprotein is enriched in multivesicular bodies and periaxonal membranes of actively myelinating oligodendrocytes. *J Cell Biol* 109:2417-2426.

Unger VM, Kumar NM, Gilula NB, Yeager M. (1999). Three-dimensional structure of a recombinant gap junction membrane channel. *Science* 283:1176-1180

Unwin PNT, Ennis PD. (1984). Two configurations of a channel-forming membrane protein. *Nature* 307:609-613

Unwin PNT, Zampighi G. (1980) Structure of the gap junction between communicating cells. *Nature* 283:545-549

Valdimarsson G, Kidder GM. (1995). Temporal control of gap junction assembly in preimplantation mouse embryos. *J Cell Sci* 1081715-1722

Valiunas V, Gemel J, Brink PR, Beyer EC. (2001). Gap junction channels formed by coexpressed connexin40 and connexin43. *Am J Physiol Heart Circ Physiol* 281(4):H1675-89

Veenstra RD, Wang H-Z, Beyer EC, Ramanan SV, Brink PR. (1994a). Connexin 37 forms high conductance gap junction channels with subconductance state activity and selective and ionic permeabilities. *Biopys J* 66: 1915-1928

Veenstra RD, Wang H-Z, Beyer EC, Brink PR. (1994b). Selective dye and ionic permeability of gap junction channels formed by connexin45. *Circ. Res.* 75:483-490

Veenstra RD. (1996). Size and selectivity of gap junction channels formed from different connexins. *J Bioenerg Biomemb* 28:327-337

Veenstra RD. (2001). Voltage clamp limitations of dual whole-cell gap junction current and voltage recordings. I. Conductance measurements. *Biophys J* 80:2231-2247

Verity AN, Campagnoni AT. (1988). Regional expression of myelin protein genes in the developing mouse brain: in situ hybridization studies. *J Neurosci Res* 21:238-248.

Verselis VK, Ginter C, Bargiello TA. (1994). Opposite voltage gating polarities of two closely related connexins. *Nature* 368:348-351

Warner AE. (1985).The role of gap junctions in amphibian development. *J Embryol Exp Morphol* 89 Suppl:365-80

Waxman SG, Black JA. (1984). Freeze-fracture ultrastructure of the perinodal astrocyte and associated glial junctions. *Brain Res* 308:77-87.

Waxman SG. (1996). Correlative neuroanatomy 24th edition. Lange Medical Books

Webster HF. (1965). The relationship between Schmidt-Lanterman incisures and myelin segmentation during Wallerian degeneration. *Ann NY Acad Sci* 122:29-38.

Weidmann S. (1952). The electrical constants of Purkinje fibers. J *Physiol* 118:348-360

Weingart R, Bukauskas FF. (1993). Gap junction channels of insect cells exhibit a residual conductance. *Pflügers Arch* 424:192-194

Werner RE, Levine C, Rabadan-Diehl C, Dahl G. (1989). Formation of hybrid channels. *Proc Natl Acad Sci* USA 86:5380-5384.

White RL, Spray DC, Campos de Carvalho AC, Wittenberg BA, Bennett MV. (1985). Some electrical and pharmacological properties of gap junctions between adult ventricular myocytes. *Am J Physiol* 249:C447-C455

White TW, Bruzzone R, Woflfram S, Paul DL, Goodenoughy DA. (1994a). Selective interactions among the multiple connexin proteins expressed in the vertebrate lens: the second extracellular domain is a determinant of compatibility between connexins. *J Cell Biol* 125:879-892

White TW, Bruzzone R, Goodenough DA, Paul DA. (1994b). Voltage gating of connexins. *Nature* 371:208-209

White TW, Paul DL, Goodenough DA, Bruzzone R. (1995). Functional analysis of selective interactions among rodent connexins. *Molec Biol Cell* 6:459-470

White TW, Bruzzone R. (1996). Multiple connexin proteins in single intercellular channels: connexin compatibility and functional consequences. *J Bioenerg Biomem* 28:339-349.

Willecke K, Heynkes R, Dahl E, Stutenkemper R, Hennemann H, Jungbluth S, Suchyna T, Nicholson BJ. (1991a). Mouse connexin37: cloning and functional expression of a gap junction gene highly expressed in lung. *J Cell Biol* 114:1049-1057

Willecke K, Hennemann H, Dahl E, Jungbluth S, Heynkes R. (1991b). The diversity of connexin genes encoding gap junctional proteins. *Eur J Cell Biol* 56(1):1-7

Willecke K, Eiberger J, Degen, J, Eckardt D, Romualdi, A, Guldenagel, M, Deutsch, U, Sohl G. (2002). Structural and functional diversity of connexin genes in the mouse and human genome. *Biol Chem* 383:725-737

Williams PL, Hall SM. (1970). In vivo observations on mature myelinated nerve fibers of the mouse. *J Anat* 107:31-38

Williams PL, Hall SM. (1971a). Prolonged in vivo observations of normal peripheral nerve fibers and their acute reactions to crush and deliberate trauma. *J Anat* 108:397-408.

Williams PL, Hall SM. (1971b). Chronic Wallerian degeneration - an in vivo and ultrastructural study. *J Anat* 109:487-503.

Williams DB, Akabas MH. (1999). Gamma-aminobutyric acid increases the water accessibility of M3 membrane-spanning segment residues in gamma-aminobutyric acid type A receptors. *Biophys J* 77:2563-7254

Williamson MP. (1994). The structure and function of proline-rich regions in proteins. *Biochem J* 297:249-260.

Winterhager E, Von Ostau C, Gerke M, Gruemmer R, Traub O, Kaufmann P. (1999). Connexin expression patterns in human trophoblast cells during placental development. *Placenta* 20:627-38

Wolburg H, Rohlmann A. (1995). Structure-function relationships in gap junctions. *Int Rev Cytol* 157:315-373

Yamamoto T, Shiosaka S, Whittaker ME, Hertzberg EL, Nagy JI. (1989). Gap junction protein in rat hippocampus: light microscope immunohistochemical localization. *J Comp Neurol* 281:269-81

Yamamoto T, Ochalski PAY, Hertzberg EL, Nagy JI. (1990a). LM and EM immunolocalization of the gap junctions protein connexin43 in rat brain. *Brain Res* 508:313-319

Yamamoto T, Ochalski PAY, Hertzberg EL, Nagy JI. (1990b). On the organization of astrocytic gap junctions in rat brain as suggested by LM and EM immunohistochemistry of connexin43 expression. *J Comp Neurol* 302:853-883.

Yamamoto T, Hertzberg EL, Nagy JI. (1991). Subsurface cisterns in alpha-motoneurons of the rat and cat: immunohistochemical detection with antibodies against connexin32. *Synapse* 8:119-136

Yu H, Chen JK, Feng S, Dalgarno DC, Brauer AW, Schreiber SL. (1994). Structural basis of the binding of proline-rich peptides to SH3 domains. *Cell* 76:933-945

Zhang JT, Nicholson BJ. (1989). The topological structure of connexin 26 and its distribution compared to connexin 32 in hepatic gap junctions. *J Membr Biol* 139:15-29

Zhou XW, Pfahnl R, Werner R, Hudder A, Llanes A, Luebke A, Dahl G. (1997). Identification of the pore lining segment in gap junctions hemichannels. *Biophys J* 72:1946-1953

Zhou L, Kasperek EM, Nicholson BJ. (1999). Dissection of the molecular basis of pp60v-src induced gating of connexin43 gap junctions. *J Cell Biol* 144:1033-1045

Zimmer DB, Green CR, Evans WH, Gilula NB. (1987). Topological analysis of the major protein in isolated intact rat liver gap junctions and gap junction-derived single membrane structures. *J Biol Chem* 262:7751-7763